Enhanced Efficacy of Plasmid DNA Vaccines for Cancer Therapy

A DISSERTATION
SUBMITTED TO THE FACULTY OF THE GRADUATE SCHOOL
OF THE UNIVERSITY OF MINNESOTA
BY

Wynette Marie Dietz

IN PARTIAL FULFILLMENT OF THE REQUIREMENTS
FOR THE DEGREE OF
DOCTOR OF PHILOSOPHY

Adviser: Christopher A. Pennell, Ph.D.

November 2010

Acknowledgements

First, I want to acknowledge my advisor, Dr. Christopher Pennell, for his guidance and support throughout my graduate education. His encouragement enabled me to persevere through times of frustration and his kindness made working in his lab a pleasure. I am indebted to him for the knowledge and wisdom he has imparted to me through his excellent teaching and mentoring abilities. Additionally, I would like to thank the members of the Pennell lab including Michelle Jund and Nicole Skinner, who contributed both their scientific expertise and their friendship. I will miss working with them.

I would like to give credit to my committee members—Drs. Matthew Mescher, James McCarthy and Kaylee Schwertfeger—for their advice and support. Their expertise and guidance shaped my research and contributed to making me the scientist that I am today. In addition, I would like to thank the members of the Farrar, Mescher and Ohlfest labs for providing ideas and reagents which contributed greatly to my research.

Finally, my most heartfelt thanks go to my family and friends for their prayers, encouragement, understanding and support. I would like to thank my husband, James, for being patient, loving and understanding. I also owe a great deal to my parents, Clark and Susan Will, for teaching me that I can do anything I put my mind to, for believing in me and for encouraging me along the way. I am blessed to have such wonderful friends and family as a part of my life and could not have done this without them.

Dedication

This dissertation is dedicated to my husband, to my family and to God.

Without them, this would not have been possible.

Abstract

Since cancer is the second most common cause of death in the United States, it is of great importance to pursue new and improved methods for treating cancer. The goal of cancer immunotherapy is to exploit the specificity and longevity of immune responses through the use of vaccines to treat cancer. DNA vaccines have many advantages over protein and viral vaccine-based strategies including low cost, ease of production, flexibility and low toxicity. Plasmid DNA vaccines encoding tumor antigens can produce powerful anti-tumor immune responses in animal models, but clinical trials have shown only modest responses. This lack of clinical efficacy is thought to reflect the two major limitations of plasmid DNA vaccines: transient protein expression and low transfection efficiency. Transient protein expression is likely the result of gene silencing due to transcriptionally repressive chromatin within the plasmid backbone. To overcome this limitation, we removed the bacterial backbone sequences and produced a minicircle DNA consisting of the gene expression cassette with only a few bases of the bacterial backbone. This resulted in persistent protein expression, increased transfection efficiency and enhanced immunogenicity. In an effort to further enhance the transfection efficiency, we produced cationic carriers that bind plasmid DNA and protect it from degradation. The addition of these cationic carriers significantly increased transfection efficiency *in vitro* but has yet to show the same effect *in vivo*. Additionally, we administered these vaccines transdermally using a tattoo device and achieved rapid and potent immune responses. Our results suggest transdermal delivery of a minicircle DNA vaccine elicits potent antigen-specific immune responses, and as such, holds great promise for cancer

therapy. Future work will include increasing transfection efficiency *in vivo* and increasing the immunogenicity of the vaccines through the use of adjuvants with the goal of producing feasible, efficacious DNA vaccines for cancer therapy.

Table of Contents

List of Figures

List of Abbreviations

APC: Antigen presenting cell

Ag: Antigen

BpA: Bovine growth hormone polyadenylation signal

CFA: Complete Freund's adjuvant

CFSE: 5-(and-6)-carboxyfluorescein diacetate, succinimidyl ester

CTL: Cytotoxic T lymphocyte

DC: Dendritic Cell

dLN: Draining lymph node

DNA: Deoxyribonucleic acid

eff: Enhanced firefly luciferase

EGFR: Epidermal growth factor receptor

ELISA: Enzyme-linked immunosorbent assay

ELISpot: Enzyme-linked immunosorbent spot assay

EMSA: Electrophoretic mobility shift assay

FL: Full-length

FL-Ag: Full-length plasmid encoding the antigen cassette

FL-eff: Full-length plasmid encoding enhanced firefly luciferase

GFP: Green fluorescent protein

HA2: Hemagglutinin 2

His: Histidine

HPV: Human papilloma virus

Hsp: Heat shock protein

Hsp70: Heat shock protein 70

hUBC: Human ubiquitin C promoter

IFN-γ: Interferon-γ

MC: Minicircle

MC-Ag: Minicircle encoding the antigen cassette

MC-eff: Minicircle encoding enhanced firefly luciferase

MHC: Major histocompatibility complex

NK: Natural killer

NP: Nucleoprotein

OVA: Ovalbumin

PBS: Phosphate buffered saline

pDNA: Plasmid DNA

SDS: Sodium dodecyl sulfate

SDS-PAGE: Sodium dodecyl sulfate polyacrylamide gel electrophoresis

TCR: T cell receptor

UbC: Ubiquitin C promoter

VC: Empty control vector

VEGF: Vascular endothelial growth factor

Chapter 1:
Introduction

Cancer therapy:

It is predicted that 1,529,560 new cancer cases and 569,490 deaths will occur in the United States alone in 2010 (1). Despite recent advances in cancer therapy, currently one in four deaths in the United States is caused by cancer. This high mortality rate is mainly due to recurrence following standard treatments including surgery, radiation and/or chemotherapy. Therefore, there is a great need for more effective cancer treatment strategies. Imunotherapy, or using the immune system to kill cancer cells selectively, may be one answer.

Cancer immunotherapy:

Immunity and cancer

The immune system protects an individual against disease or infection due to pathogens such as bacteria and viruses. Immunosurveillance is the theory that the immune system also protects individuals against tumor formation by detecting and killing nascent tumor cells. Strong evidence for this theory comes from data showing that RAG2-/- mice (which lack both T and B cells) have a higher rate of spontaneous tumors than immunocompetent mice (2). In addition, Shankaran and colleagues showed that the tumor rate was even higher in RAG2-/- mice that also lacked interferon type I and type II signaling.

There are two types of immune responses: innate and adaptive. The innate immune system serves as a first line of defense and functions in the non-antigen-specific

killing of pathogens and virus-infected cells. Innate immune cells include granuloctyes, mast cells, natural killer cells, macrophages and dendritic cells (DCs). There are three types of granulocytes: neutrophils, eosinophils and basophils. Neutrophils, the most common of the granulocytes, are phagocytic cells that engulf and destroy extracellular bacteria. Eosinophils kill parasites that are coated with antibodies while basophils likely function in allergic responses. Mast cells trigger local inflammatory responses and also function in allergic responses by releasing granules that contain histamine. Natural killer cells release lytic granules that can kill some virus-infected or tumor cells. Macrophages are phagocytic cells and can also act as antigen presenting cells (APCs). APCs take up antigens and display them on their cell surface along with either major histocompatibility complex (MHC) class I or MHC class II molecules. DCs are specialized APCs whose primary role is to take up, process and present antigen to T cells, resulting in an adaptive immune response.

Unlike innate immune responses, adaptive immune responses develop slowly (over the course of days) and are antigen-specific and long-lived. The adaptive immune system was named due to the nature of the responses to adapt throughout the life of the individual due to infection and disease. The adaptive immune system consists of T and B lymphocytes. The antigen-specific receptors displayed by these cells are produced through somatic rearrangements of germline-encoded gene segments. The combinatorial assembly of multiple gene segments, plus the inexact nature of the joining process, leads to a great diversity of specificities. This diverse repertoire enables T and B lymphocytes to detect a virtually limitless array of antigens. In addition, memory T or B cells remain

after primary immune responses, leading to faster secondary responses and immune memory. It is due to the specificity and long-lived memory responses that immunotherapy is so attractive for cancer treatment.

Humoral immunity

Humoral immunity is mediated by antibodies secreted by terminally differentiated B cells. Surface immunoglobulin expressed on B cells can recognize extracellular pathogens including bacteria, fungi and parasites. B cells require two signals for activation: the binding of the antigen to the B cell receptor and an additional signal such as one from a $CD4^+$ helper T cell. Once activated, the B cell proliferates and differentiates into a plasma cell that secretes antibodies. These antibodies can bind extracellular toxins or pathogens, leading to their ingestion and destruction by macrophages or they can bind extracellular pathogens and activate complement leading to pathogen lysis or ingestion.

Cell-mediated immunity

Cell-mediated immunity in the adaptive immune system is composed of both $CD4^+$ and $CD8^+$ T cells. $CD4^+$ T cells, which include helper T cells and regulatory T cells, recognize peptides presented by MHC Class II molecules. These peptides are typically derived from the proteolysis of internalized, extracellular proteins. Regulatory T cells play a role in suppressing the immune system whereas helper T cells aid in the activation of $CD8^+$ T cells, B cells, macrophages and DCs. $CD8^+$ T cells, which

differentiate into cytotoxic T lymphocytes (CTLs), recognize peptides presented on MHC Class I, which include intracellular proteins including those produced in virus-infected cells and tumor cells. $CD8^+$ T cells kill target cells by release of cytotoxins such as perforins, granzymes and granulysins. Perforins form pores in the target cell's plasma membrane, allowing granzymes to enter the cell, leading to caspase activation and apoptosis. Granulysin leads to pore formation and apoptosis of the target cell and has antimicrobial function. Additionally, $CD8^+$ T cells can to kill cells through receptor/ligand interactions such as the binding of Fas ligand on their cell surface with Fas on the target cell. This interaction between Fas ligand and Fas leads to caspase activation and apoptosis of the target cell. The TRAIL pathway is another mechanism of receptor mediated killing by effector $CD8^+$ T cells. Since $CD8^+$ T cells can recognize and kill tumor cells, they are often the target of cancer immunotherapy approaches.

Recognition of tumors by the immune system

The adaptive immune system responds to tumor cells via recognition of tumor-specific or tumor-associated antigens. Tumor-specific antigens are only expressed by tumor cells and not by normal cells while tumor-associated antigens are differentially expressed by tumor cells versus normal cells (3). Tumor-specific antigens include proteins produced by mutations caused by carcinogens (4) and by viral proteins, such as E6 and E7 of the human papillomavirus, in viral-induced tumors (5). Examples of tumor-associated antigens include tyrosinase (6), human epidermal growth factor receptor 2 (HER2)/neu (7), prostate-specific antigen (PSA) (8) and gp100 (9).

Following tumor cell death, tumor antigens can be internalized by APCs such as DCs, which are constantly sampling the extracellular fluid. The APC can then process and present peptides derived from the antigen on MHC Class I along with co-stimulatory molecules on its cell surface. A $CD8^+$ T cell bearing a T cell receptor (TCR) specific for that MHC Class I:antigen complex can then be activated. Following activation, the $CD8^+$ T cell proliferates and differentiates into a CTL. It can then travel to the site of the tumor and release cytotoxins to kill the tumor cells that express its specific antigen. Additionally, following expansion and contraction of this particular $CD8^+$ T cell clone; memory $CD8^+$ T cells will remain and respond if the tumor recurs.

Cancer vaccines:

Vaccines have been used to prevent bacterial and viral diseases for centuries, but only in the last 30 years has their potential for cancer treatment been explored. There has been investigation into both prophylactic and therapeutic cancer vaccines. Vaccines that prevent infection with tumor-associated viruses, such as Hepatitis B virus which can lead to hepatocellular carcinoma and human papilloma virus (HPV) which causes cervical cancer, have been shown to prevent tumor occurrence (10, 11). The long-term goal of this thesis work is to improve therapeutic cancer vaccines that are aimed at curing established tumors.

There are two types of immunotherapy, passive immunotherapy and active immunotherapy. Passive immunotherapy involves the adoptive transfer of tumor-specific antibodies or immune stimulators (such as cytokines), or ex-vivo activated antigen-

specific $CD8^+$ T cells. In contrast, the goal of active immunotherapy is to activate the patient's immune system through a vaccine consisting of either tumor-specific or tumor-associated proteins/peptides, live vectors or plasmid DNA encoding tumor antigens, or tumor antigen-loaded DCs. The benefit of active over passive immunotherapy is that it results in a long-lasting memory response that can prevent tumor recurrence. It is the goal of cancer immunotherapy to elicit an adaptive immune response due to both its specificity (ability to kill tumor cells while leaving normal cells unharmed) and its longevity (ability to prevent tumor recurrence).

There are four broad categories of cancer vaccines: tumor cell lysates and derivative proteins, synthetically produced proteins and peptides, live microbial vectors and plasmid DNA (12). Examples of tumor cell vaccines include tumor-antigen loaded DCs and ex-vivo activated and expanded tumor-antigen specific $CD8^+$ T cells. Production of these DC or $CD8^+$ T cell vaccines is labor-intensive and costly. Live vector vaccines include viral and bacterial vectors and have many advantages including high transfection efficiency, high immunogenicity, large variety to choose from and the flexibility to modify the gene or genes that they encode. However, they also have a risk of toxicity, possibility of pre-existing immunity and potential for immunity toward viral proteins which can decrease their effectiveness.

Protein and peptide vaccines typically encode 8-10 linear amino acid stretches that can be detected by $CD8^+$ T cells. Protein-based vaccines can contain multiple $CD8^+$ T cell epitopes (sequences recognized by the T cell receptor) and can be used with multiple adjuvants, but they can be difficult to produce, have low immunogenicity and

often elicit better antibody than CTL responses. Peptide-based vaccines are easier to produce, can also contain multiple $CD8^+$ T cell epitopes and the epitopes can be optimized for better T cell responses. However, the T cell epitopes must first be discovered and the problem of low immunogenicity remains.

The protein and peptide group of vaccines includes antibody-based vaccines, a specific type of protein vaccine, which has shown great promise in the clinic. Antibody-based vaccines consist of antibodies that are specific for tumor antigens or block ligand binding and/or signaling of pathways critical for tumor growth including vascular endothelial growth factor (VEGF) or epidermal growth factor receptor (EGFR). Antibody-based vaccines have led to complete tumor regression in many individuals (13). Examples of this type of vaccine include Rituximab (non-Hodgkins lymphoma), Trastuzumab (breast cancer), and Cetuximab (colorectal cancer along with head and neck cancers) (14).

The final type of cancer vaccines consists of plasmid DNA that encode one or more tumor antigens. DNA vaccines are typically administered either intramuscularly or intradermally (15-18). Following vaccination, resident cells (either myocytes and DCs in the case of intramuscular vaccination or keratinocytes and DCs in the case of intradermal vaccination) take up the plasmid and express the encoded antigen (Figure 1) (19). The antigen can then be presented to $CD8^+$ T cells either directly by DCs that have been transfected with the plasmid or indirectly following the release of antigen from keratinocytes or myocytes and their uptake by and presentation on DCs. The $CD8^+$ T

cells are activated, proliferate and migrate to the site of the tumor where they release cytotoxins to specifically kill antigen-bearing target cells.

DNA plasmids have many advantages over proteins and peptides including their flexibility (easy to manipulate), ease of production, stability, ability to activate cellular and humoral immunity, ability to be administered repeatedly, low cost for production and safety (20-22). There are some limitations, however, which include transient transgene expression, low transfection efficiency and low immunogenicity. Transient transgene expression is a result of low levels of protein production and short-lived expression. *The aim of this thesis is to test approaches designed to overcome these limitations.*

Adjuvants:

Adjuvants are substances that enhance an immune response to an antigen. The need for adjuvants was discovered when it was found necessary to add killed bacteria or bacterial extracts to antigens to produce adaptive immune responses. Examples of adjuvants include bacterial components such as endotoxin or lipopolysaccharide, Complete Freund's adjuvant (an oil and water emulsion including muramyldipeptide, a component of mycobacteria) and aluminum hydroxide gel. Adjuvants function by increasing uptake by APCs, by enhancing the APCs ability to produce an immune response through increasing its antigen-presentation or through production of inflammatory cytokines.

One adjuvant is heat shock protein 70 (Hsp70). Hsp70 belongs to a highly conserved, ubiquitous superfamily of stress proteins. In 1962, Ritossa and colleagues

discovered heat shock proteins in Drosophila larvae following thermal stress (23). In the 1980's, Srivastava and colleagues tested fractions of tumor cell lysates for immunoprotective effects and found that it was the heat shock proteins that were producing these effects (24).

Hsp70 has three major functional domains: an ATPase domain, a substrate-binding domain composed of neutral, hydrophobic residues and an alpha-helical C-terminal domain which acts as lid that helps keep bound peptide in place (Figure 2). Hsp70 can be found both intracellularly and extracellularly. Intracellular Hsp70 functions in protein folding & transmembrane transport and protects cells from environmental stresses including heat, cold and oxygen deprivation (25, 26). Extracellular Hsp70 can be membrane-bound or in exosomes and either peptide-bound or free.

It is the extracellular Hsp70 that has immunostimulatory functions (Figure 3) (27). Hsp70 is a potent adjuvant that links innate and adaptive immune responses by activating and delivering peptides to APCs such as DCs. To activate T cells fully, DCs must also provide costimulatory- and cytokine-derived stimuli that result from receipt of "danger" or "stranger" signals. Hsp70 provides a strong "danger" signal to DCs that leads to protective $CD8^+$ T cell-mediated responses in models of viral and tumor immunity (28-32). Heat shock proteins have been used for immunotherapy/cancer vaccines in many types of cancer, including melanoma, renal cell carcinoma, colon cancer, chronic myelogenous leukemia, lymphoma and pancreatic cancer (33)(27). In addition, an HspE7 fusion protein vaccine (Nventa) has been produced (29, 32, 34).

Vaccination methods:

Vaccines can be administered subcutaneously, intramuscularly, intravenously or intradermally. The primary methods of vaccination for plasmid DNA vaccines are intramuscular or intradermal since the plasmid needs to be taken up by cells for the genes to be expressed. The typical procedure for intramuscular vaccination involves injection into the muscle every two weeks for a total of three immunizations. The immune response is then detected two weeks following the last vaccination, resulting in a total of six weeks for the optimal response. Since there are relatively few APCs in muscle tissue, it takes longer for a detectable immune response to occur than in other tissues such as the skin.

The skin is a barrier organ relatively rich in APCs. While intradermal vaccination still involves three immunizations, they are spaced closer together and the resultant response is quicker, typically in less than two weeks total. The most common device used for intradermal immunization is the gene gun (35)(36). A gene gun is a device that shoots gold coated particles into cells using a low pressure helium pulse. This device was designed for transformation of plant cells, but is now commonly used for delivering genetic material to all types of cells. Nanogram amounts of DNA administered using a gene gun can elicit humoral and cytotoxic T lymphocyte responses (18).

In 2005 Bins and colleagues described a DNA vaccination method that employs a tattoo device (37). The rotary tattoo device contained multiple needles, was set to a depth of 0.5mm and oscillated at 100Hz. They administered 20 μg of plasmid in 10 μl of saline

solution to a shaved hind leg. They compared antigen-specific T cell responses elicited by tattooing to responses obtained via more conventional routes of DNA vaccination such as intramuscular injection and intradermal administration via a gene gun. The responses with tattooing were similar to that achieved with the gene gun, but a tattoo device is much cheaper and easier to use. Compared to intramuscular vaccination, intradermal administration via tattooing consistently activated higher frequencies of antigen-specific $CD8^+$ T cells and it did so in a shorter time. The authors suggested the higher frequency of APCs in the skin versus the muscle and the greater surface area over which the DNA was applied, accounted for this enhanced response. They determined the optimal vaccination via this method was tattooing every three days for three immunizations and measuring the $CD8^+$ T cell response six days after the last immunization. Due to the advantages of using a tattoo device for DNA delivery, we use this method for DNA immunization.

Synthetic vehicles for DNA vaccination/Carrier proteins:

To increase the efficacy of DNA vaccines, synthetic particles have been used as carrier systems for the plasmids. For this, the DNA is either complexed with or encapsulated into the synthetic carrier producing micro- or nanoparticles. This technique has been widely used for nucleic acid delivery (38)(39)(40). Most of these complexes are formed by the electrostatic interaction between cationic carriers and anionic phosphate groups in the plasmid. This complex has numerous advantages over naked plasmid DNA including protection against endonucleases, increased cellular uptake and increased

uptake by APCs. Examples of synthetic vehicles that have been used for DNA delivery include cationic lipids, cationic polymers and non-cationic polymers such as poly(lactide) or poly(lactide-co-glycolide).

In 2007 Lawrence and colleagues described a mutant, supercharged green fluorescent protein (GFP) that had a +36 charge and increased resistance to aggregation and consequent precipitation (41). They further showed that this +36GFP bound DNA and led to DNA transfection *in vitro*. The use of this protein as a cationic carrier for DNA vaccines may increase transfection efficiency.

Thesis Statement:

Immunotherapy using DNA vaccines is a promising approach for the treatment of cancer. DNA vaccines encoding tumor antigens produce powerful anti-tumor immune responses in animal models, but clinical trials show only modest responses. Although DNA plasmids have many advantages including low cost, ease of production, flexibility and safety; they also have disadvantages, including transient protein expression and low transfection efficiency. The primary goal of this dissertation research was to overcome these barriers and thereby increase the efficacy of plasmid DNA vaccines.

Chapter 2 of this dissertation shows the prelimary DNA vaccine research necessary for the following chapters. The data show that we can produce and administer DNA vaccines and can track the resulting antigen-specific $CD8^+$ T cell responses. We have chosen to administer the vaccines intradermally using a tattoo device in order to achieve rapid and potent immune responses.

Chapter 3 of this dissertation is focused on increasing both the level and duration of protein expression following DNA vaccine immunization. Transient protein expression is likely the result of gene silencing due to transcriptionally repressive chromatin within the plasmid backbone. We overcame this by removing the bacterial backbone sequences and thereby producing a minicircle plasmid consisting of the gene expression cassette with only a few bases of the bacterial backbone. This resulted in persistent protein expression and in greater resulting immune responses.

Chapter 4 of this dissertation is focused on overcoming the low transfection efficiency previously seen with DNA vaccination. We produced cationic carriers that bind the plasmid and then increase transfection efficiency *in vitro*. Further optimization of the vaccine strategy may result in highly efficacious DNA vaccines in a clinical setting.

Figure 1. DNA vaccination and the resulting immune response (From "DNA vaccines: ready for prime time?" (9)). *This diagram shows the process of intramuscular immunization with a DNA vaccine and the resulting activation of T cells. First, the gene of interest is chosen and the plasmid is constructed. The vaccine is then administered intramuscularly. Following vaccination, myocytes and some APCs are transfected with the plasmid and express the gene of interest. There are two ways that lead to antigen presentation to $CD8^+$ T cells: either by antigen secretion from transfected myocytes (1) or by direct transfection of APCs (2). Antigen can be released in apoptotic or necrotic bodies (3) or shed (4) and then can be taken up by APCs. APCs travel through an afferent lymphatic vessel (5) into a draining lymph node (6) where they process and present the antigen to T cells (7). The activated antigen-specific $CD8^+$ T cells leave the draining lymph node via the efferent lymphatic vessel (8) and travel to the site of the tumor where they selectively kill antigen-bearing tumor cells.*

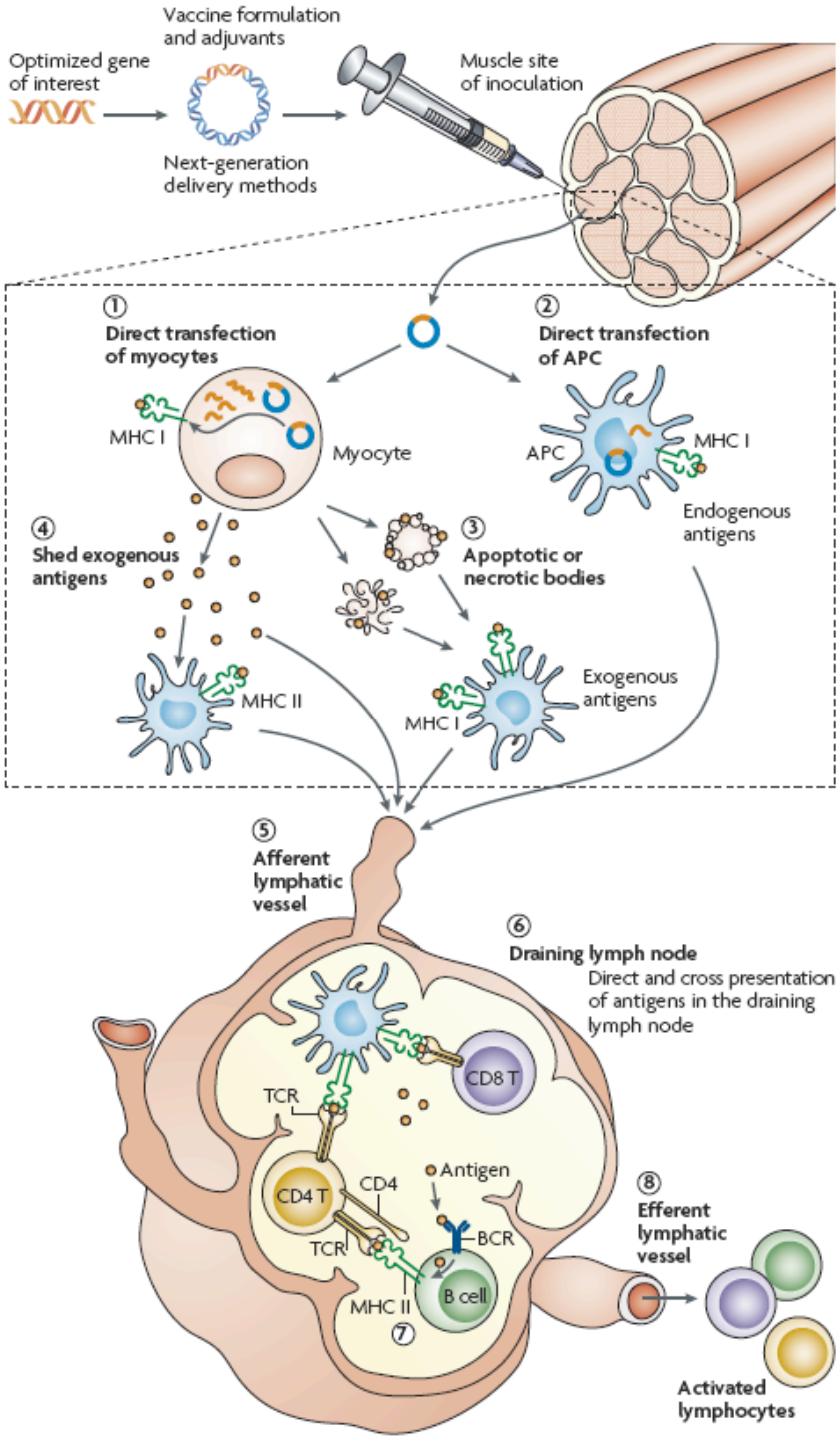
Vaccine formulation
and adjuvants
Optimized gene
of interest
Next-generation
delivery methods
Muscle site
of inoculation
① Direct transfection
of myocytes
MHC I
Myocyte
② Direct transfection
of APC
APC
MHC I
Endogenous
antigens
④ Shed exogenous
antigens
③ Apoptotic or
necrotic bodies
MHC II
MHC I
Exogenous
antigens
⑤ Afferent
lymphatic
vessel
⑥ Draining lymph node
Direct and cross presentation
of antigens in the draining
lymph node
CD8 T
TCR
CD4 T
CD4
Antigen
BCR
TCR
B cell
MHC II
⑦
⑧ Efferent
lymphatic
vessel
Activated
lymphocytes

Figure 2. Structure of heat shock protein 70 (Hsp70). *Hsp70 consists of three major functional domains, an ATPase domain, a substrate-binding domain and a α-helical domain.*

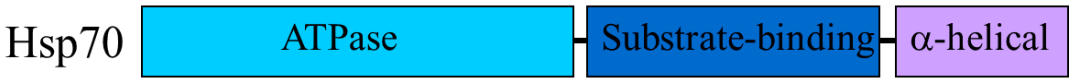
Hsp70
ATPase
Substrate-binding
α-helical

Figure 3. Immunostimulatory properties of heat shock proteins (From "Heat shock proteins as vaccine adjuvants in infections and cancer" (27)). *Heat shock proteins (Hsps) are potent adjuvants that can activate both the innate and adaptive immune systems following induction during physiological stress. Hsps can activate APCs leading to their maturation and the production of immunostimulatory cytokines. Additionally, when bound with client proteins, Hsps can deliver these proteins to the APC. These proteins are presented by MHC Class I to $CD8^+$ T cells, leading to a $CD8^+$ T cell response that is capable of killing tumor cells. In addition, Hsps can activate natural killer (NK) cells which also have the ability to lyse tumor cells.*

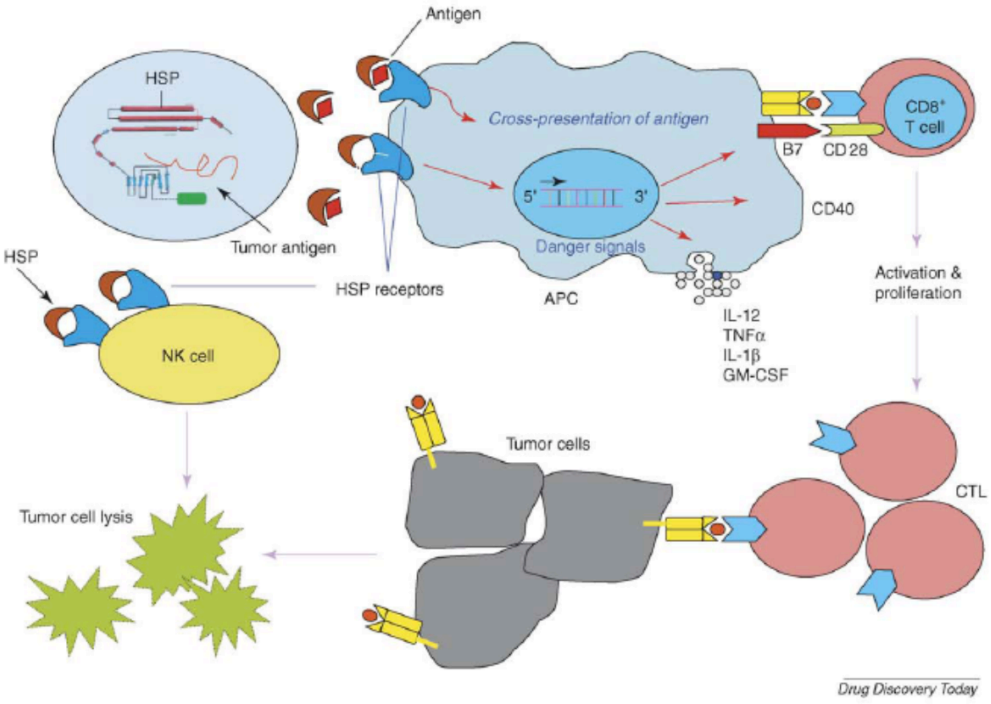
Antigen
HSP
Cross-presentation of antigen
CD8+
T cell
B7
CD28
5'
3'
CD40
Tumor antigen
Danger signals
HSP
HSP receptors
APC
Activation &
proliferation
IL-12
TNFα
IL-1β
GM-CSF
NK cell
Tumor cells
CTL
Tumor cell lysis
Drug Discovery Today

Chapter 2:

Transdermal Delivery of Plasmid DNA Elicits Antigen-Specific $CD8^+$ T cell Responses

DNA vaccines encoding tumor antigens produce powerful anti-tumor immune responses in animal models, but clinical trials show only modest responses. Although DNA plasmids have many advantages including low cost, ease of production, flexibility and safety, they also have disadvantages, including low transfection efficiency, transient protein expression and low immunogenicity. These barriers must be overcome to increase the efficacy of plasmid DNA vaccines. To this end, we produced a series of DNA plasmids designed to elicit antigen-specific $CD8^+$ T cell responses. The plasmids encoded the potent immune adjuvant heat shock protein 70 (Hsp70), a secretion sequence and several model antigens. The plasmids were delivered transdermally using a tattoo device. We found that the DNA plasmids led to protein production *in vitro* and *in vivo* and led to functional antigen-specific $CD8^+$ T cell responses. One immunization was as effective as multiple immunizations and the secretion sequence did not appear to enhance the resulting immune response. These plasmids will serve as the foundation for future plasmid DNA-based vaccines.

Introduction:

Vaccines have been used to prevent bacterial and viral diseases for over a century, but only in the last 30 years have their potential for cancer treatment been explored. This delay reflects the difficulties in producing potent immune responses against self-tumor

antigens and the immunosuppressive nature of cancer. Over the past several decades, our understanding of tumor immunity has evolved to the point where the development of prophylactic and therapeutic cancer vaccines are now a reality (10)(42).

Our goal is to produce vaccines that can elicit $CD8^+$ T cell responses against tumor-associated and tumor-specific antigens. $CD8^+$ T cells recognize peptides presented on MHC Class I molecules, which include intracellular proteins produced in virus-infected cells and tumor cells. Activated $CD8^+$ T cells differentiate into cytotoxic T cells that kill target cells by release of cytotoxins such as perforins, granzymes and granulysins and through cell contact via the Fas and TRAIL death pathways. Therefore, $CD8^+$ T cells play a critical role in anti-tumor immune responses. Our long term goal is to optimize anti-tumor vaccines to produce potent and long-lived immune responses capable of rejecting spontaneous tumors and preventing tumor recurrence.

This chapter describes our initial efforts to produce and characterize plasmid DNA (pDNA) vaccines. pDNA vaccines have several advantages over protein/peptide vaccines including low cost, ease of production and manipulation, high stability and low toxicity (20-22). DNA vaccines are typically administered intramuscularly or intradermally (15-18). Following vaccination, resident cells (e.g. myocytes or keratinocytes) take up the plasmid and express the encoded antigen. The antigen can then be presented to $CD8^+$ T cells either directly by antigen presenting cells (APCs) that have been transfected with the plasmid or indirectly following the release of antigen from keratinocytes or myocytes and their subsequent uptake by and presentation on APCs.

The $CD8^+$ T cells are activated, proliferate and migrate to the site of the tumor where they can specifically kill antigen-bearing target cells.

We constructed a series of plasmids that all encoded the same three peptides: two were derived from chicken ovalbumin (OVA) and the third was derived from the mouse MHC class II molecule, I-Eα. All three epitopes were chosen due to the availability of mice bearing the transgenic T cell receptors (TCR) that recognize the peptides presented by $H\text{-}2^b$ molecules. OT-I and OT-II mice bear TCRs that specifically recognize the OVA peptides 257-264 and 323-339 presented by K^b and $I\text{-}A^b$, respectively (43, 44). TEa mice bear a TCR specific for the mouse I-Eα 52-68 peptide presented by $I\text{-}A^b$ (45). In addition, there are antibodies specific for the OT-I and I-Eα peptides presented by K^b and $I\text{-}A^b$, respectively (46, 47). Collectively these peptides will enable us to track peptide presentation by APCs and antigen-specific T cell responses for both $CD4^+$ and $CD8^+$ T cells.

In an effort to elicit a powerful immune response, the DNA vaccines included a gene encoding the adjuvant heat shock protein 70 (Hsp70). Heat shock proteins (Hsps) are intracellular chaperones, some of which protect cells from chemical and physical stress (25, 26). Several Hsps, including Hsp70, are also potent immunostimulants (29, 32, 48, 49). Following stress or necrotic cell death, Hsps and their client proteins are released from the cell and may be subsequently bound by receptors on APCs. This can lead to the cross-presentation of client protein-derived peptides on MHC class I molecules and the activation of antigen-specific $CD8^+$ T cells that mature into cytolytic

effectors. The net result is a protective $CD8^+$ T cell response in animal models of viral and tumor immunity (28-32)(50).

Finally, we chose to deliver the plasmid DNA to the skin instead of intramuscular injection. The skin is a barrier organ relatively rich in APCs whereas the muscle has very few APCs. Additionally, while both intradermal and intramuscular vaccination typically require three immunizations, they are spaced closer together and the resultant response is much quicker with intradermal immunization, typically in less than two weeks versus six weeks or more via the intramuscular route (37).

The most common device used for intradermal immunization is the gene gun (34-35). A gene gun is a device that shoots gold coated particles into cells using a low pressure helium pulse. This device was designed for transformation of plant cells, but is now commonly used for delivering genetic material to all types of cells. Nanogram amounts of DNA administered using a gene gun can elicit humoral and cytotoxic T lymphocyte responses (18).

However, in 2005 Bins and colleagues described a new DNA vaccination method that employs a tattoo device for transdermal delivery (37). They compared antigen-specific T cell responses elicited by tattooing to responses obtained via intramuscular injection and intradermal administration via a gene gun. The responses with tattooing were similar to that achieved with the gene gun, but a tattoo device is less expensive and easier to use. Compared to intramuscular vaccination, intradermal administration via tattooing consistently activated higher frequencies of antigen-specific $CD8^+$ T cells and it

did so in a shorter time. Due to the advantages of using a tattoo device for DNA delivery, we chose this method for DNA immunization.

We show that transfection with plasmid DNA results in protein production and secretion (with the encoded secretion sequence) and it elicits functional antigen-specific $CD8^+$ T cell responses. Furthermore, we show that addition of the secretion sequence does not enhance the resulting immune response and that one immunization results in an equivalent immune response to two or three immunizations. Future work will include characterizing the $CD4^+$ T cell response and antigen presentation by DCs following plasmid administration.

Materials and Methods:

DNA constructs. The plasmids were constructed in the pcDNA3.1(+) backbone (Invitrogen, Carlsbad, CA) which contains the cytomegalovirus (CMV) promoter for expression in mammalian cells. A codon-optimized insert was synthesized (GenScript, Piscataway, NJ) to encode a Kozak consensus sequence, a signal sequence, a 10x histidine (His) tag and mouse heat shock protein 70 (Hsp70), and was inserted into the *Nhe*I and *Pme*I sites in pcDNA3.1(+). The resultant plasmid was designated pWMD1S. A double stranded oligonucleotide with NheI and SwaI compatible 5' and 3' ends, respectively, was synthesized to encode the Kozak consensus sequence and a 10x His tag. This oligonucleotide was cloned into pWMD1S restricted with NheI and SwaI, thereby removing the signal sequence and creating pWMD1. A cassette encoding green fluorescent protein (dGFP), a Gly_4Ser linker, and three model peptides was codon-

optimized for expression in mouse cells, synthesized (GenScript), and subcloned from a separate vector into pWMD1S and pWMD1 to form pWMD2S and pWMD2, respectively.

All plasmids were transformed into Mach1 *E. coli* cells (Invitrogen). Transformed bacteria were grown in LB-broth (Invitrogen) supplemented with ampicillin. Plasmids were isolated with the PureLink HiPure Filter Plasmid Purification Maxiprep kit (Invitrogen) according to the manufacturer's instructions. Following elution in water, the plasmids were concentrated to 4-6 μg/μl by ethanol precipitation, resuspended in water and stored at -20°C. All constructs were sequence verified.

Cell lines and transfections. HEK293T cells (a gift from the Polunovsky lab at the University of Minnesota, Minneapolis, MN) were maintained in complete Dulbecco's modified Eagle's medium (Invitrogen) supplemented with 10% fetal bovine serum (Invitrogen) at 37°C with 5% CO_2. Adherent cells were dissociated from tissue culture flasks with TrypLE Express (Invitrogen) and plated in 6 well tissue culture-treated plates (BD Biosciences, San Jose, CA) at equal numbers (2-5 x 10^5 cells) per well without antibiotics. The following day cells were transfected with 4 μg per well of pWMD2 or pWMD2S using Lipofectamine 2000 (Invitrogen) according to the manufacturer's protocol. Cells were harvested 24 to 48 hours later for flow cytometry and Western blot analyses.

Western blot analysis. HEK293T cells were transfected with pWMD2 or pWMD2S and two days later the cells and supernatants were harvested. The cells were lysed using RIPA lysis buffer (Millipore, Billerica, MA) and the proteins within the cell lysate (and supernatant) were purified over His SpinTrap columns from GE Healthcare (Piscataway, NJ) and eluted according to the manufacturer's protocol. The samples were denatured using sodium dodecyl sulfate (SDS), run on NuPAGE 4-12% Bis-Tris gradient gels (Invitrogen), transferred to Hybond-ECL nitrocellulose membranes (GE Healthcare) and probed using anti-His-HRP from AbD Serotec (Raleigh, NC).

Flow cytometry analysis of 293T cells. HEK293T cells were transfected with pWMD2 or pWMD2S and 24 hours later the cells were harvested and analyzed for GFP expression by flow cytometry on a BD FACSCalibur flow cytometer (BD Biosciences) using BD CellQuest Pro software (BD Biosciences) and analyzed with FlowJo software (Tree Star, Inc., Ashland, OR).

Mice. Four to eight week old female C57BL/6 mice were purchased from the Jackson Laboratory (Bar Harbor, ME) or the National Cancer Institute (Frederick, MD). C57BL/6-Tg(TcraTcrb)1100Mjb/J (OT-I) Thy1.1^{+}/Thy1.2^{+} mice were a generous gift from Dr. Stephen Jameson at the University of Minnesota (Minneapolis, MN). All mice were housed under specific pathogen free-conditions at the University of Minnesota (Minneapolis, MN). All animal procedures were carried out according to protocols approved by the Institutional Animal Care and Use Committee.

OT-I adoptive cell transfer. All work was carried out under asceptic conditions using sterile reagents. OT-I mice were euthanized and lymph nodes were harvested. Single cell suspensions were prepared and cells were washed in phosphate buffered saline (PBS) supplemented with 2% (v/v) fetal bovine serum (Invitrogen). Cells were counted and analyzed by flow cytometry to determine the percentage and number of OT-I cells. Antibodies used were CD44-FITC, B220-PE, and CD8α-APC (eBiosciences, San Diego, CA) and Thy1.1-PerCP (BD Pharmingen, San Diego, CA). The OT-I phenotype was $B220^{-}CD8^{+}Thy1.1^{+}$. Additionally, the OT-I cells were $CD44^{low}$, indicating they were naïve at the time of transfer. To determine the cell count, PKH26 Reference Beads (Sigma-Aldrich, St. Louis, MO) were mixed with cells; 5,000 bead events were collected on the flow cytometer. The following equation was used to determine the number of lymphocytes: # cells/ml = (# cells acquired x dilution factor of cells x # singlet beads/ml) / (# beads acquired x dilution factor beads). Cell counts were verified manually using a hemocytometer. Data were acquired on a BD FACSCalibur flow cytometer (BD Biosciences) using BD CellQuest Pro software (BD Biosciences) and analyzed with FlowJo software (Tree Star, Inc.). Cells were washed in PBS with 1% (v/v) fetal bovine serum and then in PBS before being resuspended at 10^7 cells/ml in PBS. 10^6 cells were transferred into each anesthetized mouse via retro-orbital injection using 1ml tuberculin syringes and 27 gauge needles.

DNA immunizations. Mice were anesthetized and their inner hind legs were shaved and wiped with 70% ethanol. The mice were immunized with 40 μg of plasmid DNA in 10-15 μl volumes on the indicated days. The plasmids were delivered transdermally using a Cheyenne Hawk PU II tattoo device (Unimax Supply Co. Inc., New York, NY) set at 110 Hz using 9-point needles. The needle was adjusted to a depth of 0.5mm. DNA was delivered over an area of approximately $1cm^2$ for 30 seconds.

$CD8^+$ T cell proliferation and function assays. Mice were adoptively transferred with 10^6 OT-I cells on -d1 and immunized with DNA using a tattoo device on d0, d3 and d6. Splenocytes and the draining inguinal lymph nodes were harvested on d12 and analyzed by flow cytometry for percentages of OT-I cells ($B220^-CD8^+Thy1.1^+$). Functionality was assessed by IFN-γ production following a brief exposure of cells to antigen *in vitro*. Splenocytes were incubated with or without 1μM SIINFEKL for 4 hours at 37°C and then examined for extracellular expression of CD8 and Thy1.1 (to identify OT-I cells) and intracellular expression of IFN-γ using BD Cytofix/Cytoperm kit (BD Biosciences). Data were acquired on a BD FACSCalibur flow cytometer (BD Biosciences) using BD CellQuest Pro software (BD Biosciences) and analyzed with FlowJo software (Tree Star, Inc.).

Statistical analysis. All statistical analyses were performed by the unpaired two-tailed Student's *t*-test unless noted otherwise.

Results:

DNA plasmid construction:

As a first step towards developing potent plasmid DNA-based cancer vaccines, we constructed a series of vectors encoding model antigens with and without a signal sequence for secretion. The parental plasmid was pcDNA3.1(+), which contains the CMV promoter to drive expression in mammalian cells (Figure 1). This plasmid is commonly used for DNA vaccines as the CMV promoter leads to high levels of protein production. All of our constructs include a Kozak consensus sequence upstream of the start codon for optimal eukaryotic translation initiation. Two constructs (pWMD1S and pWMD2S) include a signal sequence (called a secrecon) to permit protein secretion (51). A secretion sequence was included since the Haanen group found that ~99% of the cells transfected with a DNA plasmid using transdermal delivery were keratinocytes and only ~1% of the transfected cells were Langerhans cells, a type of dendritic cell (78). We reasoned that secretion by keratinocytes would permit more protein to be internalized and presented by APCs, leading to a more powerful immune response than if protein release by keratinocytes was solely due to cell death. All plasmids were sequence verified (data not shown).

The plasmids include two methods of detection, a 10X histidine (His) tag used both for detection and purification, and a modified green fluorescent protein (dGFP) for detection. The 10X His tag and dGFP enable both easy purification and easy detection *in vitro*. There are three peptides encoded in the plasmids: two are derived from chicken ovalbumin (OVA) and one from the mouse MHC class II molecule I-Eα. In addition,

murine Hsp70, a potent immune adjuvant, is fused to the carboxy terminus of the peptide cassette. Hsp70 is a commonly used immune adjuvant that has been shown to produce potent $CD8^+$ T cell responses (49)(52).

Production and secretion of plasmid-encoded proteins:

Following plasmid production and purification, HEK293T cells were transfected with pWMD2 or pWMD2S and both the cells and supernatant were harvested 48 hours later. The proteins were purified from the cell lysate and supernatant using His-tag purification and Western blots were performed using His-tag detection antibodies (Figure 2A). The protein was produced but not secreted following transfection with pWMD2 (which lacks the secretion sequence) as evidenced by an immunoreactive protein in the cell lysate sample but not in the supernatant. An immunoreactive protein was detected in the supernatant, but not in the cell lysate, of HEK293T cells transfected with pWMD2S (which includes the secretion sequence). The lack of a detectable immunoreactive protein in the cell lysate may be due to the rapid secretion of the protein. We conclude the protein is expressed and that the His tag and signal sequence are functional.

Next, HEK293T cells were transfected with either pWMD2 or pWMD2S and analyzed by flow cytometry 24 hours later. As Figure 2B shows, about 8% of the pWMD2S-transfected cells were GFP+ whereas 29% of the pWMD2-transfected cells were GFP+. We speculate that the lower percentage of GFP+ cells within the pWMD2S-transfected cells is due to protein secretion. We conclude the GFP within the protein is also functional as detected by fluorescence using flow cytometry.

Immunization strategy:

To detect the antigen-specific $CD8^+$ T cell response following DNA plasmid administration, an OT-I adoptive transfer system was used (Figure 3). The $CD8^+$ T cells in OT-I mice bear a transgenic TCR specific for the SIINFEKL peptide (aa 257-264 in OVA) when presented by the MHC class I molecule H-$2K^b$ (43). This peptide is the $CD8^+$ T cell epitope of OVA contained in the pWMD2 and pWMD2S plasmids. OT-I/PL mice express the OT-I TCR and the Thy1.1 allelic marker. $CD8^+$ OT-I (Thy1.1) cells adoptively transferred into C57BL/6 mice can be distinguished from host $CD8^+$ T cells (Thy1.2) based on this allelic difference.

C57BL/6 mice were adoptively transferred with 10^6 OT-I/PL cells one day prior (-d1) to immunization. On d0, d3 and d6 the mice were immunized transdermally on the left hind leg with 40 μg plasmid DNA using a rotary tattoo device containing an 8-prong needle. The DNA administration on d0, d3 and d6 was chosen based on optimization by the Hannen group (53). On d12, the mice were sacrificed, the spleens harvested and antigen-specific OT-I cell responses were measured.

Expansion of antigen-specific $CD8^+$ T cells following immunization:

Following validation that the plasmids produced protein and that the protein was secreted, we tested the immunogenicity of the plasmid-encoding OT-I epitope. Following adoptive transfer of equal numbers of OT-I cells on -d1, mice were immunized with either a control or pWMD2S on d0, d3 and d6. On d12, splenocytes were harvested

and stained with fluorescently labeled antibodies for CD8, Thy1.1 and B220 (a marker used to exclude B cells). The number of OT-I cells ($CD8^+Thy1.1^+B220^-$) was quantitated by flow cytometry. As seen in Figure 4, immunization with pWMD2S led to significantly greater numbers and percentages of antigen-specific $CD8^+$ T cells than immunization with PBS or the vector control. pWMD2S immunization resulted in a greater than 3.5 fold increase in OT-I cells compared to the controls, showing the immunogenicity of this vaccine.

Effect of the secretion sequence on the resultant immune response and the functional ability of the activated $CD8^+$ T cells:

Because our goal is not only to establish a system in which to test DNA vaccines, but also to begin vaccine optimization, we next compared the plasmids with and without the secretion sequence. C57BL/6 mice were adoptively transferred with equal numbers of OT-I cells on –d1 and immunized on d0, d3 and d6 with a control vector, pWMD2 or pWMD2S using a tattoo device. On d12, OT-I cells were identified by their expression of CD8 and the allelic marker Thy1.1. The proliferative responses of OT-I cells were similar in mice immunized with either pWMD2 or pWMD2S (~0.6% and ~0.7% of $CD8^+$ T cells, respectively), with the percentage slightly higher for pWMD2S-immunized mice (Figure 5A). We conclude that the secretion sequence does not have a significant effect on the resulting $CD8^+$ T cell response.

To assess their functionality, we briefly stimulated OT-I cells *in vitro* with their cognate antigen, SIINFEKL peptide presented by $H\text{-}2K^b$, and examined them for IFN-γ

expression (an effector cytokine) by intracellular staining followed by flow cytometry analysis. The resultant antigen-specific $CD8^+$ T cells are functional as shown by the significant increase in intracellular staining for IFN-γ following peptide stimulation (Figure 5B).

Effect of the number of immunizations on the $CD8^+$ T cell response:

Finally, we asked if three immunizations were required for the optimal OT-I T cell response, as reported for endogenous $CD8^+$ T cell responses elicited by plasmid DNA immunization via tattooing (53). For this, we immunized mice one, two or three times and compared the resulting T cell responses. C57BL/6 mice were adoptively transferred with equal numbers of OT-I cells on -d1 and immunized either once (on d0) or twice (on d0 and d3) with pWMD2S. Six days after the last immunization, OT-I cells were identified by flow cytometry. The proliferative responses of OT-I cells in mice immunized with one or two immunizations were similar (~0.45% and ~0.4% of $CD8^+$ T cells, respectively) (Figure 6). Additionally, this is not significantly different than the percentage of OT-I cells from three immunizations, suggesting that one immunization is sufficient.

Discussion:

The goal of these studies was to establish a platform in which to optimize DNA vaccines for cancer therapy. For this, we addressed both the plasmid DNA vaccine components and the route/strategy for administration of the vaccine. These studies show

that the DNA plasmids encode functional proteins expressed both *in vitro* and *in vivo*. We validated functional expression of the His-tag via immobilized metal ion affinity chromatography and detection using a specific monoclonal antibody. Inclusion of the signal sequence permitted expression of a secreted protein. Finally, expression of plasmid-encoded GFP was detected by flow cytometry.

We evaluated the immunogenicity of the plasmids by adoptively transferring congenically marked antigen-specific $CD8^+$ T cells into C57BL/6 mice and tracking the cell expansion following immunization. The frequency of antigen-specific $CD8^+$ T cells following plasmid immunization increased significantly and these cells were functional as measured by their ability to produce IFN-γ following a brief antigen pulse *in vitro*. The secrecon signal led to the secretion of proteins *in vitro*, but there was no significant difference in the resulting $CD8^+$ T cell response *in vivo*. This suggests that secretion is not necessary.

Recently, directly transfected $langerin^+$ dermal DCs and dermal DCs have been shown to be responsible for $CD8^+$ T cell activation following intradermal DNA administration, with $langerin^+$ dermal DCs playing the primary role (54). Consequently, proteins produced in transfected keratinocytes may not be necessary for the resulting $CD8^+$ T cell response, making protein secretion unnecessary.

Finally, we compared one, two and three immunizations and found that one immunization is sufficient for a significant OT-I T cell response. The sufficiency of one immunization may be due to the increased frequency of precursor antigen-specific $CD8^+$

T cells as a result of the adoptive transfer. Future work will include comparing the endogenous $CD8^+$ T cell response following one or multiple immunizations.

Following transdermal DNA administration using a tattoo device, 0.4% to 0.7% of the $CD8^+$ T cells in the spleen were OT-I cells. Bins and colleagues found that ~5% of the $CD8^+$ T cells in the peripheral blood were specific for the influenza A nucleoprotein epitope (NP) at the peak of the response following DNA tattoo administration (53). The lower percentage of resulting OT-I cells than NP-specific $CD8^+$ T cells may be due to differences in immunogenicity of the encoded proteins, differences in the adjuvants used, differences in the plasmids or differences in the kinetics of the responses.

We chose to use the OT-I adoptive transfer system versus tracking endogenous responses since we have previous experience with this system and the reagents were readily available. Future work will include tracking endogenous responses to OVA, examining responses to the OT-II and I-Eα epitopes encoded in the plasmids and using tumor models to examine the resulting anti-tumor response. The OT-II epitope will be used to examine the $CD4^+$ T cell response to DNA vaccination. Both the OT-I epitope and I-Eα epitopes will be used to determine antigen presentation by DCs following transdermal delivery of the pDNA. Additionally, OVA-expressing tumors can be used to examine the anti-tumor immune response following DNA vaccination.

In conclusion, the plasmids were made successfully and immunization via a tattoo device resulted in functional antigen-specific $CD8^+$ T cell responses. This DNA vaccine platform is now ready to be used for vaccine optimization. Future directions for

this work include the optimization of DNA vaccines by overcoming transient protein expression (Chapter 3) and by increasing transfection efficiency (Chapter 4).

Figure 1. pWMD plasmid constructs. *We produced the pWMD series of plasmids in pcDNA3.1(+) which contains the CMV promoter. Kozak – sequence for eukaryotic translation initiation; SS – secrecon signal sequence for secretion; 10xHis – detection tag; dGFP – detection; Linker – flexible linker; Antigen – encodes OT-I and OT-II epitopes of ovalbumin and mouse I-Ea derived peptides; Mhsp70 – murine Hsp70: an adjuvant. A. Cloning strategy and representation of plasmid inserts. B. Sequences of vaccine components. C. Diagram of pWMD2S. D. Nucleotide sequence of insert in pWMD2S (cloned in between the NheI/PmeI sites in pcDNA3.1+).*

A.

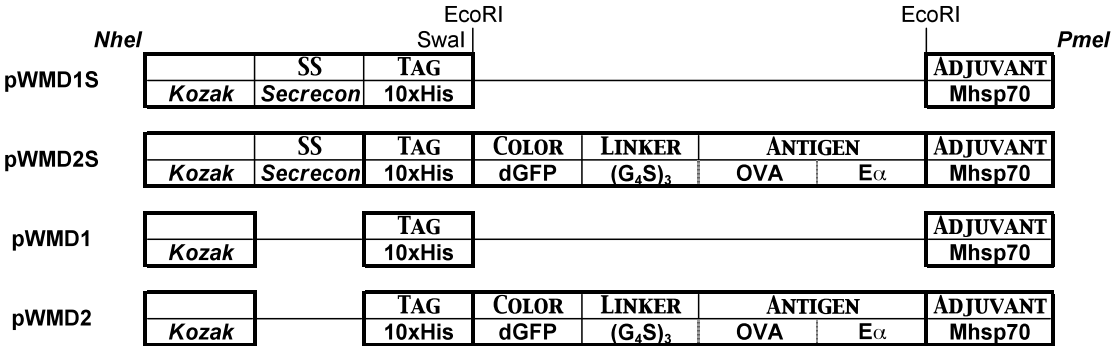

pWMD1S: The Kozak/SS/Tag/Adjuvant insert was codon optimized by GenScript for expression in mouse cells and inserted into the NheI/PmeI sites contained within pcDNA3.1(+).

pWMD2S: The Color/Linker/Antigen cassette was codon optimized by GenScript for expression in mouse cells and was subcloned from a separate vector into pWMD1S as an EcoRI fragment.

pWMD1: A double stranded oligonucleotide with NheI and SwaI compatible 5' and 3' ends, respectively, was synthesized to encode the Kozak consensus sequence and a 10xHis tag. This oligonucleotide was cloned into pWMD1S restricted with NheI and SwaI, thereby removing the secrecon signal sequence.

pWMD2: The Color/Linker/Antigen cassette was codon optimized by GenScript for expression in mouse cells and was subcloned from a separate vector into pWMD1 as an EcoRI fragment.

B.

Kozak: gccgccaccatg

Secrecon (51) : MWWRLWWLLLLLLLLWPMVWA

dGFP:
MSKGEELFTGVVPVLVELDGDVNGQKFSVSGEGEGDATYGKLTLNFICTTGKLP
VPWPTLVTTFSYGVQCFSRYPDHMKQHDFFKSAMPEGYVQERTIFYKDDGNYK
TRAEVKFEGDTLVNRIELKGIDFKEDGNILGHKMEYNYNSHNVYIMGDKPKNGI
KVNFKIRHNIKDGSVQLADHYQQNTPIGDGPVLLPDNHYLSTQSALSKDPNEKR
DHMILLEFVTAARITHGMDELYK

OVA epitopes: (OT-I = $OVA_{257-264}$; OT-II = $OVA_{323-339}$) epitopes in bold face.
Other residues are naturally occurring flanking amino acids included to facilitate antigen processing.
GLEQLE**SIINFEKL**TEWTSSSSAESLK***ISQAVHAAHAEINEAGR***EVVGSAE

Ea epitope: EEFAKF**ASFEAQGALANIAVDKA**NLDVME

Mhsp70: M A K N T A I G I D L G T T Y S C V G V F Q H G K V E I I A N D Q G N
R T T P S Y V A F T D T E R L I G D A A K N Q V A L N P Q N T V F D A K R L I
G R K F G D A V V Q S D M K H W P F Q V V N D G D K P K V Q V N Y K G E S
R S F F P E E I S S M V L T K M K E I A E A Y L G H P V T N A V I T V P A Y F N
D S Q R Q A T K D A G V I A G L N V L R I I N E P T A A A I A Y G L D R T G K
G E R N V L I F D L G G G T F D V S I L T I D D G I F E V K A T A G D T H L G G
E D F D N R L V S H F V E E F K R K H K K D I S Q N K R A V R R L R T A C E R
A K R T L S S S T Q A S L E I D S L F E G I D F Y T S I T R A R F E E L C S D L F
R G T L E P V E K A L R D A K M D K A Q I H D L V L V G G S T R I P K V Q K L
L Q D F F N G R D L N K S I N P D E A V A Y G A A V Q A A I L M G D K S E N V
Q D L L L L D V A P L S L G L E T A G G V M T A L I K R N S T I P T K Q T Q T F
T T Y S D N Q P G V L I Q V Y E G E R A M T R D N N L L G R F E L S G I P P A P
R G V P Q I E V T F D I D A N G I L N V T A T D K S T G K A N K I T I T N D K G
R L S K E E I E R M V Q E A E R Y K A E D E V Q R D R V A A K N A L E S Y A F
N M K S A V E D E G L K G K L S E A D K K K V L D K C Q E V I S W L D S N T
L A D K E E F V H K R E E L E R V C S P I I S G L Y Q G A G A P G A G G F G A
Q A P P K G A S G S G P T I E E V D

C.

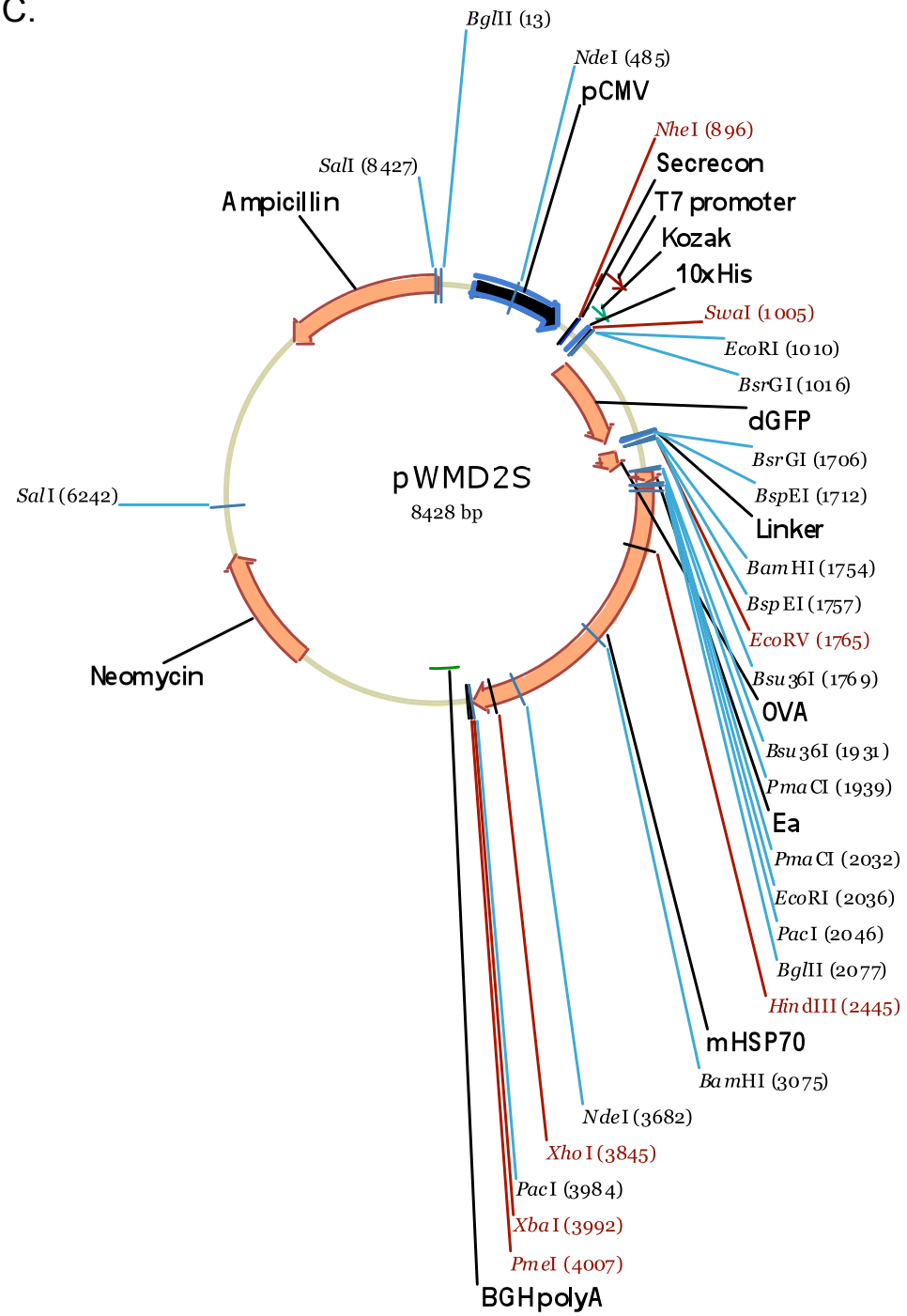
pWMD2S
8428 bp
BglII (13)
NdeI (485)
pCMV
NheI (896)
Secrecon
T7 promoter
Kozak
10xHis
SwaI (1005)
EcoRI (1010)
BsrGI (1016)
dGFP
BsrGI (1706)
BspEI (1712)
Linker
BamHI (1754)
BspEI (1757)
EcoRV (1765)
Bsu36I (1769)
OVA
Bsu36I (1931)
PmaCI (1939)
Ea
PmaCI (2032)
EcoRI (2036)
PacI (2046)
BglII (2077)
HindIII (2445)
mHSP70
BamHI (3075)
NdeI (3682)
XhoI (3845)
PacI (3984)
XbaI (3992)
PmeI (4007)
BGHpolyA
Neomycin
SalI (6242)
SalI (8427)
Ampicillin

D.

gctagcgccgccaccatgtggtggcggctctggtggcttcttttgctgctcctgcttctgtggcccatggtgtgggcac
accatcaccatcaccatcatcaccaccatttaaatgaattctgtacaatgaaggggtgaaggaagtaatgaagatca
gtctggagatggactgcactgttaacggcgacaaatttaagatcactggggatggaacaggagaaccttacgaagga
acacagactttacatcttacagagaaggaaggcaagcctctgacgttttctttcgatgtattgacaccagcatttcagtat
ggaaaccgtacattcaccaaatacccaggcaatataccagacttttcaagcagaccgtttctggtggcgggtatacct
gggagcgaaaaatgacttatgaagacgggggcataagtaacgtccgaagcgacatcagtgtgaaaggtgactctttc
tactataagattcacttcactggcgagtttcctcctcatggtccagtgatgcagaggaagacagtaaaatgggagccat
ccactgaagtaatgtatgttgacgacaagagtgacggtgtgctgaagggagatgtcaacatggctctgttgcttaaag
atggccgccatttgagagttgactttaacacttcttacatacccaagaagaaggtcgagaatatgcctgactaccatttta
tagaccaccgcattgagattctgggcaacccagaagacaagccggtcaagctgtacgagtgtgctgtagctcgctatt
ctctgctgcctgagaagaacaagtgtacatccggaggaggaggaagcggaggaggaggcagcggaggaggag
gatccggagatatcctgaggggcctggagcagctggagtcgatcatcaacttcgagaagttgaccgagtggacctc
ctccagcagcgccgagagcctgaagattagccaggccgtgcacgccgcccacgctgagattaacgaggccggcc
gcgaggtggtgggaagtgctgagtccctgaggcacgtggaggagtttgccaagttcgcctccttcgaggcccaggg
cgccctggccaacatcgccgtggataaggccaacctggatgtgatggagcacgtggaattcttaattaatatggccaa
gaacactgctattggcatagatctgggaactacatattcttgcgtgggcgtctttcaacacggaaaggtcgagattatcg
ccaacgatcagggtaatcgaacaacacctagctacgtcgcattcaccgacacagagcgtctcatcggagacgcagc
caagaaccaggtggccctcaatccccagaatacagtgtttgatgccaagcgcctcatcgggcgcaagtttggagatg
ctgtggttcagtcagacatgaagcattggcccttccaagtggtgaacgatggcgacaaaccaaaggtccaggtcaac
tacaaaggcgagtctcggagcttcttccccgaggaaattagcagcatggtgctcacaaagatgaaggagatagccg
aagcttatttgggccatcccgtcaccaacgcagtgatcaccgtgcctgcctattttaacgattcccaaagacaggctact
aaggatgccggcgtgatcgccggactcaacgtgctgagaatcatcaacgagcctacagccgccgccatcgcctac
ggattggaccggacagggaaaggcgagcgtaatgtcctgatattcgacctcggaggtgggactttcgatgtcagcat
cctcactatagacgatggaatttttgaggtgaaggccaccgctggggatactcatctgggaggcgaggacttcgataa
cagactggtcagtcatttcgtcgaggagttcaagcgaaaacacaaaaaagacatcagtcaaaacaaacgcgccgtc
cggcgtctgcgcaccgcctgtgagagggctaagagaaccctgagcagttccacccaggcaagccttgaaatcgata
gtctgtttgagggcatcgacttctatacatccataacaagggctcgattcgaggagctgtgtagcgacctgttcagggg
aacactggaaccagtggagaaggccctgagagacgccaaaatggacaaggctcagattcacgacctggtcctggt
gggcggaagtactcggatccccaaggtgcagaagctccttcaggatttcttcaacggacgcgacctcaacaagtcta
tcaatcctgatgaggccgtggcatacggcgcagccgtgcaagcagcaatactcatgggagacaagagcgagaacg
tgcaggacctgctgctgctggatgtggcccccctgtcactcggactcgaaacagccgggggcgtgatgactgccct
gatcaagcgaaattctaccattccgaccaagcagactcagacattcacaacctactcagataaccagccaggcgtgct
gatccaggtgtacgaaggagagagagcaatgactagggacaacaacctgctgggcagattcgagctctccggcat
ccctccagctcctcggggagttcctcagattgaggtgacttttgacatcgacgcaaacggtattttgaacgttaccgcta
ccgataagtctaccggcaaggccaacaaaattaccataactaatgataaggggcggttgagtaaggaggagatcga
gcgaatggtgcaggaagctgagagatacaaggctgaggatgaggtccagcgcgaccgggtggcagccaagaac
gccctcgaatcatatgcctttaacatgaaatcagctgtggaagatgaaggcctgaaagggaagctctccgaggccga
taagaaaaaggtgctggataagtgtcaggaagtgattagttggttggatagcaataccctggccgataaggaggaatt
tgtgcacaagagggaggaactcgagagagtctgcagtcccatcatcagtgggctctatcagggtgctggcgctccc
ggggccggaggcttcggggcccaagctccccccaaaggtgcctccggctccgggccaaccatcgaggaggtgg
attgattaattaactgatctaga

Figure 2. Protein expression and secretion in 293T cells. HEK293T cells were transfected with pWMD2 or pWMD2S and the cells and supernatant were harvested either 24 (B) or 48 (A) hours later. A. Western blot using anti-His-HRP 48 hours after transfection. Proteins were first purified by means of the His tag. Lane 1: Cells transfected with pWMD2. Lane 2: Supernatant from cells transfected with pWMD2. Lane 3: Cells transfected with pWMD2S. Lane 4: Supernatant from cells transfected with pWMD2S. B. Flow cytometry contour plots of control cells or cells transfected with pWMD2 or pWMD2S 24 hours prior to analysis (expression of GFP-containing proteins).

A. 1 2 3 4

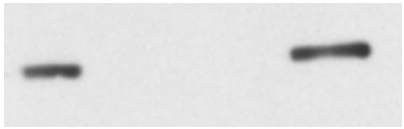

B

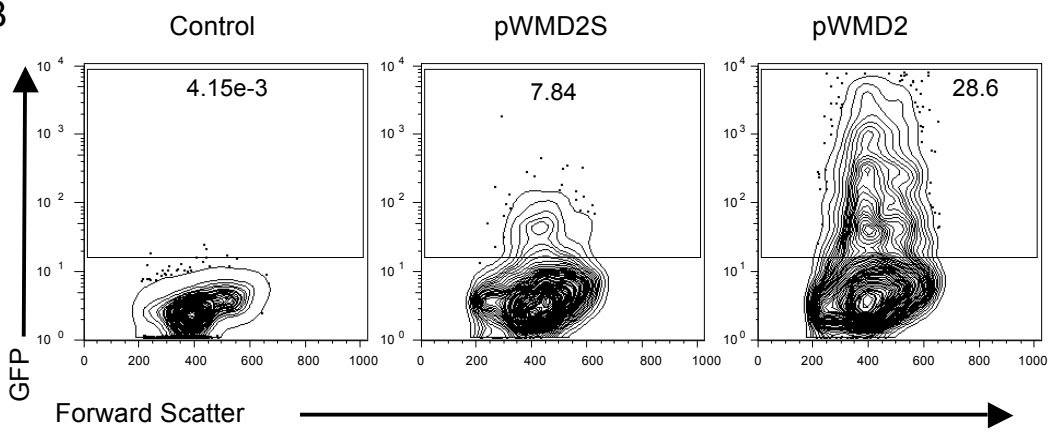

Figure 3. DNA tattooing procedure. *C57BL/6 (Thy1.2) mice were adoptively transferred with 10^6 allelically marked (Thy1.1) OT-I cells one day prior (-d1) to immunization. Mice were then immunized intradermally on the left hind leg with a rotary tattoo device for 16 seconds with 40 μg DNA on the indicated days. Readouts were the numbers and percentages of OT-I cells ($CD8^+Thy1.1^+$) as measured by flow cytometry on d12.*

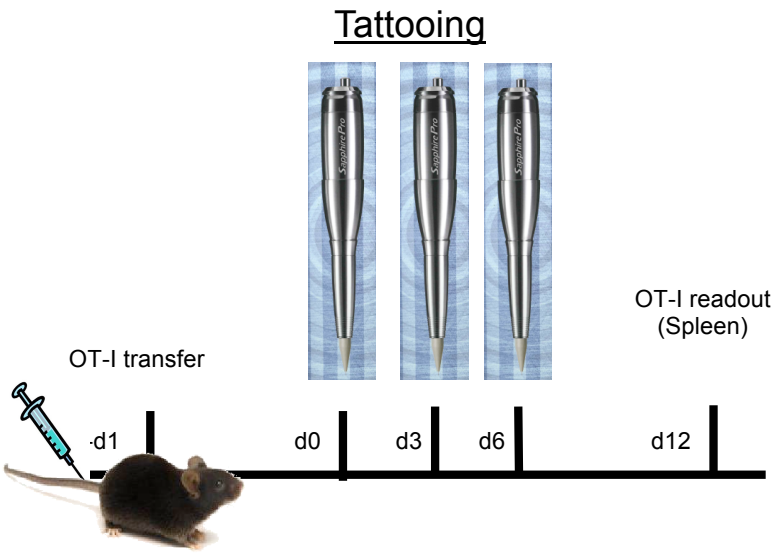
Tattooing
OT-I transfer
OT-I readout
(Spleen)
d1
d0
d3
d6
d12

Figure 4. Antigen specific $CD8^+$ T cell response to pWMD2S following DNA tattooing. *C57BL/6 (Thy1.2) mice were adoptively transferred with 10^6 OT-I cells one day prior to immunization. The mice were then immunized intradermally on the left hind leg using a tattoo device with 40µg DNA on d0, d3 and d6. A. Dot plots of OT-I cells ($CD8^+Thy1.1^+$) as measured by flow cytometry on d12. B-C. Percentage and number of OT-I cells of total splenocytes measured by flow cytometry on d12. ***P=<.001 TTEST, 1 Tail, Type 2.*

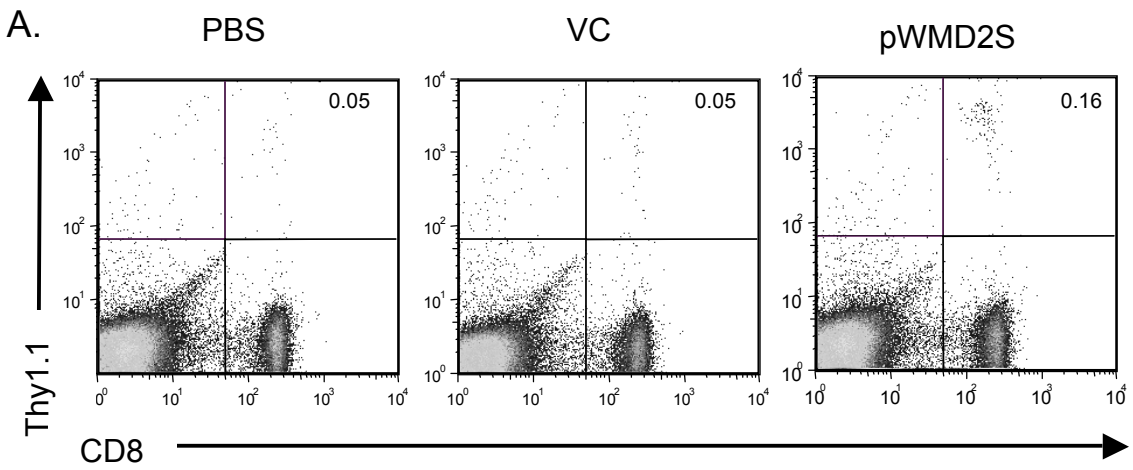
A.
PBS
VC
pWMD2S
0.05
0.05
0.16
Thy1.1
CD8

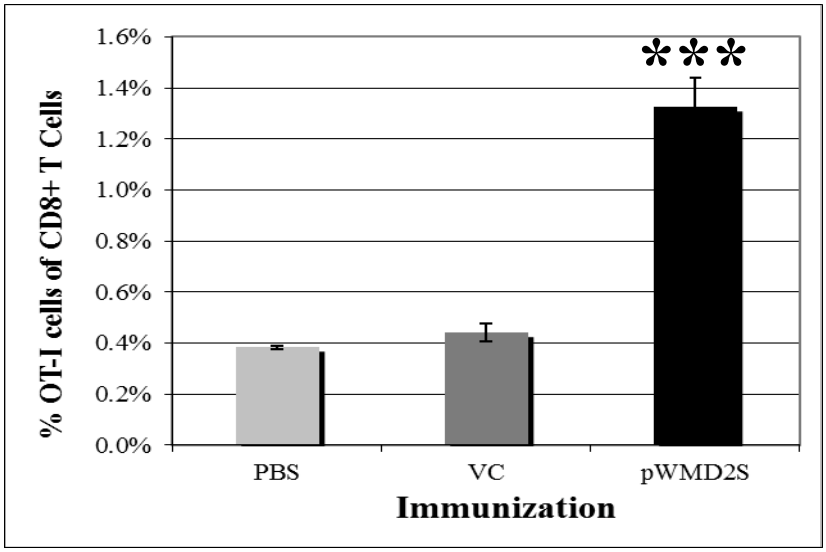
B.
% OT-I cells of CD8+ T Cells
1.6%
1.4%
1.2%
1.0%
0.8%
0.6%
0.4%
0.2%
0.0%
***
PBS
VC
pWMD2S
Immunization

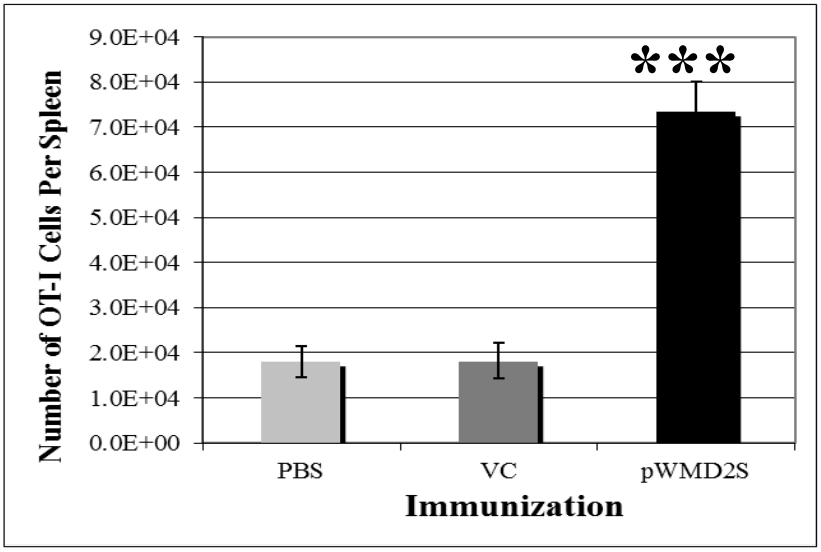
C.
Number of OT-I Cells Per Spleen
9.0E+04
8.0E+04
7.0E+04
6.0E+04
5.0E+04
4.0E+04
3.0E+04
2.0E+04
1.0E+04
0.0E+00
***
PBS
VC
pWMD2S
Immunization

Figure 5. Functional antigen specific $CD8^+$ T cell response with and without the secretion sequence. *C57BL/6 (Thy1.2) mice were adoptively transferred with 10^6 OT-I cells one day prior to immunization. The mice were then immunized intradermally on the left hind leg using a tattoo device with 40μg DNA on d0, d3 and d6. A. Percentage of OT-I cells ($CD8^+Thy1.1^+$) as measured by flow cytometry as percentage of $CD8^+$ T cells on d12. B. Percentage of IFN-γ^+ OT-I cells following ex vivo peptide stimulation on d12. *P=<.05 (pWMD2 P=0.022, pWMD2S P=0.029) TTEST 1 Tail, Type 2.*

A.

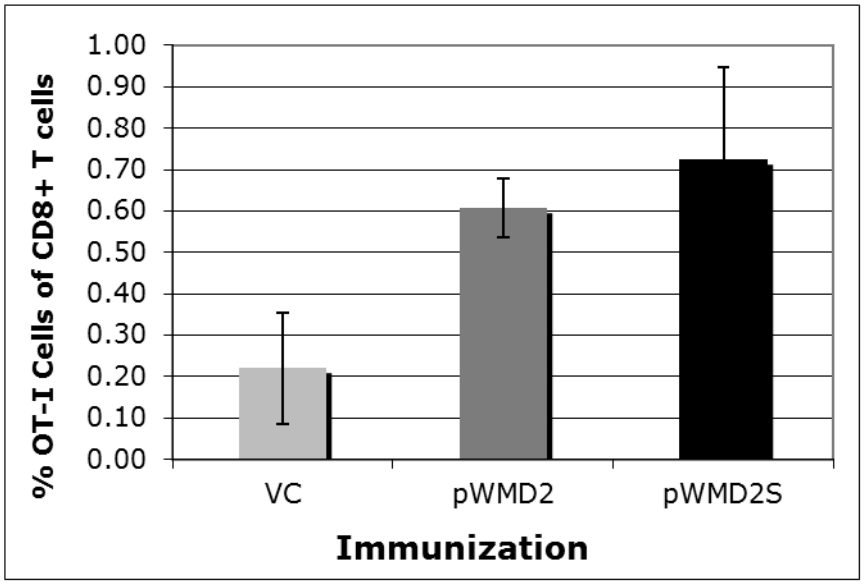
% OT-I Cells of CD8+ T cells
1.00
0.90
0.80
0.70
0.60
0.50
0.40
0.30
0.20
0.10
0.00
VC
pWMD2
pWMD2S
Immunization

B.

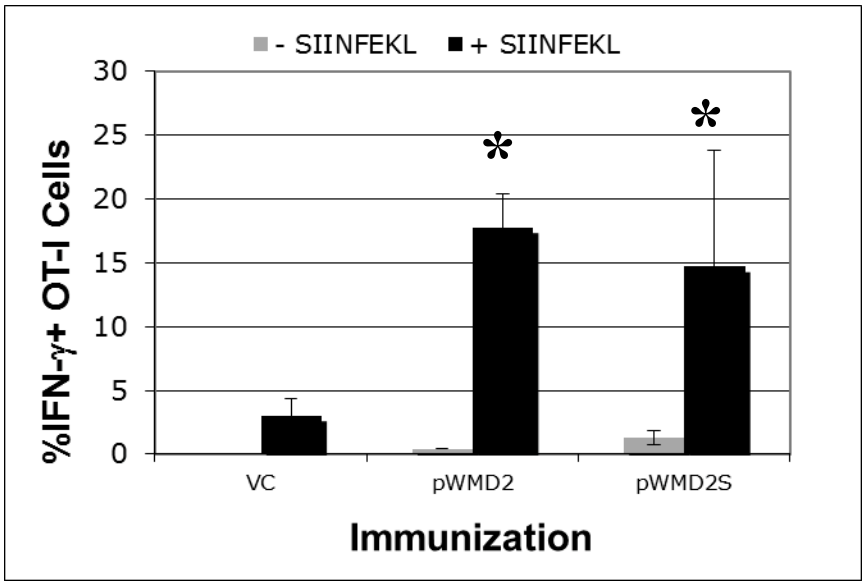
- SIINFEKL
+ SIINFEKL
%IFN-γ+ OT-I Cells
30
25
20
15
10
5
0
*
*
VC
pWMD2
pWMD2S
Immunization

Figure 6. Antigen specific $CD8^+$ T cell response following one, two or three immunizations. *C57BL/6 (Thy1.2) mice were adoptively transferred with 10^6 OT-I cells one day prior to immunization. The mice were then immunized intradermally on the left hind leg using a tattoo device with 40μg DNA either on d0, on d0 and d3, or on d0, d3 and d6. Splenocytes were harvested 6 days after the last immunization. Percentage of OT-I cells ($CD8^+Thy1.1^+$) as measured by flow cytometry (as percentage of $CD8^+$ T cells). *P=<.05 (pWMD2 P=0.022, pWMD2S P=0.029) TTEST 1 Tail, Type 2.*

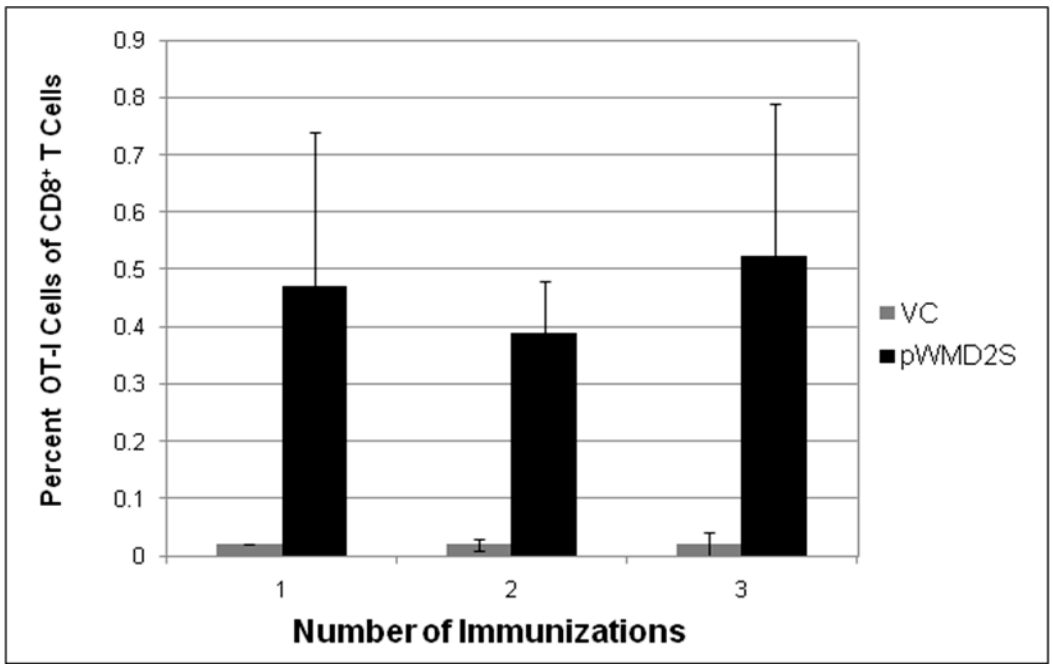
Percent OT-I Cells of CD8+ T Cells
0.9
0.8
0.7
0.6
0.5
0.4
0.3
0.2
0.1
0
1
2
3
Number of Immunizations
VC
pWMD2S

Chapter 3:

Transdermal Vaccination with Minicircle DNA Enhances Protein Expression and Antigen-Specific CD8$^+$ T Cell Responses

Wynette M Dietz[1], Nicole E B Skinner[1], Michelle D Jund[1], Patrick Hwu[2], Zhi-Ying Chen[3], Mark A Kay[3], Bruce R Blazar[4], Christopher A Pennell[1]* and Mark J Osborn[4]*

[1]Department of Laboratory Medicine and Pathology and Masonic Cancer Center, University of Minnesota School of Medicine, Minneapolis, Minnesota, USA

[2]Department of Melanoma Medical Oncology, The University of Texas MD Anderson Cancer Center, Houston, TX

[3]Departments of Genetics and Pediatrics, Stanford University School of Medicine, Stanford, California, USA

[4]Department of Pediatrics and Masonic Cancer Center, University of Minnesota School of Medicine, Minneapolis, Minnesota, USA

*These authors contributed equally.

Correspondence should be addressed to C.A.P. (penne001@umn.edu)

Address: Mayo Mail Code 806, 420 Delaware St. SE, Minneapolis, MN 55455; Phone 612-625-7138; Fax 612-626-5135).

Work was done in Minneapolis, Minnesota, USA

Short title: Enhanced Immunogenicity of a Minicircle Vaccine

Plasmid DNA-based gene delivery in mammals can result in brief transgene expression. This is most likely due to the spread of transcriptionally repressive chromatin initially deposited on plasmid bacterial backbone sequences. Minicircle DNA lacks plasmid backbone sequences and correspondingly, confers higher levels of relatively durable transgene expression upon gene delivery. In this study we show minicircle DNA also elicits enhanced antigen-specific $CD8^+$ T cell responses *in vivo*. We first used a luciferase reporter transgene to demonstrate that transdermal delivery of minicircle DNA, as compared to full-length plasmid DNA, resulted in significantly higher and persistent levels of luciferase expression in the skin. Minicircle DNA encoding an epitope recognized by $CD8^+$ T cells similarly elicited more potent and durable specific immune responses than the corresponding full-length plasmid DNA. Together our results suggest transdermal delivery of minicircle DNA vaccines may prove to be more efficacious for prophylaxis and therapy than traditional plasmid DNA vaccines.

Introduction:

Minicircle (MC) DNA is potentially superior to plasmid DNA (pDNA) as a nonviral vector for gene delivery (55, 56). Although both vector types contain expression cassettes that permit transgene products to be made at high levels shortly after delivery *in vivo*, expression rapidly wanes following delivery with standard full-length (FL) pDNA vectors because transcriptionally repressive heterochromatin is deposited on the plasmid bacterial backbone (57, 58). Heterochromatin then spreads *in cis* to silence transgene expression, independent of CpG content and methylation status (59-61). In contrast to pDNA, MC-encoded transgenes avoid this fate because MCs are devoid of essentially all prokaryotic sequence elements (e.g. origin of replication and antibiotic-resistance genes). Removal of these plasmid backbone sequences is achieved via site-specific recombination in *Escherichia coli* prior to episomal DNA isolation (62-64). The lack of these prokaryotic sequence elements also reduces MC size relative to its parental FL pDNA, leading to enhanced transfection efficiencies (65). The net result is that compared to their FL pDNA counterparts, MCs transfect a higher frequency of cells and permit durable high level transgene expression upon delivery *in vivo*.

In vivo gene delivery has broad appeal because of its potential as a therapeutic agent that mediates long-term gene expression. While MC-based vectors have been employed for gene therapy (66, 67), to our knowledge they have not been tested for their potential in DNA vaccine therapy. pDNA vaccines enjoy several advantages over protein and viral vaccine-based strategies including low cost, ease of production, flexibility in design and fewer safety concerns (68-70). While pDNA vaccines encoding pathogen or

tumor antigens (Ags) elicit immunity against infections or tumors in optimized animal models, clinical trials show only modest responses (71). These disappointing results likely are influenced by transient protein expression and low efficiency of gene delivery *in vivo* characteristic of FL pDNA. Because MC DNA does not have these limitations, we reasoned immune responses elicited by MC vaccines would be more potent than responses to FL pDNA vaccines encoding the Ags.

The two main routes for administering DNA vaccines are intramuscular and intradermal. The intradermal route is preferred because the skin is a barrier organ relatively rich in cells that present Ag to the immune system (72, 73). Intradermal delivery methods for DNA include injection with a hypodermic needle, bombardment of the skin with DNA-coated gold particles ejected from a gene gun, topical application, electroporation and tattooing (74-78). Tattooing has the advantage of being relatively inexpensive and rapid, and the infliction of thousands of perforations likely serves as a potent adjuvant. We therefore used tattooing to deliver FL pDNA and their derivative MC vaccines transdermally to mice. We found that the level, duration and immunogenicity of the MC transgene-encoded proteins were all significantly greater than those elicited by the FL pDNA vaccines. We discuss these results relative to future strategies involving DNA-based vaccines.

Materials and Methods:

DNA constructs. The plasmid backbone for the FL constructs (pMC.BESPX) contains the requisite sequences for bacterial propagation (e.g. the pUC origin of replication), the

øC31 integrase recognition sites attB and attP, and a block of 32 tandem repeats of the recognition sequence for the I-*Sce*I homing endonuclease (64).

To generate the FL-eff construct, eff was amplified from the pUltra Bright eff luciferase^{+} plasmid (79) and inserted into a vector containing the bovine growth hormone polyadenylation signal (BpA). The luciferase-BpA fragment was then PCR amplified. In a parallel PCR reaction the hUbC promoter (a generous gift from Michael Kyba, University of Minnesota, Minneapolis, MN) was amplified. The hUbC amplicon contains a 5' overlap region with the pMC.BESPX plasmid upstream of the EcoRI site and an overlapping region with the eff 5' sequence. The luciferase/BpA amplicon contains an overlap region with the pMC.BESPX plasmid downstream of the EcoRV site. The two PCR products and the EcoRI/EcoRV digested pMC.BESPX were subjected to a one-step isothermal DNA assembly protocol (80) allowing for seamless joining of the overlapping fragments.

A similar strategy was utilized to generate the FL-Ag construct containing the hUbC promoter-driven Ag cassette. The cassette encodes a signal sequence, a 10x histidine tag, a linker and a region that includes the chicken ovalbumin-derived peptide SIINFEKL (**Supplementary Figure 1**). It was amplified from a codon-optimized synthetic gene (GenScript, Piscataway, NJ) and inserted upstream of BpA. Overlapping PCR products for cloning hUbC-antigen-BpA were generated and isothermally assembled into pMC.BESPX. Sequences of all amplifying primers are available upon request from the authors.

All PCR reactions were performed using Phusion® High-Fidelity DNA Polymerase (New England BioLabs, Ipswich, MA) under the following conditions: 98°C x 30 seconds, followed by 35 cycles of 98°C x 10 seconds, 60°C x 30 seconds and 72°C x 120 seconds. Plasmids containing the eff or Ag cassettes were then transformed into the ZYCY10P3S2T bacterial strain. ZYCY10P3S2T bears ten copies of the øC31 integrase gene, three copies of the *I-Sce1* homing endonuclease gene, and the araC.BAD promoter-controlled araE and LacY arabinose transporter genes that induce øC31 integrase and I-*Sce*1 endonuclease expression (64). For FL pDNA preparation, transformed bacteria were grown in LB-broth (Invitrogen, Carlsbad, CA) supplemented with kanamycin. pDNA was by isolation using the PureLink HiPure Filter Plasmid Purification Maxiprep kit (Invitrogen) according to the manufacturer's instructions. For MC generation, bacteria transformed with FL pDNA were grown overnight in Terrific Broth supplemented with kanamycin (Invitrogen). The following day MC induction media (fresh LB broth containing 0.04 volumes of 1N NaOH and 0.02% *L*-arabinose (Sigma-Aldrich, St Louis, MO)) were added and the culture temperature was decreased from 37˚C to 32˚C for 5-8 hours. The culture was centrifuged and MC DNA was purified with the PureLink HiPure Filter Plasmid Purification Maxiprep kit (Invitrogen) by increasing the recommended volumes of buffers six-fold and using four columns. Following elution in water, the DNA was concentrated to 4-6 µg/µl by ethanol precipitation, resuspended in water and stored at -20°C. Sequence analyses verified the genes encoded by the FL pDNAs and their derivative MCs were identical.

Cell lines and transfections. COS cells were maintained in complete Dulbecco's modified Eagle's medium (Invitrogen) supplemented with 10% fetal bovine serum (Invitrogen) and DC2.4 cells were maintained in complete RPMI 1640 (Invitrogen) supplemented with 10% fetal bovine serum at 37°C with 5% CO_2. Adherent cells were dissociated from tissue culture flasks with TrypLE Express (Invitrogen) and plated in 6 well tissue culture-treated plates (BD Biosciences, San Jose, CA) at equal numbers (2-5 x 10^5 cells) per well without antibiotics. The following day, cells were transfected using Lipofectamine LTX with PLUS Reagent (Invitrogen) according to the manufacturer's protocol. COS cells were transfected with 2.5 μg (1.1 pmol) per well of MC-eff or equal molar amounts of VC or FL-eFF and were harvested two days later for flow cytometry analysis. DC2.4 cells were transfected with 2.6 μg (1.8 pmol) of MC-Ag per well or equal molar amounts of VC or FL-Ag and were harvested one, three and five days later for flow cytometry analysis.

Measurements of eff and Ag expression by flow cytometry. Staining for intracellular eff luciferase in COS cells was carried out using the BD Cytofix/Cytoperm kit (BD Biosciences) according to the manufacturer's protocol. Fixed and permeabilized cells were incubated with an anti-luciferase-FITC conjugate (Lifespan Biosciences, Seattle, WA) for 20 minutes. The DC2.4 cells were analyzed for cell surface antigen presentation using a 25-D1.16-APC conjugate (eBioscience, San Diego). 25-D1.16 is an antibody specific for the SIINFEKL/H-$2K^b$ complex (46). Cells were stained at 4°C for 30 minutes. Data were acquired on a BD FACSCalibur flow cytometer (BD Biosciences)

using BD CellQuest Pro software (BD Biosciences) and analyzed with FlowJo software (Tree Star, Inc., Ashland, OR).

Mice. Four to eight week old female C57BL/6 mice were purchased from the Jackson Laboratory (Bar Harbor, ME) or the National Cancer Institute (Frederick, MD). C57BL/6-Tg(TcraTcrb)1100Mjb/J (OT-I) $Thy1.1^{+}/Thy1.2^{+}$ mice were a generous gift from Dr. Stephen Jameson at the University of Minnesota (Minneapolis, MN). All mice were housed under specific pathogen free-conditions at the University of Minnesota (Minneapolis). All animal procedures were carried out according to protocols approved by the Institutional Animal Care and Use Committee.

OT-I adoptive cell transfer. All work was carried out under asceptic conditions using sterile reagents. OT-I mice were euthanized and lymph nodes were harvested. Single cell suspensions were prepared and cells were washed in phosphate buffered saline (PBS) supplemented with 2% (v/v) fetal bovine serum (Invitrogen). Cells were counted and analyzed by flow cytometry to determine the percentage and number of OT-I cells with the following antibody-fluorochrome conjugates: CD44-FITC, B220-PE, and CD8-APC (eBioscience) and Thy1.1-PerCP (BD Pharmingen, San Diego, CA). The OT-I phenotype was $B220^{-}CD8^{+}Thy1.1^{+}$. Additionally, the OT-I cells were $CD44^{low}$, indicating they were naïve at the time of transfer. To determine the cell count, PKH26 Reference Beads (Sigma-Aldrich) were mixed with cells; 5,000 bead events were collected on the flow cytometer. The following equation was used to determine the number of lymphocytes: #

cells/ml = (# cells acquired x dilution factor of cells x # singlet beads/ml) / (# beads acquired x dilution factor beads). Cell counts were verified manually using a hemocytometer. Data were acquired on a BD FACSCalibur flow cytometer (BD Biosciences) using BD CellQuest Pro software (BD Biosciences) and analyzed with FlowJo software (Tree Star, Inc.). Cells were washed in PBS with 1% (v/v) fetal bovine serum and then in PBS before being resuspended at 10^6 cells/ml in PBS. 10^5 cells were transferred into each anesthetized mouse via retro-orbital injection using 1 ml tuberculin syringes and 27 gauge needles.

DNA immunizations. Mice were anesthetized and their inner hind legs were shaved and sterilized with 70% ethanol. Based on pilot experiments, mice were immunized with 20 µg of MC DNA in 10-15 µl volumes. This mass converts to 9.2 and 13.9 pmol for MC-eff and MC-Ag, respectively. Equimolar amounts of VC and the corresponding FL pDNA samples were diluted in sterile water to the same volumes. All DNA was delivered transdermally over an area of approximately 1 cm^2 for 30 seconds using a Cheyenne Hawk PU II tattoo device (Unimax Supply Co. Inc., New York, NY) set at 110 Hz using 9-point needles adjusted to a depth of 0.5 mm.

Bioluminescence measured in vivo. Mice were imaged for bioluminescence using a Xenogen IVIS Imaging System (Caliper Life Sciences, Hopkinton, MA). Data were analyzed using Living Image 2.5 Software (Caliper Life Sciences). Briefly, mice were

injected intraperitoneally with 100 µl of 30 mg/ml luciferin and anesthetized with isoflurane. Bioluminescence was measured for 5 minutes.

CD8$^+$ T cell proliferation and function assays. Mice were adoptively transferred with 10^5 OT-I cells and the next day immunized with DNA using a tattoo device as described above. Splenocytes and the draining inguinal lymph nodes were harvested seven days later and analyzed by flow cytometry for percentages of OT-I cells. Functionality was assessed by IFN-γ production following a brief exposure of cells to antigen *in vitro*. Splenocytes were incubated with or without 1 µM SIINFEKL for 4 hours at 37°C and then examined for extracellular expression of CD8 and Thy1.1 (to identify OT-I cells) and intracellular expression of IFN-γ using BD Cytofix/Cytoperm kit (BD Biosciences). Data were acquired on a BD FACSCalibur flow cytometer (BD Biosciences) using BD CellQuest Pro software (BD Biosciences) and analyzed with FlowJo software (Tree Star, Inc.).

In vivo cytotoxicity. C57BL/6 mice were adoptively transferred with 10^6 OT-I cells and were immunized the next day with equimolar amounts of DNA using the tattoo device as described above. Eight days later these mice were adoptively transferred with equal numbers (10^7 each) of syngeneic splenocytes that had been pulsed or not with SIINFEKL peptide (1 µg peptide per 2.5 x 10^7 cells for one hour at 37˚C). To distinguish the cells from one another and from host cells, peptide-pulsed and unpulsed splenocytes were respectively labeled with 5 µM 5-(and-6)-carboxyfluorescein diacetate, succinimidyl

ester (CFSE) and 0.5 μM CFSE. Fourteen hours later, the mice were euthanized and their splenocytes harvested and analyzed by flow cytometry for percentages of $CFSE^{high}$ (peptide pulsed) and $CFSE^{low}$ (unpulsed control) cells. The percent specific killing was determined using the following formula: [1-(ratio in VC-immunized mouse/ratio in FL-Ag or MC-Ag-immunized mouse)] X 100 (81).

Statistical analysis. All statistical analyses were performed by the unpaired two-tailed Student's *t*-test unless noted otherwise.

Results:

Efficient production of MC-based expression vectors:

We constructed two series of expression vectors. One encoded enhanced firefly (eff) luciferase as a reporter to track expression. The other encoded a model peptide to monitor specific T cell responses. We chose eff luciferase as a reporter because of its sensitivity; mouse cells expressing eff luciferase emit >100 times more light than cells expressing standard firefly luciferase (79). The model peptide was the chicken ovalbumin-derived peptide SIINFEKL. When the SIINFEKL peptide is bound by the mouse major histocompatibility class I molecule $H\text{-}2K^b$, it forms an Ag recognized by mouse $CD8^+$ T cells bearing the Vα2/Vβ5 OT-I transgenic T cell receptor (43). Ag-specific OT-I responses are easily tracked after these cells are adoptively transferred into C57BL/6 ($H\text{-}2^b$) recipients who are subsequently immunized with chicken ovalbumin or the SIINFEKL peptide plus adjuvant (82). Expression of the eff and Ag genes was

controlled by the human ubiquitin C (hUbC) promoter, chosen because it efficiently drives transgene expression in many mouse tissues including skin (83).

MC constructs encoding eff or Ag (MC-eff and MC-Ag, respectively) were generated from FL pDNA precursors (**Fig. 1a**). Briefly, we cloned the hUbC-driven expression cassettes between the øC31 integrase recognition sites attB and attP contained within the minicircle producer plasmid backbone (64). Upstream of the attP site was a block of 32 tandem repeats of the I-*Sce*I homing endonuclease recognition sequence (83). FL pDNA was transformed into an *E. coli* strain (ZYCY10P3S2T) engineered to inducibly express øC31 integrase and I-*Sce*I endonuclease (64). Upon induction, øC31 integrase activity generated the MC and circular plasmid backbone; the latter was subsequently degraded by host bacterial exonucleases following linearization by the I-*Sce*I endonuclease. Densitometry analyses of ethidium bromide-stained agarose gels revealed that less than 5% of FL-eff pDNA remained in the purified MC-eff preparations (**Fig. 1b**). MC-Ag preparations were comparably pure (data not shown).

Enhanced expression of MC-encoded eff luciferase *in vitro:*

To determine if the expression levels or transfection efficiencies of MC-encoded genes were enhanced as compared to FL plasmid-encoded genes, we transfected COS cells transiently with equimolar amounts of MC-eff or FL-eff DNA. Two days later the cells were analyzed by flow cytometry for intracellular luciferase expression (**Fig. 2a**). On average about 14% of cells transfected with MC-eFF expressed luciferase, more than twice the frequency (6%) of luciferase-expressing cells transfected with an equimolar

amount of FL-eff (**Fig. 2b**). However, the median fluorescent intensities of the two luciferase-expressing populations were comparable (P=0.65). Together these data suggest that under the conditions used, the smaller MC-eff (3348 bp) transfected COS cells more efficiently than the larger FL-eff (7262 bp). On a per cell basis, though, cells transfected with either construct expressed equivalent levels of eff luciferase two days post-transfection.

Enhanced expression of MC-encoded eff luciferase in skin:

Because our goal is to develop MC-based vaccines, we next determined the intensity and duration of MC gene expression *in vivo*. We immunized mice intradermally since the skin is a barrier organ relatively rich in immune sentinel cells. Epidermal cells (e.g. keratinocytes) are critical for maintaining the immunological barrier function of the skin by initiating inflammation via recognition of damage- and pathogen-associated molecular patterns by pattern recognition receptors (84). Dermal dendritic cells similarly initiate proinflammatory responses but they also can internalize and present antigen to B and T cells (72). Work by the Haanen group demonstrated pDNA delivery to the skin via tattooing elicited more rapid and robust immune responses specific for the pDNA-encoded antigens than did intramuscular delivery (37). Therefore we tattooed the skin of mice with MC or FL DNA initially to compare the intensity and duration of gene expression, and later the immunogenicity of the proteins they encode.

Each mouse in the experimental cohort was tattooed on the left and right thighs with equimolar amounts of FL-eff and MC-eff DNA, respectively. Mice in a separate

cohort were tattooed with equimolar amounts of FL pDNA lacking an expression cassette (empty vector control, VC). The mice were then injected with saturating amounts of luciferin substrate on the indicated days and imaged for bioluminescence (**Fig. 3a**). Consistent with previous reports of standard firefly luciferase expression resulting from pDNA tattooing (37), expression peaked two to three days post-delivery in both groups (**Fig. 3b**). However, luciferase activity encoded by MC-eff was consistently and significantly higher than that of FL-eff. Luciferase activity decayed to background levels by day 42 in the FL-eff cohort but it remained detectable in the MC-eff cohort throughout the 63-day observation period. It is noteworthy that the MC-eff luciferase activity on day 63 was comparable to the FL-eff peak response on day 3. It took 49 days for luciferase activity in MC-eff mice to decay back to the levels measured on day 1 ($P = 0.23$; paired two-tailed *t* test). Together these data indicate that luciferase expression in the skin persists significantly longer and at significantly higher levels in mice tattooed with MC-eff relative to FL-eff.

Enhanced presentation of MC-encoded Ag *in vitro*:

To compare the intensity and duration of MC-encoded Ag presentation *in vitro*, we transfected a dendritic cell line, DC2.4 (H-2^b haplotype), with equimolar amounts of VC, FL-Ag or MC-Ag. The Ag cassette encoded the chicken ovalbumin-derived peptide SIINFEKL linked to a secretion sequence and a histidine tag (**Supplemental Fig. 1**). Western blot analysis of transiently transfected COS cells revealed the Ag was secreted (data not shown). To measure presentation of the SIINFEKL peptide, we analyzed DC2.4

cells one, three and five days after transfection for reactivity with 25-D1.16 (**Fig. 4a**). This monoclonal antibody specifically binds SIINFEKL only when presented by H-2K^b (46). The frequency of Ag-presenting cells was significantly higher and persisted longer in the MC-Ag transfectants as compared to the FL-Ag transfectants (**Fig. 4b**). The MC-Ag transfectants also expressed significantly higher Ag levels on each day than the FL-Ag transfectants. These data demonstrate Ag presentation persists longer, at higher levels, and in more DC2.4 cells transiently transfected with MC-Ag as compared to FL-Ag.

Enhanced immunogenicity of MC-encoded Ag *in vivo:*

To determine if the enhanced presentation of MC-encoded Ag observed *in vitro* corresponded to increased immunogenicity *in vivo*, we adoptively transferred equal numbers of CD8$^+$ OT-I (Thy1.1$^+$) cells into congenic C57BL/6 (Thy1.2$^+$) mice and tracked their responses following DNA immunization. One day after OT-I cell adoptive transfers, recipients were tattooed with equimolar amounts of VC, FL-Ag or MC-Ag DNA. Seven days later OT-I cells were identified by their expression of CD8 and the allelic marker Thy1.1. The proliferative responses of OT-I cells in mice immunized with MC-Ag were significantly greater than the responses in mice immunized with FL-Ag. This was true in the spleen (**Fig. 5a**) and draining lymph nodes (data not shown). To assess their functionality, OT-I cells from immunized mice were stimulated briefly *in vitro* with cognate Ag and examined for interferon-γ (IFN-γ) expression. IFN-γ was expressed by significantly more OT-I cells from mice immunized with MC-Ag than from mice immunized with FL-Ag (**Fig. 5b**). Moreover, the levels of intracellular IFN-γ tended

to be higher in OT-I cells from MC-Ag immunized mice than in FL-Ag immunized mice (median fluorescent intensities of 370 versus 235, respectively).

The *in vivo* cytolytic activity of OT-I cells was also significantly greater than in mice immunized with MC-Ag versus FL-Ag. To assess *in vivo* cytotoxicity, C57BL/6 mice were adoptively transferred with OT-I cells and the next day immunized with VC, MC-Ag or FL-Ag DNA via tattooing. One week later these mice were injected with equal numbers of SIINFEKL-pulsed syngeneic splenocytes labeled with CFSE ($CFSE^{high}$) and unpulsed syngeneic splenocytes labeled with 10-fold less CFSE ($CFSE^{low}$). The loss of $CFSE^{high}$ (Ag-positive) relative to $CFSE^{low}$ (Ag-negative) cells provided a measure of OT-I cytolytic activity *in vivo* (**Fig. 6a**) (81). Antigen-specific cytolytic activity in MC-Ag immunized mice was significantly greater than that in FL-Ag immunized mice (**Fig. 6b**). Together these data indicate MC-Ag immunization elicits a significantly greater OT-I response than does immunization with FL-Ag pDNA.

Discussion:

Our data indicate MC DNAs delivered via tattooing are superior to their FL counterparts in terms of the expression levels and duration, as well as the immunogenicity, of the proteins they encode. The enhanced levels and duration of protein expression we observe in the skin corroborate studies of MC DNA delivered to various tissues via other routes for gene therapy (62, 85, 86). The novelty of our report lies in the enhanced antigen-specific CD8 T cell response to an epitope encoded by a MC delivered transdermally.

Standard pDNA has two components: the bacterial backbone required for plasmid propagation in bacteria and the transcription cassette for expression in mammalian cells. Removal of the bacterial backbone reduced the size of MC DNA relative to pDNA by about half. pDNA size is inversely related to transfection efficiency (65) and correspondingly, the transfection efficiency and expression levels of MC are higher than pDNA (55, 56, 86). Accordingly we showed cells transfected *in vitro* with MC consistently expressed higher levels of luciferase or Ag compared to parental pDNA (**Fig. 2a**). This was also true *in vivo*, as evidenced by the $\geq$ 10-fold levels of luciferase activity in mice tattooed with MC-eff compared to FL-eff at all time points measured (**Fig. 3b**).

A second critical benefit to the removal of the backbone elements is their role in gene silencing. We have shown that the deposition of heterochromatin on the bacterial sequences causes the loss of expression that is independent of DNA methylation, CpG content, immune cell clearance, and plasmid copy number (59-61, 67)(58). The near complete absence of plasmid backbone elements most likely allowed expression of the eff transgene encoded by MC DNA to persist throughout the duration of the nine-week observation period. It is noteworthy that MC-eff expression at seven weeks was comparable to that at one day. This was unexpected because 33-44% of C57BL/6 keratinocytes are replaced weekly (87) and keratinocytes are the predominant cell type in the skin. Moreover, van den Berg *et al.* reported that 99% of human skin cells transfected by pDNA delivered via tattooing were keratinocytes (37). The persistence of eff

luciferase expression we observe is consistent with the transfection of longer-lived progenitor cells in the skin, such as hair follicle-associated dermal precursors (88).

Enhanced Ag expression following transdermal administration of MC-Ag DNA most likely caused the significant increases in the frequencies of effector OT-I cells. We speculate that the Ag provided by the MC DNA and the adjuvant effect resulting from the thousands of needle pricks inflicted by the tattoo device combined to produce a local microenvironment conducive for naïve $CD8^+$ T cell activation. Because the majority of cells transfected by tattooing pDNA are likely keratinocytes, we included a secretory signal in the Ag expression cassette. Our rationale was that secreted antigen by transfected cells could be internalized by resident antigen-presenting cells in the skin. These cells could then migrate to the draining lymph node and cross-present SIINFEKL/K^b to naïve OT-I cells. This is consistent with reports that dermal dendritic cells are required to stimulate naïve $CD8^+$ T cells upon intradermal immunization with pDNA (89).

Recent studies with pDNA-encoded Ags delivered transdermally suggest, though, that transfection of antigen-presenting cells themselves is the key event required to elicit specific $CD8^+$ T cell responses. Ag expression in keratinocytes failed to elicit specific $CD8^+$ T cell responses upon transdermal delivery of pDNA containing a K14 promoter, whereas Ag expression in dermal dendritic cells (via a CD11c promoter) did (54). Moreover, depletion of $langerin^+$ dermal dendritic cells ablated the response of $CD8^+$ T cells to Ag encoded by pDNA delivered transdermally, suggesting that specific delivery of MC to dermal dendritic cells should further enhance immunogenicity upon tattooing.

The duration of Ag expression following transdermal immunization with pDNA affects $CD8^+$ T cell responses to the encoded Ags (90). Hovav et *al.* reported that Ag-presenting cell activity slowly increased over a two-week period following injection of pDNA into the ear pinnae of mice (91). Removal of the ear pinnae at various times post-immunization diminished this activity, and the resultant specific $CD8^+$ T cell responses. These data suggest a depot of Ag controls $CD8^+$ T cell expansion at the level of Ag-presentation. A persistent Ag depot afforded by MC immunization arguably could permit sustained $CD8^+$ T cell responses first through activation of naïve $CD8^+$ T cells and then persistent reactivation of resultant memory cells. The combination of Ag and coadministered proinflammatory cytokines/chemokine all encoded by MC may establish a long-lived immunostimulatory microenvironment in the skin, leading to efficacious anti-pathogen and anti-tumor immunity.

In conclusion we show the applicability of the MC to mediate long-term expression of transgenes when delivered transdermally. This clinically relevant delivery method and the inherent safety benefits of the non-integrating MC DNA represents a novel approach toward DNA-based therapies.

Acknowledgements:

We thank Steve Jameson for the OT-I mice and Michael Kyba for the hUbC promoter (University of Minnesota). We also thank the staff of the University of Minnesota Masonic Cancer Center Flow Cytometry Core for their assistance. This work

was supported by a kind and generous gift to the University of Minnesota Masonic Cancer Center from Rosella Qualey, and grants NIH R01 CA72669 and CA113576.

Figure 1. Minicircle derivation. (a) Plasmid construct and minicircle generation. The expression cassette contains the human ubiquitin C promoter, genes encoding enhanced firefly luciferase (eff) or the chicken ovalbumin-derived SIINFEKL peptide (antigen; Ag), and the bovine growth hormone polyadenylation signal. The cassette is cloned between the øC31 integrase recognition sites attB and attP in the minicircle producer plasmid pMC.BESPX. This plasmid also contains a block of 32 tandem repeats of the I-*Sce*I homing endonuclease recognition sequence. The full-length (FL) parental plasmids are propagated in the ZYCY10P3S2T *E. coli* strain engineered to express øC31 integrase and the I-*Sce*I endonuclease under an arabinose-inducible promoter. Upon induction, øC31 integrase activity generates the minicircle (MC) and circular plasmid backbone; the latter is subsequently degraded by host exonucleases following linearization by the I-*Sce*I endonuclease. **(b)** Agarose gel electrophoresis analysis of the FL plasmid encoding eff (FL-eff) and its MC derivative (MC-eff). Products were linearized by digestion with K*pn*I (FL-eff) or S*tu*I (MC-eff). The arrow indicates residual FL plasmid in the purified MC-eff DNA preparation. Sizes of the DNA species are noted next to each band. eff, enhanced firefly luciferase; FL-eff, full-length plasmid encoding eff; I-*Sce*I x32, 32 tandem repeats of the I-*Sce*I homing endonuclease recognition sequence; Kan^r, kanamycin resistance gene; MC-eff, minicircle encoding eff; mw, molecular weight standards; pUC, plasmid origin of replication.

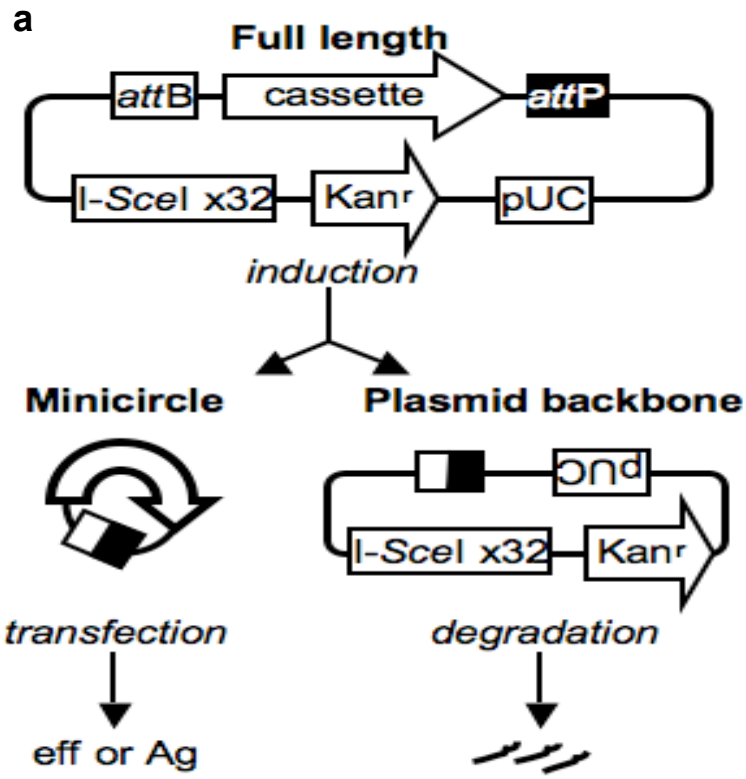
a
Full length
attB
cassette
attP
I-SceI x32
Kanr
pUC
induction
Minicircle
Plasmid backbone
pUC
I-SceI x32
Kanr
transfection
degradation
eff or Ag

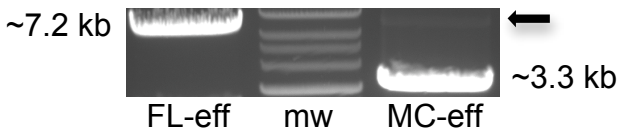
~7.2 kb
~3.3 kb
FL-eff
mw
MC-eff

Figure 2. Enhanced expression of minicircle-encoded eff *in vitro*. COS cells were transiently transfected with equimolar amounts (1.1 pmol; 2.5 μg MC-eff) of each DNA species. A luciferase-specific antibody was used to determine the frequencies of luciferase-expressing cells 48 hours later. (**a**) Flow cytometric analysis of transfected COS cells. These are representative flow cytometry contour plots used to determine the frequencies of eff-positive COS cells shown in **b**. (**b**) Frequencies of luciferase-positive COS cell transfectants. Data are presented as mean ± SEM (n =3)(*P***<0.01). eff, enhanced firefly luciferase; FL-eff, full-length plasmid encoding eff; MC-Ag, minicircle encoding eff; VC, empty full-length plasmid vector control.

a

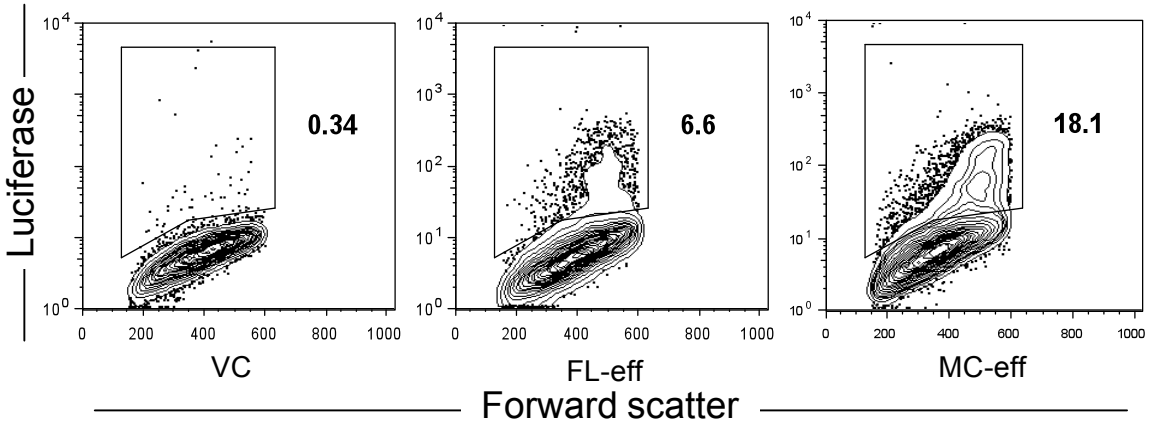
Luciferase
0.34
6.6
18.1
VC
FL-eff
MC-eff
Forward scatter

b

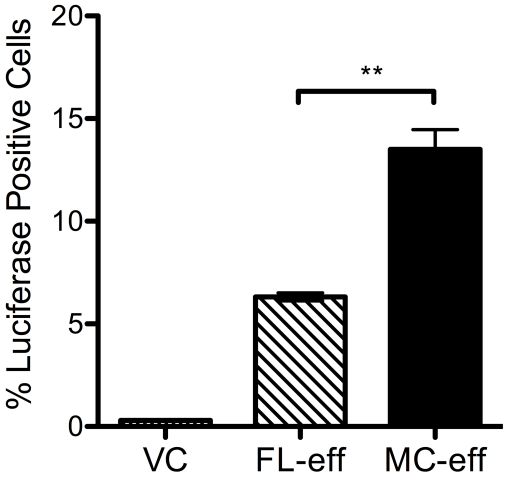
% Luciferase Positive Cells
**
VC
FL-eff
MC-eff

Figure 3. Enhanced intensity and duration of minicircle-encoded eff expression in the skin. The ventral skin on both thighs of C57BL/6 mice was tattooed with equimolar (9.2 pmol; 20 μg MC-eff) amounts of empty full-length plasmid vector control (VC), full-length plasmid encoding enhanced firefly luciferase (FL-eff), or the eff-encoding minicircle derivative (MC-eff). **(a)** Representative Xenogen IVIS imaging of *in vivo* luciferase activity (four days post-gene delivery). The left and right thighs of the first four mice show FL-eff and MC-eff activity, respectively. **(b)** Quantitative long-term *in vivo* luciferase expression**.** Animals were imaged daily for 18 days and then weekly from days 21 to 63. The data for the FL-eff and MC-eff cohorts are presented as the mean ± SEM (n = 4), corrected for background bioluminescence. Values for the VC cohort (n = 4) never exceeded background and are not shown. Luciferase activity in the FL-eff cohort decayed to background levels on day 42. Luciferase activity in the FL-eff and MC-eff cohorts was significantly different (P *<0.05) on each day analyzed except the first day ($P<0.06$). eff, enhanced firefly luciferase; FL-eff, full-length plasmid encoding eff; MC-eff, minicircle encoding eff; VC, empty full-length plasmid vector control.

a

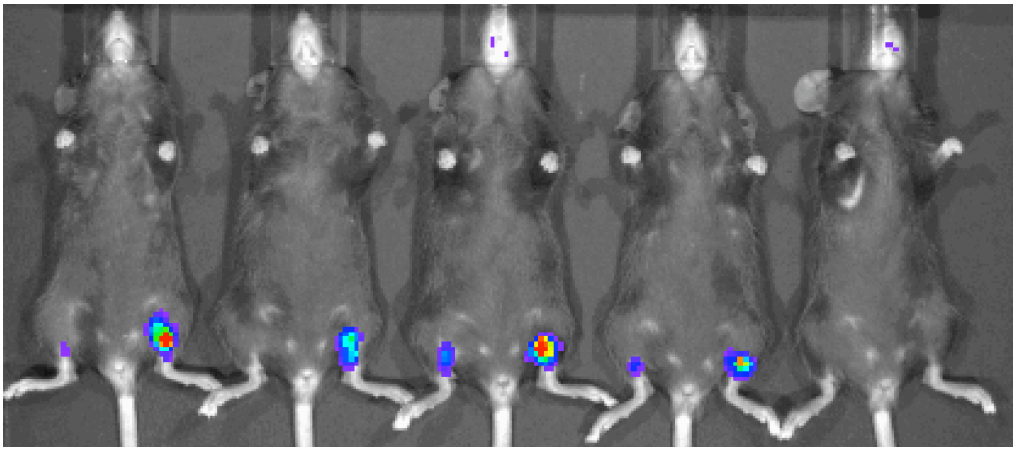

FL-eff/MC-eff VC

b

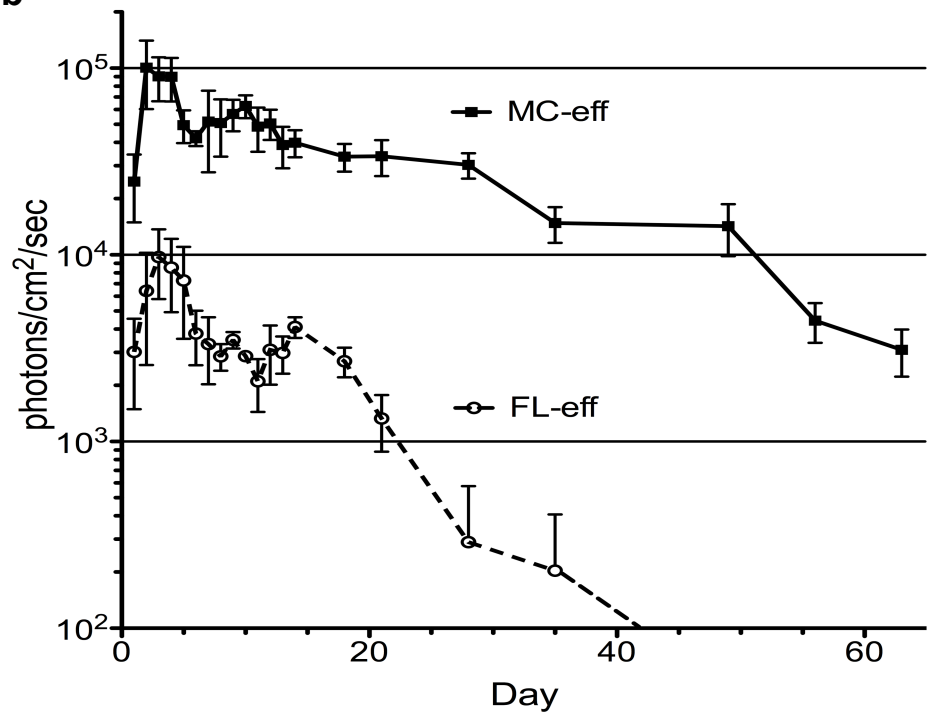

Figure 4. Enhanced presentation of minicircle-encoded antigen by dendritic cells. Cells from the C57BL/6-derived dendritic cell line DC2.4 were transiently transfected with equimolar (1.8 pmol) amounts of empty full-length plasmid vector control (VC), full-length plasmid encoding the chicken ovalbumin-derived peptide SIINFEKL (FL-Ag), or the SIINFEKL-encoding minicircle derivative of the full-length plasmid (MC-Ag). SIINFEKL presented by the MHC class I molecule H-2K^b is an antigen (Ag) recognized by specific CD8$^+$ T cells. Cells were analyzed by flow cytometry one, three and five days post-transfection for presentation of SIINFEKL by H-2K^b, as determined by reactivity with the monoclonal antibody 25.D1-16. (**a**) Flow cytometric analysis of transfected DC2.4 cells. These are representative flow cytometry contour plots (day three) used to determine the frequencies of Ag-positive DC2.4 cells shown in **b**. (**b**) Frequencies of Ag-positive DC2.4 cells. Data are presented as the mean ± SEM (n = 3)(*P****<0.001). Ag, antigen (SIINFEKL/H-2K^b); FL-Ag, full-length plasmid encoding SIINFEKL; MC-Ag, minicircle encoding SIINFEKL: VC, empty full-length plasmid vector control.

a

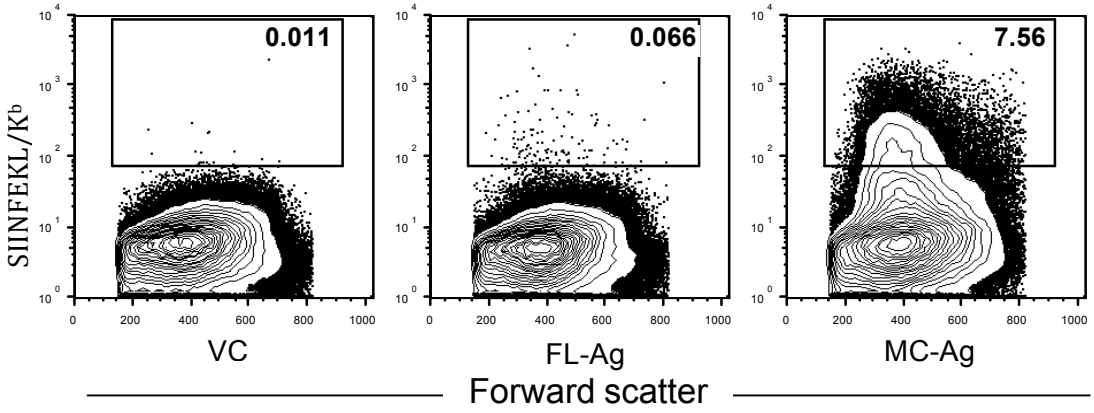
SIINFEKL/Kb
0.011
0.066
7.56
VC
FL-Ag
MC-Ag
Forward scatter

b

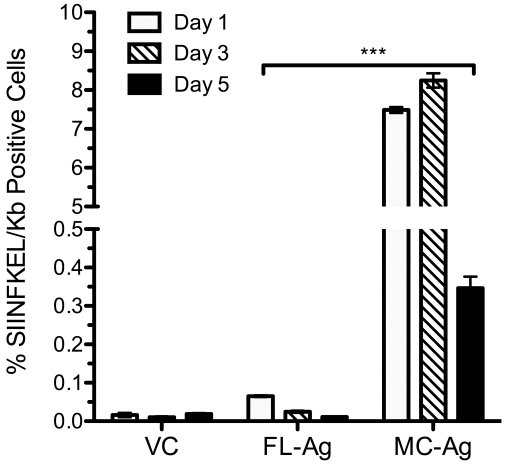
% SIINFKEL/Kb Positive Cells
Day 1
Day 3
Day 5
***
VC
FL-Ag
MC-Ag

Figure 5. Enhanced activation of antigen-specific $CD8^+$ T cells *in vivo* following immunization with MC-Ag. C57BL/6 mice were adoptively transferred with $Thy1.1^+/Thy1.2^+$ $CD8^+$ OT-I cells. OT-I cells bear a transgenic T cell receptor specific for the chicken ovalbumin-derived peptide SIINFEKL presented by the MHC class I molecule H-$2K^b$. Twenty-four hours after OT-I cell adoptive transfer, recipients were tattooed with equimolar (13.8 pmol; 20 μg MC-Ag) amounts of vector control (VC), full-length plasmid encoding SIINFEKL (FL-Ag), or the SIINFEKL-encoding minicircle derivative (MC-Ag). Mice were sacrificed one week later and their splenocytes analyzed by flow cytometry. (**a**) OT-I cell quantification. Donor OT-I cells were identified by their expression of CD8 and Thy1.1 (recipient $CD8^+$ T cells express Thy1.2). (**b**) Frequencies of interferon-γ^+ (IFN-γ^+) OT-I cells. The frequencies of OT-I cells expressing intracellular IFN-γ were determined to assess functional activity. Splenocytes from adoptively transferred, immunized mice were incubated with or without SIINFEKL peptide *in vitro* before analysis by flow cytometry for intracellular IFN-γ expression. Data are presented as the mean ± SEM (n = 3)($P^*<0.05$). FL-Ag, full-length plasmid encoding SIINFEKL; MC-Ag, minicircle-encoding SIINFEKL; VC, empty full-length plasmid vector control.

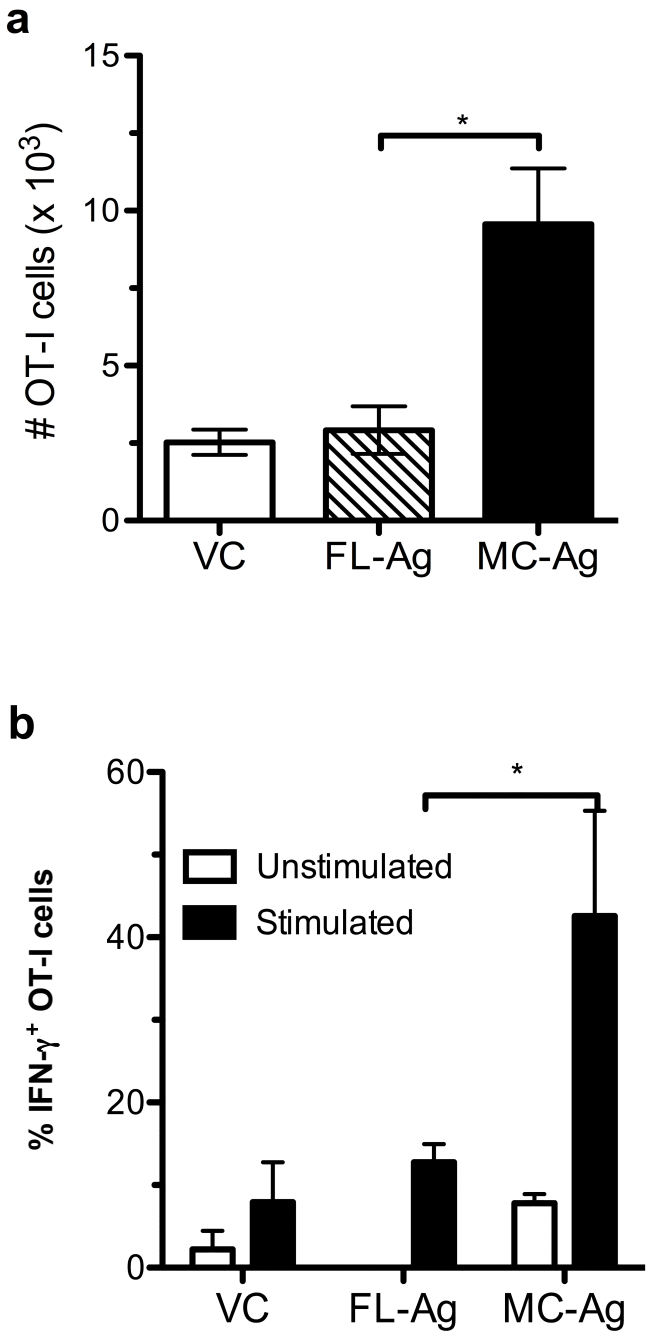
a
15
10
5
0
OT-I cells (x 10^3)
*
VC
FL-Ag
MC-Ag
b
60
40
20
0
% IFN-γ+ OT-I cells
Unstimulated
Stimulated
*
VC
FL-Ag
MC-Ag

Figure 6. Enhanced cytolytic activity of antigen-specific $CD8^+$ T cells following immunization with MC-Ag. C57BL/6 mice were adoptively transferred with OT-I cells. The next day recipients were tattooed with equimolar (13.8 pmol; 20 μg MC-Ag) amounts of empty full-length plasmid vector control (VC), full-length plasmid encoding the SIINFEKL peptide (FL-Ag), or the SIINFEKL-encoding minicircle derivative (MC-Ag) of the full-length plasmid. Control mice were immunized subcutaneously with SIINFEKL peptide emulsified in complete Freund's adjuvant (CFA). Eight days later, mice were adoptively transferred with equal numbers of syngeneic splenocytes pulsed with SIINFEKL peptide and unpulsed splenocytes. To distinguish them, peptide-pulsed and unpulsed splenocytes were respectively labeled with 5 μM and 0.5 μM CFSE. Mice were sacrificed 14 hours after cell transfer and their splenocytes analyzed by flow cytometry for the frequencies of $CFSE^{low}$ (unpulsed) and $CFSE^{high}$ (peptide-pulsed) cells. (**a**) Representative histograms of $CFSE^{low}$ and $CFSE^{high}$ cells. The numbers show the frequencies of $CFSE^{low}$ and $CFSE^{high}$ cells in the $CFSE^+$ populations in immunized mice. **(b)** Antigen-specific *in vivo* cytolytic activity. The frequency of unpulsed cells ($CFSE^{low}$) was divided by the frequency of peptide-pulsed cells ($CFSE^{high}$) to determine the ratio of antigen-negative to antigen-positive target cells in each mouse. These ratios were then used to calculate the percent antigen-specific cytolytic activity by the equation: [1-(VC ratio/FL-Ag or MC-Ag ratio)] x 100]. Data are presented as mean ± SEM (n = 5)($P^*<0.05$;$P^{**}<0.01$). CFA, complete Freund's adjuvant; CFSE, 5-(and-6)-carboxyfluorescein diacetate, succinimidyl ester; FL-Ag, full-length plasmid encoding

SIINFEKL; MC-Ag, minicircle encoding SIINFEKL; VC, empty full-length plasmid vector control.

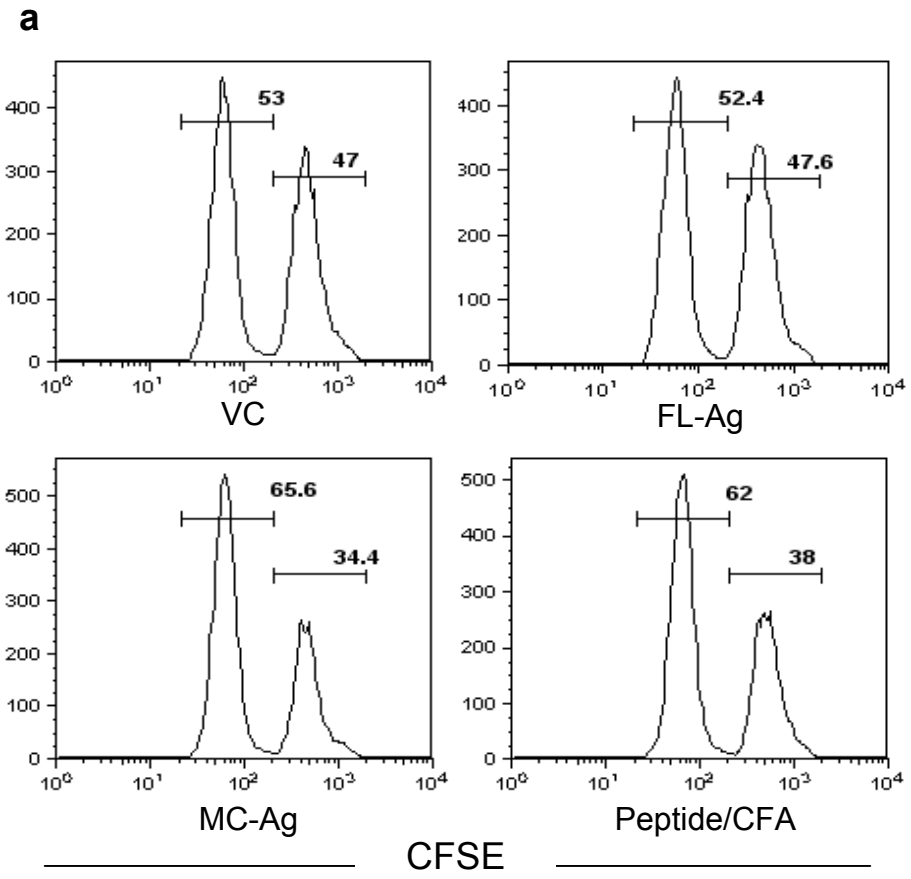
a
53
47
VC
52.4
47.6
FL-Ag
65.6
34.4
MC-Ag
62
38
Peptide/CFA
CFSE
b
% Specific lysis
30
20
10
0
*
**
FL-Ag
MC-Ag
Peptide

Supplementary Material:

Figure S1.

Single letter amino acid sequence of Ag insert. The signal sequence is underlined. The 10x histidine tag is italicized. The OVA-derived SIINFEKL peptide is bold faced. The SIINFEKL epitope is embedded in a larger peptide to facilitate antigen processing.

M W W R L W W L L L L L L L L W P M V W A *H H H H H H H H H H* L N E F C T S G L A V G A T K V P R N Q D W L G V S R Q L D I L R G L E Q L E **S I I N F E K L** T E W T S S S S A E S L K I S Q A V H A A H A E I N E A G R E V V G S A E S

Chapter 4:

Effect of +36GFP-HA2 Cationic Carrier on *in vitro* and *in vivo* Transfection Efficiency of Plasmid DNA

Two major limitations to the use of plasmid DNA for immunotherapy are transient protein expression and low transfection efficiency *in vivo*. The work presented in this chapter focuses on increasing the transfection efficiency of plasmid DNA vaccines through the use of highly cationic mutants of green fluorescent protein: +36GFP and +36GFP linked to a peptide derived from influenza hemagglutinin (HA2) known to enhance nuclear localization. We show that these cationic carriers bind plasmid DNA and significantly increase transfection efficiency *in vitro*. In addition, we show that +36GFP-HA2 leads to plasmid transfection *in vivo*, albeit not as efficiently as naked plasmid. By further increasing transfection efficiency we plan to produce plasmid DNA vaccines capable of tumor rejection.

Introduction:

In vivo gene delivery is an umbrella term for the introduction of exogenous nucleic acids into multicellular organisms. Gene delivery has broad appeal because of its potential for addition or replacement gene therapy, vaccination and gene silencing (92-94). These diverse applications permit its use to study normal and abnormal cell biology, and to treat diseases such as cancer.

DNA can be packaged in viruses or delivered as "naked" plasmid DNA (pDNA) to cells *in vivo*. pDNA delivery has the advantages of low cost, ease of production,

flexibility (several genes can be introduced simultaneously) and safety (e.g. pDNA does not cause insertional mutagenesis) (69). Gene delivery requiring multiple administrations is also best served with pDNA because immunity developed against viral proteins blocks viral vector delivery (70). Because of these advantages, pDNA-mediated gene delivery *in vivo* has been evaluated in almost 300 clinical trials to date (95). Together these trials reveal that while pDNA has promise, its efficacy *in vivo* is limited primarily by poor transfection efficiency, transient protein production, and for pDNA vaccines, low immunogenicity.

The efficiency of pDNA transfection *in vivo* is five to eight orders of magnitude lower than that *in vitro* (78). This relatively poor efficiency results from pDNA degradation by extracellular nucleases, nonspecific pDNA uptake and inefficient trafficking to the nucleus (96, 97). To enhance transfection efficiency *in vivo*, pDNA is often complexed to synthetic particles. For this, the DNA is either complexed with or encapsulated into the synthetic carrier producing micro- or nanoparticles. This technique has been widely used for nucleic acid delivery (38)(39)(40). Most of these complexes are formed by the electrostatic interaction between cationic carriers and anionic phosphate groups in the plasmid. Condensation of plasmid DNA by cationic carriers protects DNA from degradation by endonucleases and enhances transfection efficiency (both general cellular uptake and uptake by APCs in particular) (98). Examples of synthetic vehicles that have been used for DNA delivery include cationic lipids, cationic polymers and non-cationic polymers such as poly(lactide) or poly(lactide-co-glycolide).

We employed a supercharged GFP with a net theoretical +36 charge (+36GFP) as a cationic carrier (41). Lawrence and colleagues have shown that +36GFP has increased resistance to aggregation and consequent precipitation. This highly cationic protein also binds DNA and can be used as a transfection reagent *in vitro*. To facilitate escape from endosomes following cellular uptake, a variant of +36GFP (+36GFP-HA2) was made that contains the N-terminal 20 amino acids of the viral influenza hemagglutinin protein (HA2) fused to the C-terminus of GFP (99). The HA2 residues destabilize the endosomal membrane and allow escape (100-102). We show that use of these cationic carriers leads to significantly increased transfection efficiency *in vitro* but lower levels of transfection *in vivo*.

Materials and Methods:

Design and production of the cationic carriers +36GFP and +36GFP-HA2. Plasmids encoding +36GFP and +36GFP-HA2 were generous gifts from Dr. David Liu, Howard Hughes Medical Institute, Harvard University, Cambridge, MA. The proteins encode a 6X Histidine tag for purification purposes. Arctic Express (DE3) bacteria from Agilent Technologies, Inc. (Santa Clara, CA) were electroporated with the DNA encoding +36GFP or +36GFP-HA2. A single clone of each was verified by restriction endonuclease digestion and glycerol stocks were prepared and frozen at -20°C.

The proteins, +36GFP and +36GFP-HA2, were expressed in Arctic Express bacteria. Briefly, the bacteria were grown in 2.8L low form flasks containing 1L of LB supplemented with carbenicillin until they reached an OD_{600} of 0.6 to 0.8. Protein

expression was induced by the addition of 0.4mM IPTG and incubation at 15°C for an additional 6-8 hours. Following centrifugation, the bacterial pellets were resuspended in ice cold 1.5M NaCl/PBS and sonicated. Following sonication, the samples were spun down at 10,000 x g for 15 min at 4°C and the soluble protein was harvested. The protein was purified using His Gravitrap columns from GE Healthcare (Piscataway, NJ) and samples taken throughout the purification process were analyzed by SDS gel electrophoresis. Eluted proteins were dialyzed in 1.5M NaCl/PBS and stored at -20°C protected from light. Protein concentrations were determined spectrophotometrically using the extinction coefficient of GFP (M = OD_{488}/(8.33 X 10^4/M X 1 cm)(1cm)). The proteins were concentrated using Amicon Ultra-4 Centrifugal Filter Units with 10kDa filters from Millipore (Billerica, MA) and stored at -20°C protected from light.

SDS-PAGE. Sodium dodecyl sulfate polyacrylamide gel electrophoresis (SDS-PAGE) was used to separate the proteins according to their electrophoretic mobility, a function of their molecular weight, or size. Following protein production, +36GFP and +36GFP-HA2 were purified over His SpinTrap columns (GE Healthcare) and eluted according to the manufacturer's protocol. The samples were denatured by boiling for 5min with SDS and then run on NuPAGE 4-12% Bis-Tris gradient gels from Invitrogen (Carlsbad, CA). The gels were stained with SimplyBlue SafeStain (Invitrogen) for protein visualization.

DNA Plasmid production. The minicircle (MC) DNA encoding enhanced firefly (eff) luciferase was constructed and produced from a full-length (FL) plasmid encoding eff as

previously described in Chapter 3. Briefly, MC-eff DNA is devoid of the bacterial backbone sequences(62)(95). The eff was amplified from the pUltra Bright eff luciferase^{+} plasmid (kindly provided by Patrick Hwu, M.D. Anderson Cancer Center (Houston, TX)) (79) and inserted into a vector containing the human ubiquitin C promoter (UbC; a generous gift from Michael Kyba, University of Minnesota, Minneapolis, MN).

For MC-eff generation, bacteria transformed with FL-eff plasmids (full-length plasmid encoding eff) were grown overnight in Terrific Broth supplemented with kanamycin (Invitrogen). The following day MC induction media (fresh LB broth containing 0.04 volumes of 1N NaOH and 0.02% *L*-arabinose (Sigma-Aldrich, St Louis, MO)) were added and the culture temperature was decreased from 37˚C to 32˚C for 5-8 hours in order for the production of MC from FL plasmid. The culture was centrifuged and purified using the PureLink HiPure Filter Plasmid Purification Maxiprep kit (Invitrogen) by increasing the recommended volumes of buffers six-fold and purifying the MC over four columns. Following elution in water, the plasmids were concentrated to 4-6 μg/μl by ethanol precipitation, resuspended in water and stored at -20°C. All constructs were sequence verified.

Electrophoretic mobility shift assays. The abilities of the purified +36GFP and +36GFP-HA2 proteins to bind DNA were tested in electrophoretic mobility shift assays (EMSA). Briefly, a 0.7% agarose gel was pre-run at 4°C for 1 hour at 93V (to remove any potential contaminants). 120ng of the DsRed2 plasmid (a gift from Dr. Marc Jenkins, University

of Minnesota, Minneapolis, MN) was mixed with either +36GFP or +36GFP-HA2 in PBS at molar ratios of 0, 30:1, 100:1, 200:1 or 300:1 (protein to DNA) which corresponds to charge ratios of 0, 0.1:1, 0.3:1, 0.7:1, or 1:1 (positive to negative charge) and incubated at room temperature for 30 minutes protected from light. Following this incubation, the complexes were electrophoresed on 0.7% agarose gels at room temperature at 93V for 100 minutes without loading dye. The gels were stained in 50 ml of 0.6 μg/ml ethidium bromide for 15 minutes and analyzed using UV light.

HEK293T cells. HEK293T cells (a gift from the Polunovsky lab at the University of Minnesota, Minneapolis, MN) were maintained in complete Dulbecco's modified Eagle's medium (Invitrogen) supplemented with 10% fetal bovine serum (Invitrogen) at 37°C with 5% CO_2.

HEK293T cell transfections with +36GFP or +36GFP-HA2 and flow cytometry analysis. Adherent HEK293T cells were dissociated from tissue culture flasks with TrypLE Express (Invitrogen) and plated in 6 well tissue culture-treated plates (BD Biosciences, San Jose, CA) at equal numbers (2-5 x 10^5 cells) per well without antibiotics. The following day, the cells were treated with equimolar (0.23 nmol) amounts of protein, +36GFP or +36GFP-HA2, and incubated for 48 hours. The cells were harvested and analyzed for GFP expression by flow cytometry on a BD FACSCalibur flow cytometer using BD CellQuest Pro software (BD Biosciences) and analyzed with FlowJo software (Tree Star, Inc., Ashland, OR).

HEK293T cell transfections with +36GFP or +36GFP-HA2 and MC-eff plasmid.

Adherent cells were dissociated from tissue culture flasks with TrypLE Express (Invitrogen) and plated in 80 cm^2 tissue culture-treated flasks (Thermo Scientific, Rochester, NY) at 1.5 x 10^6 cells per well without antibiotics. Two days later, the cells were incubated with +36GFP or +36GFP-HA2 (with or without MC-eff plasmid). Briefly, +36GFP or +36GFP-HA2 was incubated with MC-eff (a luciferase-encoding plasmid) for 30 minutes at room temperature at a charge ratio of 0.7:1 (positive to negative) as determined by EMSA (20 µg MC-eff with either 54 µg +36GFP or 60 µg +36GFP-HA2). The cells were harvested 48 hours later for luminescence assays on a plate reader.

Measurements of transfection efficiency in vitro. Two days after transfection with +36GFP or +36GFP-HA2 (with or without MC-eff plasmid), 1 x 10^6 HEK293T cells were resuspended in 100 µl Reporter Lysis Buffer (Promega, Madison, WI), sheared by repetitive passage through 29 gauge needles and centrifuged at 12,000 x g for 15 seconds in 1.5 ml Eppendorf tubes to pellet debris. Supernatant (20 µl) was added to 15 µl Luciferase Assay Reagent (Promega) substrate and 35 µl PBS in a 96 well plate, mixed and read on a Synergy HT Multi-Detection Microplate Reader (BioTek, Winooski, VT) for 1 second each using a 590/20 nm bandpass filter. The data were analyzed using Gen5 Data Analysis Software (BioTek).

Mice. Four to eight week old female BALB/c mice were purchased from the Jackson Laboratory (Bar Harbor, ME). All mice were housed under specific pathogen free-conditions at the University of Minnesota (Minneapolis). All animal procedures were carried out according to protocols approved by the Institutional Animal Care and Use Committee.

Plasmid DNA immunizations (with and without +36GFP-HA2). Mice were anesthetized and their inner hind legs were shaved and wiped with 70% ethanol. The mice were immunized with the specified amounts of plasmid DNA (with or without +36GFP-HA2) or with +36GFP-HA2 alone in 10-15 µl volumes. The plasmids were incubated at room temperature with +36GFP-HA2 for 30 minutes prior to immunization. The plasmids were delivered transdermally using a Cheyenne Hawk PU II tattoo device (Unimax Supply Co. Inc., New York, NY) set at 110 Hz using 9-point needles. The needle was adjusted to a depth of 0.5mm. DNA was delivered over an area of approximately $1cm^2$ for 30 seconds.

Bioluminescence measured in vivo. Mice were imaged for bioluminescence using a Xenogen IVIS Imaging System and the data were analyzed using Living Image 2.5 Software (Caliper Life Sciences, Hopkinton, MA). Briefly, mice were injected intraperitoneally with 100 µl of 30mg/ml luciferin and anesthetized with isoflurane. Bioluminescence was measured for 5 min.

Statistical analysis. All statistical analyses were performed by the unpaired two-tailed Student's *t*-test unless noted otherwise.

Results:

Production of the cationic carriers:

In an effort to increase plasmid DNA transfection efficiency, we first produced two cationic carriers, +36GFP and +36GFP-HA2 (Figure 1A) (41). We chose these proteins since they bind DNA and can be used as transfection reagents *in vitro*. They can also be tracked by fluorescence. +36GFP and +36GFP-HA2 were produced in Arctic Express bacteria and purified using His Gravitrap columns. Samples taken throughout the purification process were analyzed by SDS gel electrophoresis (Figure 1B-C). The purified proteins are homogeneous and +36GFP-HA2 migrated slightly slower than +36GFP, consistent with their masses of 32.66 and 29.41 kDa, respectively. The carboxy terminus of +36GFP-HA2 contains the first 20 amino acids of the viral influenza hemagglutinin protein (HA2) which facilitates endosomal escape(102, 103). The proteins were concentrated and stored at -20°C protected from light.

DNA binding ability of the cationic carriers:

To test the ability of the cationic carriers to bind DNA and to determine the optimal binding ratio, we used an electrophoretic mobility shift assay (EMSA). Plasmid DNA was mixed with either +36GFP or +36GFP-HA2 in PBS at molar ratios of 0, 30:1, 100:1, 200:1 or 300:1 (protein to DNA) which corresponds to charge ratios of 0, 0.1:1,

0.3:1, 0.7:1, or 1:1 (positive to negative) and incubated at room temperature for 30 minutes. Following incubation, the complexes were electrophoresed on agarose gels and analyzed using UV light. As the protein binds to the DNA, the DNA's size and charge change, thereby leading to a shift in its position in the gel. Condensation of DNA on the cationic carriers also decreases the ability of ethidium bromide to intercalate between the DNA strands. This shift in mobility and ultimate loss in ethidium bromide labeling are indicative of DNA/protein binding and are used to determine the optimal amount of protein to bind the DNA completely. As Figure 2 shows, the DNA was completely bound by protein at a molar ratio of 200:1 (protein to DNA) or a charge ratio of 0.7:1 (positive to negative).

Ability of cationic carriers to transfect cells with plasmids *in vitro*:

To confirm that the +36GFP and +36GFP-HA2 proteins can bind cells, HEK293T cells were incubated with either +36GFP or +36GFP-HA2 for 48 hours and were analyzed by flow cytometry. As shown in Figure 3, 100% of the cells were positive for +36GFP and +36GFP-HA2, indicating that the proteins were able to bind the cells.

To determine if +36GFP and +36GFP-HA2 could transfect cells *in vitro*, +36GFP or +36GFP-HA2 was first incubated with MC-eff (a luciferase-encoding plasmid) at a charge ratio of 0.7:1 (positive to negative) as determined by EMSA. HEK293T cells were incubated with the protein/DNA complexes for 48 hours and then the cells were harvested. Following harvest, luminescence was analyzed on a plate reader. As shown in Figure 4, both +36GFP and +36GFP-HA2 led to internalization and expression of the

plasmid encoding luciferase. However, there was not a significant difference in luciferase expression between the two proteins.

Ability of cationic carriers to transfect cells with plasmids *in vivo*:

We next tested the ability of +36GFP-HA2 to enhance transfection efficiency *in vivo*. MC-eff was incubated +36GFP-HA2 at a charge ratio of 0.7:1 (positive to negative). Following incubation, either MC-eff alone, +36GFP-HA2, or a mix of MC-eff and +36GFP-HA2 were administered to BALB/c female mice intradermally using a tattoo device. The mice were imaged 48 hours later for bioluminescence. We found that +36GFP-HA2 led to transfection and expression of MC-eff *in vivo*, but was not as efficient as plasmid alone (Figure 5).

Discussion:

These studies show that the +36GFP and +36GFP-HA2 cationic carriers bind pDNA and transfect cells *in vitro*. McNaughton and colleagues have shown that +36GFP internalization is via endocytosis and is dependent on electrostatic interactions with sulfated cell surface proteoglycans (99). This process is energy-dependent, clathrin- and caveolin-independent and requires actin polymerization. Additionally, they showed that +36GFP-HA2, but not +36GFP, was able to transfect mammalian cell lines (HeLa, IMCD, 3T3-L and PC12) with pDNA. We show that both +36GFP and +36GFP-HA2 are able to transfect mammalian cells (HEK293T) with pDNA. However, +36GFP-HA2 did not result in significantly higher *in vitro* transfection efficiency than +36GFP as

expected based on McNaughton's results. Also, McNaughton showed that 2 μM +36GFP-HA2 led to transfection in several cell lines while 200 nM was insufficient for transfection, whereas we found that 95 nM was sufficient for transfection with both +36GFP and +36GFP-HA2.

The differences in transfection efficiency between +36GFP and +36GFP-HA2 may be due to variability among the cell lines or between the DNA. There is great variability in transfection efficiency among different cell types and cell line and several cell lines including adipocytes and neuronal cells have shown resistance to cationic lipid transfection reagents (104, 105). Lavorini-Doyle and colleagues have shown that this difference in transfection efficiency occurs after pDNA internalization via endocytosis and may be due to inability to escape the endosome or inability to enter the nucleus (106). HA2 residues destabilize the endosomal membrane and allow escape, but may not facilitate import into the nucleus (100-102). Additionally nuclear pDNA transcription is affected by the physiological state of the cell (107). Therefore, differences in endosomal escape, nuclear internalization or the physiological state among cell lines may account for the differences in transfection efficiencies between +36GFP and +36GFP-HA2. Finally, the use of different DNAs may have contributed to the differences in transfection efficiencies between McNauton's results and ours. McNaughton used the pSV-β galactosidase plasmid (Promega, Madison, WI) which is 6820 bp whereas we used MC-eff which is approximately 3200 bp. Smaller plasmids have been shown to have higher transfection efficiencies than larger plasmids (108) and this may have contributed to the increased transfection efficiency that we found following +36GFP administration.

In addition, use of +36GFP-HA2 led to lower transfection efficiencies *in vivo* than plasmid alone. This may be due to the positively charged carrier binding to negatively charged extracellular matrix components on the cell surface and therefore preventing plasmid uptake and expression. Van den Berg and colleagues have shown that by shielding the surface charge using PEGylation, they can improve protein expression by more than 55 fold (109). Future optimization, such as that previously described, may lead to increased transfection efficiency of carrier protein/plasmid complexes *in vivo*, thereby leading to more efficacious DNA vaccines in a clinical setting.

Figure 1. Protein sequence, expression and purification. *+36GFP and +36GFP-HA2 were expressed in* E. coli *and purified using His Gravitrap columns from GE Healthcare (Piscataway, NJ). A. Protein sequence of +36GFPHA2 (mutated residues in +36GFP relative to GFP are bold faced; HA2 peptide is underlined). B. Protein expression and purification fractions for +36GFP-HA2: (1)Protein molecular weight standards, (2) Flowthrough, (3) Wash #1, (4) Wash #2, (5) Elution. C. Purified +36GFP-HA2 (1) and +36GFP (2).*

A.

MGHHHHHHGGASKGE**R**LF**R**G**K**VPILVELKGDVNGH**K**FSVRG**K**G**K**GDA

T**R**GKLTLKFICTTGKLPVPWPTLVTTLTYGVQCFSRYP**K**HMK**R**HDFFKS

AMP**K**GYVQERTISFK**K**DG**K**YKTRAEVKFEG**R**TLVNRI**K**LKG**R**DFKE**K**G

NILGHKL**R**YNFNSH**K**VYITADK**R**KNGIKA**K**FKIRHNV**K**DGSVQLADHY

QQNTPIG**R**GPVLLP**R**NHYLST**R**S**K**LSKDP**K**EKRDHMVLLEFVTAAGI**K**H

G**R**DE**R**YKGSAGSAAGSGEFGLFGAIAGFIENGWEGMIDG

B.

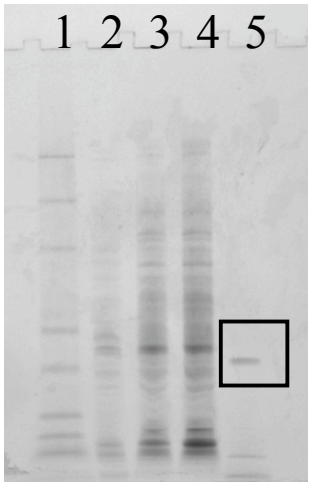

C.

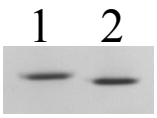

Figure 2. DNA binding ability of +36GFP and +36GFP-HA2. *+36GFP or +36GFP-HA2 were incubated for 30 minutes with DsRed2 plasmid and were found to bind DNA at a molar ratio of 200:1 (0.7:1 positive to negative charge ratio). (1) DNA ladder, (2) DsRed2 plasmid alone, (3-6) DsRed2 plasmid with various molar ratios of +36GFP, (7-10) DsRed2 plasmid with various molar ratios of +36GFP-HA2.*

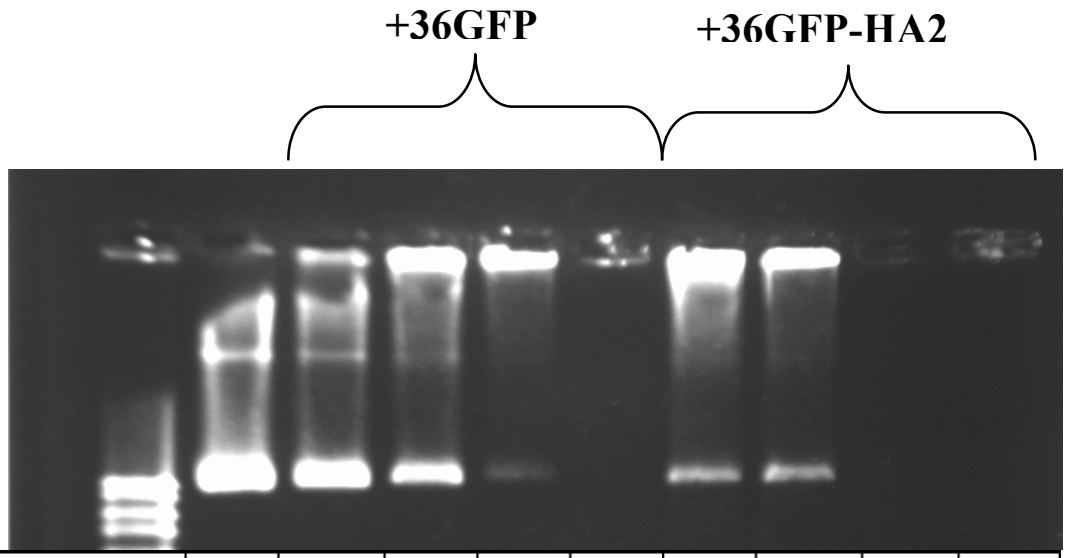

Molar Ratio	0	30	100	200	300	30	100	200	300
“+” to “-” Ratio	0	0.1	0.3	0.7	1.0	0.1	0.3	0.7	1.0

Figure 3. Ability of +36GFP and +36GFP-HA2 to bind cells *in vitro*. *HEK293T cells were incubated with either +36GFP, +36GFP-HA2 or no protein for 48 hours. The cells were harvested and analyzed by flow cytometry for GFP fluorescence.*

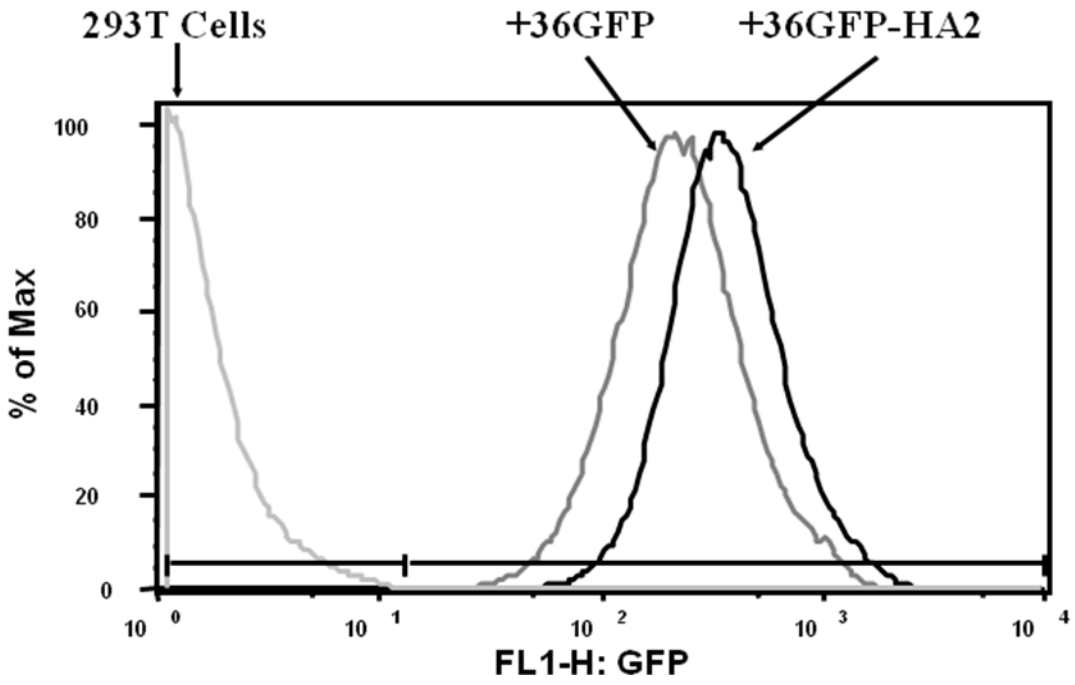
293T Cells
+36GFP
+36GFP-HA2
100
80
60
40
20
0
% of Max
10 0
10 1
10 2
10 3
10 4
FL1-H: GFP

Figure 4. Transfection efficiency of +36GFP and +36GFP-HA2 *in vitro* using a luciferase-encoding plasmid. *+36GFP or +36GFP-HA2 with or without MC-eff (a luciferase-encoding plasmid) were incubated with HEK293T cells for 48 hours. Following incubation, 1 x 10^6 cells were lysed and luminescence was detected on a plate reader.*

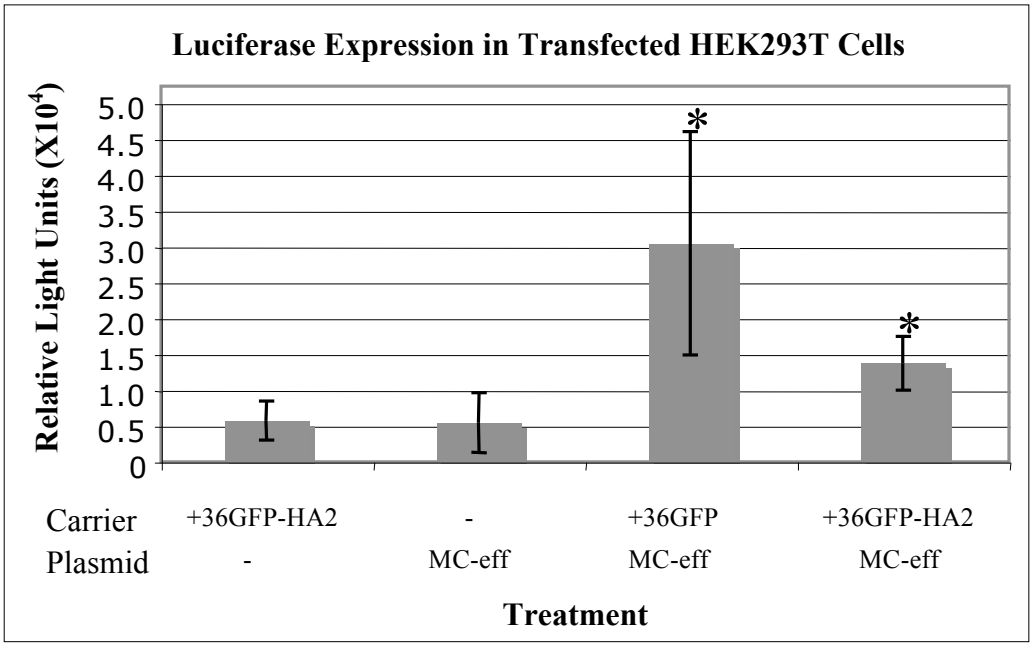
Luciferase Expression in Transfected HEK293T Cells
Relative Light Units (X10^4)
5.0
4.5
4.0
3.5
3.0
2.5
2.0
1.5
1.0
0.5
0
*
*
Carrier
Plasmid
+36GFP-HA2
-
-
MC-eff
+36GFP
MC-eff
+36GFP-HA2
MC-eff
Treatment

Figure 5. Transfection efficiency of +36GFP-HA2 *in vivo*. *MC-eff alone, +36GFP-HA2 alone or MC-eff with +36GFP-HA2 was administered to mice intradermally to the inner hind leg using a tattoo device. 48 hours after immunization, the mice were imaged for bioluminescence. Only the highest amount of +36GFP-HA2 led to luciferase expression (see mouse #3, left leg). A. Mouse image. B. Graph of data in A.*

A.

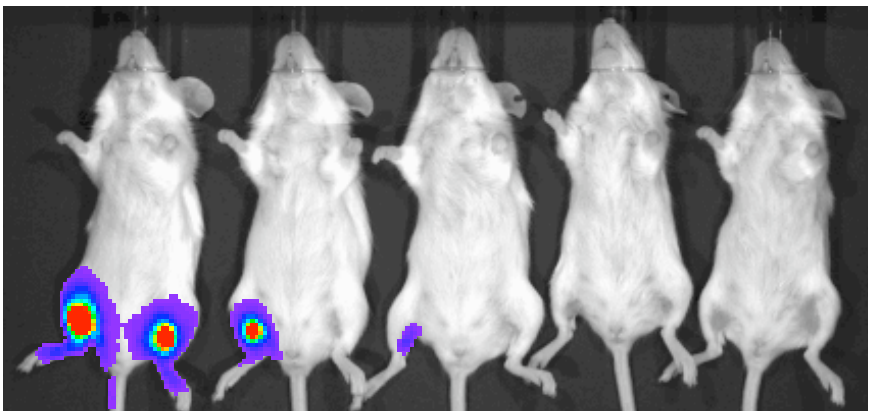

MC-eff (µg)	**20**	**10**	**5**	**-**	**20**	**-**	**10**	**-**	**5**	**-**
+36GFP-HA2 (µg)	**-**	**-**	**-**	**-**	**60**	**60**	**30**	**30**	**15**	**15**

B.

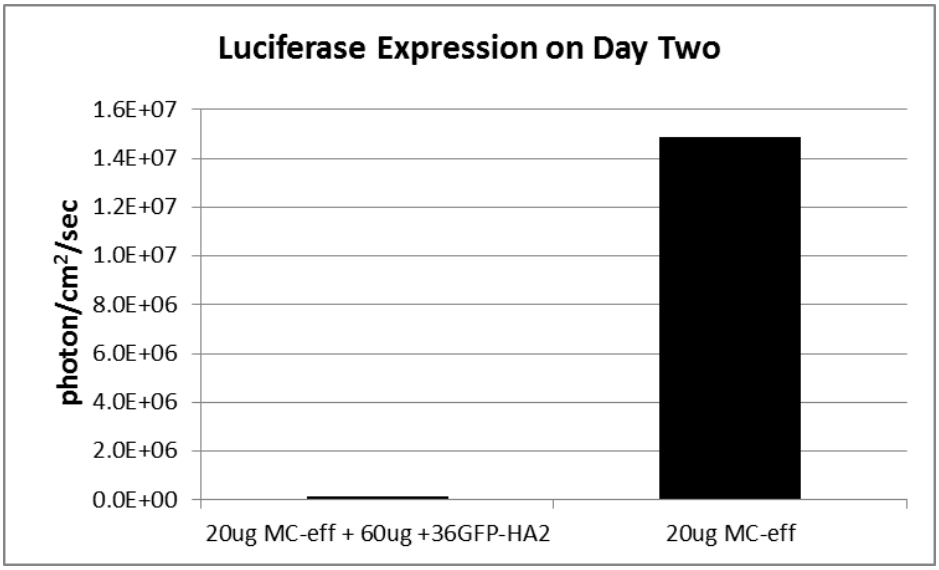

Chapter 5:

Concluding Remarks

Although there are currently over 1,000 cancer vaccines in clinical trials (132 are DNA vaccines), only one has received FDA approval (110). Provenge (Dendreon Corp., Seattle, WA), a dendritic cell based vaccine, was approved in April, 2010 for the treatment of castration-resistant prostate cancer (111, 112). The problem plaguing most cancer vaccines is their low immunogenicity in humans. Two major barriers to the immunogenicity of DNA vaccines are transient protein expression and poor transfection efficiency. The objective of this work was to overcome these limitations and thereby increase the efficacy of DNA vaccines.

First, we established a platform in which to optimize DNA vaccines for cancer therapy by addressing both the plasmid DNA vaccine components and the route/strategy for administration of the vaccines (Chapter 2). These studies showed that the DNA plasmids encoded functional proteins that were expressed both *in vitro* and *in vivo*. Furthermore, plasmid immunization via a tattoo device resulted in functional antigen-specific $CD8^+$ T cell responses *in vivo*. Lastly, we found that secretion of the plasmid-encoded protein was not necessary. Consistent with this finding, Elnekave and colleagues recently discovered that directly transfected DCs are responsible for $CD8^+$ T cell activation following intradermal DNA administration, thereby making the secretion of plasmid encoded proteins unnecessary (54).

Next, we addressed the limitation of transient protein production. Levels of plasmid DNA-encoded proteins drop rapidly following intradermal plasmid

administration (37). Therefore, multiple immunizations are required to achieve adequate immune responses. By increasing protein expression, we may reduce the need for multiple immunizations and produce more potent immune responses. As a result, DNA vaccination may become quicker, cheaper and more effective.

In Chapter 3 we overcame transient protein expression by removing essentially all of the bacterial backbone (which contains transcriptionally repressive chromatin), thereby producing minicircle (MC) DNA. We showed that the MC results in increased protein expression and in increased transfection efficiency *in vitro* and in both increased protein expression and increased duration of protein expression *in vivo* (protein expression for 63+ days with the MC compared to 5 or 6 days as shown by Bins and colleagues (53)). The increase in transfection efficiency seen following MC immunization is likely due to its decreased size as several studies have shown that smaller plasmids result in higher transfection efficiencies (55, 56, 65, 108). Furthermore, MC immunization resulted in significantly greater percentages of functional antigen-specific $CD8^+$ T cells and in greater antigen-specific killing *in vivo*, showing an enhanced antigen-specific immune response compare to the FL DNA.

Decreasing the size of the DNA resulted in increased transfection efficiency, but to further increase transfection efficiency and to decrease plasmid degradation, we tested the ability of two cationic carriers (+36GFP and +36GFP-HA2) to increase plasmid transfection efficiency (Chapter 4). Interestingly, these studies showed that both +36GFP and +36GFP-HA2 bound pDNA and transfected cells *in vitro* whereas previous research showed that only +36GFP-HA2 led to *in vitro* transfection (99). The ability of +36GFP

to transfect 293T cells with MC may be due to variability in transfection efficiency among cell lines or to the smaller size of the DNA we used (less than half the size of the other DNA). In addition, use of +36GFP-HA2 led to lower transfection efficiencies *in vivo* than plasmid alone. This may be due to the positively charged carrier binding to negatively charged extracellular matrix components on the cell surface and thereby preventing plasmid uptake and expression. Future optimization, such as shielding the surface charge using PEGylation (109), may lead to increased transfection efficiency *in vivo*.

One limitation to this work is that the immune responses were measured using an OT-I adoptive transfer system. Adoptively transferring congenically labeled T cells into mice enables easy detection and monitoring of the resultant immune response (82). However, the number of precursor cells is elevated above that of a naïve animal and therefore does not accurately reflect the endogenous response. To overcome this limitation, future work will include characterizing the endogenous response to the DNA vaccines using tetramers and T cell functional assays including enzyme-linked immunosorbent assay (ELISA), enzyme-linked immunosorbent spot (ELISpot) assay and cytotoxicity assays. Tetramers bind antigen-specific T cells and can be used to directly detect these cells using flow cytometry. ELISA and ELISpot assays can be used to monitor effector cytokine production *in vitro* following antigen stimulation whereas cytotoxicity assays can be used to directly assess antigen-specific killing *in vitro*.

Future directions include further enhancing DNA vaccine immunogenicity. One way to increase the immunogenicity is to encode an adjuvant within the DNA. The MC

DNA used in these studies included T cell antigens but did not include an adjuvant. By adding Hsp70 or another potent adjuvant, we may significantly increase its immunogenicity. Adjuvants are especially important for therapeutic vaccines since it is necessary to overcome immune tolerance for a cancer vaccine to be successful. Additionally, different adjuvants are known to result in different immune responses, such as aluminum salts lead to antibody production (113) whereas monophosphoryl lipid A results in both B and T cell responses (114-116). Therefore, it is important to choose an adjuvant that will result in a $CD8^+$ T cell response for a cancer vaccine. Another way to increase immunogenicity is to use a DNA prime followed by a protein or peptide boost. Two recent studies show that using a DNA-prime, protein/peptide-boost results in significantly greater immune responses compared to DNA vaccination alone (117, 118).

In closing, we have overcome the limitation of transient protein expression and have modestly increased transfection efficiency. Through the addition of adjuvants and by further enhancing transfection efficiency through cationic carrier optimization, we plan to increase the immunogenicity of DNA vaccines.

Bibliography:

1. Jemal, A., R. Siegel, J. Xu, and E. Ward. 2010. Cancer Statistics, 2010. *CA Cancer. J. Clin.*

2. Shankaran, V., H. Ikeda, A. T. Bruce, J. M. White, P. E. Swanson, L. J. Old, and R. D. Schreiber. 2001. IFNgamma and lymphocytes prevent primary tumour development and shape tumour immunogenicity. *Nature* 410: 1107-1111.

3. Graziano, D. F. and O. J. Finn. 2005. Tumor antigens and tumor antigen discovery. *Cancer Treat. Res.* 123: 89-111.

4. Srivastava, P. K. and L. J. Old. 1988. Individually distinct transplantation antigens of chemically induced mouse tumors. *Immunol. Today* 9: 78-83.

5. Melief, C. J., W. L. Vasmel, R. Offringa, E. J. Sijts, E. A. Matthews, P. J. Peters, R. H. Meloen, A. J. van der Eb, and W. M. Kast. 1989. Immunosurveillance of virus-induced tumors. *Cold Spring Harb. Symp. Quant. Biol.* 54 Pt 1: 597-603.

6. Robbins, P. F., M. el-Gamil, Y. Kawakami, E. Stevens, J. R. Yannelli, and S. A. Rosenberg. 1994. Recognition of tyrosinase by tumor-infiltrating lymphocytes from a patient responding to immunotherapy. *Cancer Res.* 54: 3124-3126.

7. Disis, M. L. and M. A. Cheever. 1998. HER-2/neu oncogenic protein: issues in vaccine development. *Crit. Rev. Immunol.* 18: 37-45.

8. Doehn, C., T. Bohmer, I. Kausch, M. Sommerauer, and D. Jocham. 2008. Prostate cancer vaccines: current status and future potential. *BioDrugs* 22: 71-84.

9. Kawakami, Y., S. Eliyahu, C. H. Delgado, P. F. Robbins, K. Sakaguchi, E. Appella, J. R. Yannelli, G. J. Adema, T. Miki, and S. A. Rosenberg. 1994. Identification of a human melanoma antigen recognized by tumor-infiltrating lymphocytes associated with in vivo tumor rejection. *Proc. Natl. Acad. Sci. U. S. A.* 91: 6458-6462.

10. Mao, C., L. A. Koutsky, K. A. Ault, C. M. Wheeler, D. R. Brown, D. J. Wiley, F. B. Alvarez, O. M. Bautista, K. U. Jansen, and E. Barr. 2006. Efficacy of human papillomavirus-16 vaccine to prevent cervical intraepithelial neoplasia: a randomized controlled trial. *Obstet. Gynecol.* 107: 18-27.

11. Kao, J. H. and D. S. Chen. 2002. Recent updates in hepatitis vaccination and the prevention of hepatocellular carcinoma. *Int. J. Cancer* 97: 269-271.

12. Su, J., A. Wu, E. Scotney, B. Ma, A. Monie, C. Hung, and T. Wu. 2010. Immunotherapy for cervical cancer: Research status and clinical potential. *BioDrugs* 24: 109-129.

13. Melero, I., S. Hervas-Stubbs, M. Glennie, D. M. Pardoll, and L. Chen. 2007. Immunostimulatory monoclonal antibodies for cancer therapy. *Nat. Rev. Cancer.* 7: 95-106.

14. Weiner, L. M., R. Surana, and S. Wang. 2010. Monoclonal antibodies: versatile platforms for cancer immunotherapy. *Nat. Rev. Immunol.* 10: 317-327.

15. Pokorna, D., I. Rubio, and M. Muller. 2008. DNA-vaccination via tattooing induces stronger humoral and cellular immune responses than intramuscular delivery supported by molecular adjuvants. *Genet. Vaccines Ther.* 6: 4.

16. Verstrepen, B. E., A. D. Bins, C. S. Rollier, P. Mooij, G. Koopman, N. C. Sheppard, Q. Sattentau, R. Wagner, H. Wolf, T. N. Schumacher, J. L. Heeney, and J. B. Haanen. 2008. Improved HIV-1 specific T-cell responses by short-interval DNA tattooing as compared to intramuscular immunization in non-human primates. *Vaccine* 26: 3346-3351.

17. Le, T. P., K. M. Coonan, R. C. Hedstrom, Y. Charoenvit, M. Sedegah, J. E. Epstein, S. Kumar, R. Wang, D. L. Doolan, J. D. Maguire, S. E. Parker, P. Hobart, J. Norman, and S. L. Hoffman. 2000. Safety, tolerability and humoral immune responses after intramuscular administration of a malaria DNA vaccine to healthy adult volunteers. *Vaccine* 18: 1893-1901.

18. Pertmer, T. M., M. D. Eisenbraun, D. McCabe, S. K. Prayaga, D. H. Fuller, and J. R. Haynes. 1995. Gene gun-based nucleic acid immunization: elicitation of humoral and cytotoxic T lymphocyte responses following epidermal delivery of nanogram quantities of DNA. *Vaccine* 13: 1427-1430.

19. Kutzler, M. and D. Weiner. 2008. DNA vaccines: ready for prime time? *Nature Reviews.Genetics* 9: 776-788.

20. Martin, J. E., T. C. Pierson, S. Hubka, S. Rucker, I. J. Gordon, M. E. Enama, C. A. Andrews, Q. Xu, B. S. Davis, M. Nason, M. Fay, R. A. Koup, M. Roederer, R. T. Bailer, P. L. Gomez, J. R. Mascola, G. J. Chang, G. J. Nabel, and B. S. Graham. 2007. A West Nile virus DNA vaccine induces neutralizing antibody in healthy adults during a phase 1 clinical trial. *J. Infect. Dis.* 196: 1732-1740.

21. MacGregor, R. R., J. D. Boyer, K. E. Ugen, K. E. Lacy, S. J. Gluckman, M. L. Bagarazzi, M. A. Chattergoon, Y. Baine, T. J. Higgins, R. B. Ciccarelli, L. R. Coney, R. S. Ginsberg, and D. B. Weiner. 1998. First human trial of a DNA-based vaccine for

treatment of human immunodeficiency virus type 1 infection: safety and host response. *J. Infect. Dis.* 178: 92-100.

22. Mincheff, M., S. Tchakarov, S. Zoubak, D. Loukinov, C. Botev, I. Altankova, G. Georgiev, S. Petrov, and H. T. Meryman. 2000. Naked DNA and adenoviral immunizations for immunotherapy of prostate cancer: a phase I/II clinical trial. *Eur. Urol.* 38: 208-217.

23. Ritossa, F. 1962. A new puffing pattern induced by temperature shock and DNP in *Drosophila*. *Experientia* 571-573.

24. Srivastava, P. K. and M. R. Das. 1984. The serologically unique cell surface antigen of Zajdela ascitic hepatoma is also its tumor-associated transplantation antigen. *Int. J. Cancer* 33: 417-422.

25. Higo, H., K. Higo, J. Y. Lee, H. Hori, and Y. Satow. 1988. Effects of exposing rat embryos in utero to physical or chemical teratogens are expressed later as enhanced induction of heat-shock proteins when embryonic hearts are cultured in vitro. *Teratog Carcinog. Mutagen.* 8: 315-328.

26. Morandi, A., B. Los, L. Osofsky, L. Autilio-Gambetti, and P. Gambetti. 1989. Ubiquitin and heat shock proteins in cultured nervous tissue after different stress conditions. *Prog. Clin. Biol. Res.* 317: 819-827.

27. Segal, B. H., X. Y. Wang, C. G. Dennis, R. Youn, E. A. Repasky, M. H. Manjili, and J. R. Subjeck. 2006. Heat shock proteins as vaccine adjuvants in infections and cancer. *Drug Discov. Today* 11: 534-540.

28. Pack, C. D., M. Gierynska, and B. T. Rouse. 2008. An intranasal heat shock protein based vaccination strategy confers protection against mucosal challenge with herpes simplex virus. *Hum. Vaccin* 4: 360-364.

29. Liu, H., B. H. Wu, G. J. Rowse, and P. C. Emtage. 2007. Induction of CD4-independent E7-specific CD8+ memory response by heat shock fusion protein. *Clin. Vaccine Immunol.* 14: 1013-1023.

30. Palefsky, J. M., J. M. Berry, N. Jay, M. Krogstad, M. Da Costa, T. M. Darragh, and J. Y. Lee. 2006. A trial of SGN-00101 (HspE7) to treat high-grade anal intraepithelial neoplasia in HIV-positive individuals. *AIDS* 20: 1151-1155.

31. Hunt, S. 2001. Technology evaluation: HspE7, StressGen Biotechnologies Corp. *Curr. Opin. Mol. Ther.* 3: 413-417.

32. Liu, H., B. H. Wu, G. J. Rowse, and P. C. Emtage. 2007. Induction of CD4-independent E7-specific CD8+ memory response by heat shock fusion protein. *Clin. Vaccine Immunol.* 14: 1013-1023.

33. Lee, K. P., L. E. Raez, and E. R. Podack. 2006. Heat shock protein-based cancer vaccines. *Hematol. Oncol. Clin. North Am.* 20: 637-659.

34. Einstein, M. H., A. S. Kadish, R. D. Burk, M. Y. Kim, S. Wadler, H. Streicher, G. L. Goldberg, and C. D. Runowicz. 2007. Heat shock fusion protein-based immunotherapy for treatment of cervical intraepithelial neoplasia III. *Gynecol. Oncol.* 106: 453-460.

35. Klinman, D. M., J. M. Sechler, J. Conover, M. Gu, and A. S. Rosenberg. 1998. Contribution of cells at the site of DNA vaccination to the generation of antigen-specific immunity and memory. *J. Immunol.* 160: 2388-2392.

36. Steitz, J., C. M. Britten, T. Wolfel, and T. Tuting. 2006. Effective induction of anti-melanoma immunity following genetic vaccination with synthetic mRNA coding for the fusion protein EGFP.TRP2. *Cancer Immunol. Immunother.* 55: 246-253.

37. Bins, A. D., A. Jorritsma, M. C. Wolkers, C. F. Hung, T. C. Wu, T. N. Schumacher, and J. B. Haanen. 2005. A rapid and potent DNA vaccination strategy defined by in vivo monitoring of antigen expression. *Nat. Med.* 11: 899-904.

38. De Smedt, S. C., J. Demeester, and W. E. Hennink. 2000. Cationic polymer based gene delivery systems. *Pharm. Res.* 17: 113-126.

39. El-Aneed, A. 2004. An overview of current delivery systems in cancer gene therapy. *J. Control. Release* 94: 1-14.

40. Jilek, S., H. P. Merkle, and E. Walter. 2005. DNA-loaded biodegradable microparticles as vaccine delivery systems and their interaction with dendritic cells. *Adv. Drug Deliv. Rev.* 57: 377-390.

41. Lawrence, M. S., K. J. Phillips, and D. R. Liu. 2007. Supercharging proteins can impart unusual resilience. *J. Am. Chem. Soc.* 129: 10110-10112.

42. Harzstark, A. L. and E. J. Small. 2007. Immunotherapy for prostate cancer using antigen-loaded antigen-presenting cells: APC8015 (Provenge). *Expert Opin. Biol. Ther.* 7: 1275-1280.

43. Hogquist, K. A., S. C. Jameson, W. R. Heath, J. L. Howard, M. J. Bevan, and F. R. Carbone. 1994. T cell receptor antagonist peptides induce positive selection. *Cell* 76: 17-27.

44. Barnden, M. J., J. Allison, W. R. Heath, and F. R. Carbone. 1998. Defective TCR expression in transgenic mice constructed using cDNA-based alpha- and beta-chain genes under the control of heterologous regulatory elements. *Immunol. Cell Biol.* 76: 34-40.

45. Grubin, C. E., S. Kovats, P. deRoos, and A. Y. Rudensky. 1997. Deficient positive selection of CD4 T cells in mice displaying altered repertoires of MHC class II-bound self-peptides. *Immunity* 7: 197-208.

46. Porgador, A., J. W. Yewdell, Y. Deng, J. R. Bennink, and R. N. Germain. 1997. Localization, quantitation, and in situ detection of specific peptide-MHC class I complexes using a monoclonal antibody. *Immunity* 6: 715-726.

47. Murphy, D. B., D. Lo, S. Rath, R. L. Brinster, R. A. Flavell, A. Slanetz, and C. A. Janeway Jr. 1989. A novel MHC class II epitope expressed in thymic medulla but not cortex. *Nature* 338: 765-768.

48. Radons, J. and G. Multhoff. 2005. Immunostimulatory functions of membrane-bound and exported heat shock protein 70. *Exerc. Immunol. Rev.* 11: 17-33.

49. Harmala, L. A., E. G. Ingulli, J. M. Curtsinger, M. M. Lucido, C. S. Schmidt, B. J. Weigel, B. R. Blazar, M. F. Mescher, and C. A. Pennell. 2002. The adjuvant effects of Mycobacterium tuberculosis heat shock protein 70 result from the rapid and prolonged activation of antigen-specific CD8+ T cells in vivo. *J. Immunol.* 169: 5622-5629.

50. Gao, H., Y. Yue, L. Hu, W. Xu, and S. Xiong. 2009. A novel DNA vaccine containing multiple TB-specific epitopes casted in a natural structure (ECANS) confers protective immunity against pulmonary mycobacterial challenge. *Vaccine* 27: 5313-5319.

51. Barash, S., W. Wang, and Y. Shi. 2002. Human secretory signal peptide description by hidden Markov model and generation of a strong artificial signal peptide for secreted protein expression. *Biochem. Biophys. Res. Commun.* 294: 835-842.

52. Chen, C. H., T. L. Wang, C. F. Hung, Y. Yang, R. A. Young, D. M. Pardoll, and T. C. Wu. 2000. Enhancement of DNA vaccine potency by linkage of antigen gene to an HSP70 gene. *Cancer Res.* 60: 1035-1042.

53. Bins, A., A. Jorritsma, M. Wolkers, C. Hung, T. Wu, T. N. M. Schumacher, and J. B. A. G. Haanen. 2005. A rapid and potent DNA vaccination strategy defined by in vivo monitoring of antigen expression. *Nat. Med.* 11: 899-904.

54. Elnekave, M., K. Furmanov, I. Nudel, M. Arizon, B. E. Clausen, and A. H. Hovav. 2010. Directly transfected langerin+ dermal dendritic cells potentiate CD8+ T cell responses following intradermal plasmid DNA immunization. *J. Immunol.* 185: 3463-3471.

55. Darquet, A. M., B. Cameron, P. Wils, D. Scherman, and J. Crouzet. 1997. A new DNA vehicle for nonviral gene delivery: supercoiled minicircle. *Gene Ther.* 4: 1341-1349.

56. Darquet, A. M., R. Rangara, P. Kreiss, B. Schwartz, S. Naimi, P. Delaere, J. Crouzet, and D. Scherman. 1999. Minicircle: an improved DNA molecule for in vitro and in vivo gene transfer. *Gene Ther.* 6: 209-218.

57. Chen, Z. Y., C. Y. He, A. Ehrhardt, and M. A. Kay. 2003. Minicircle DNA vectors devoid of bacterial DNA result in persistent and high-level transgene expression in vivo. *Mol. Ther.* 8: 495-500.

58. Chen, Z. Y., C. Y. He, L. Meuse, and M. A. Kay. 2004. Silencing of episomal transgene expression by plasmid bacterial DNA elements in vivo. *Gene Ther.* 11: 856-864.

59. Chen, Z. Y., E. Riu, C. Y. He, H. Xu, and M. A. Kay. 2008. Silencing of episomal transgene expression in liver by plasmid bacterial backbone DNA is independent of CpG methylation. *Mol. Ther.* 16: 548-556.

60. Riu, E., D. Grimm, Z. Huang, and M. A. Kay. 2005. Increased maintenance and persistence of transgenes by excision of expression cassettes from plasmid sequences in vivo. *Hum. Gene Ther.* 16: 558-570.

61. Riu, E., Z. Y. Chen, H. Xu, C. Y. He, and M. A. Kay. 2007. Histone modifications are associated with the persistence or silencing of vector-mediated transgene expression in vivo. *Mol. Ther.* 15: 1348-1355.

62. Chen, Z. Y., C. Y. He, and M. A. Kay. 2005. Improved production and purification of minicircle DNA vector free of plasmid bacterial sequences and capable of persistent transgene expression in vivo. *Hum. Gene Ther.* 16: 126-131.

63. Mayrhofer, P., M. Blaesen, M. Schleef, and W. Jechlinger. 2008. Minicircle-DNA production by site specific recombination and protein-DNA interaction chromatography. *J. Gene Med.* 10: 1253-1269.

64. Kay, M. A., C. He, and Z. Chen. 2010.
A robust system for production of minicircle DNA
vectors. In Press**.**. *Nat Biotech*

65. Molnar, M. J., R. Gilbert, Y. Lu, A. B. Liu, A. Guo, N. Larochelle, K. Orlopp, H. Lochmuller, B. J. Petrof, J. Nalbantoglu, and G. Karpati. 2004. Factors influencing the efficacy, longevity, and safety of electroporation-assisted plasmid-based gene transfer into mouse muscles. *Mol. Ther.* 10: 447-455.

66. Mayrhofer, P., M. Schleef, and W. Jechlinger. 2009. Use of minicircle plasmids for gene therapy. *Methods Mol. Biol.* 542: 87-104.

67. Osborn, MJ, McElmurry, RT, Lees, CJ, DeFeo, AP, Chen, Z, Kay, MA, et al. 2010. Minicircle DNA-based gene therapy coupled with immune modulation permits long-term expression of α-l-iduronidase in mice with mucopolysaccharidosis type I. In press. *Mol Ther*

68. Faurez, F., D. Dory, V. Le Moigne, R. Gravier, and A. Jestin. 2010. Biosafety of DNA vaccines: New generation of DNA vectors and current knowledge on the fate of plasmids after injection. *Vaccine* 28: 3888-3895.

69. Gill, D. R., I. A. Pringle, and S. C. Hyde. 2009. Progress and prospects: the design and production of plasmid vectors. *Gene Ther.* 16: 165-171.

70. Kundig, T. M., C. P. Kalberer, H. Hengartner, and R. M. Zinkernagel. 1993. Vaccination with two different vaccinia recombinant viruses: long-term inhibition of secondary vaccination. *Vaccine* 11: 1154-1158.

71. Apostolopoulos, V. and D. B. Weiner. 2009. Development of more efficient and effective DNA vaccines. *Expert Rev. Vaccines* 8: 1133-1134.

72. Nestle, F. O., P. Di Meglio, J. Z. Qin, and B. J. Nickoloff. 2009. Skin immune sentinels in health and disease. *Nat. Rev. Immunol.* 9: 679-691.

73. Romani, N., B. E. Clausen, and P. Stoitzner. 2010. Langerhans cells and more: langerin-expressing dendritic cell subsets in the skin. *Immunol. Rev.* 234: 120-141.

74. Barry, M. A. and S. A. Johnston. 1997. Biological features of genetic immunization. *Vaccine* 15: 788-791.

75. Kang, M. J., C. K. Kim, M. Y. Kim, T. S. Hwang, S. Y. Kang, W. K. Kim, J. J. Ko, and Y. K. Oh. 2004. Skin permeation, biodistribution, and expression of topically applied plasmid DNA. *J. Gene Med.* 6: 1238-1246.

76. Meykadeh, N., A. Mirmohammadsadegh, Z. Wang, E. Basner-Tschakarjan, and U. R. Hengge. 2005. Topical application of plasmid DNA to mouse and human skin. *J. Mol. Med.* 83: 897-903.

77. Gothelf, A., J. Eriksen, P. Hojman, and J. Gehl. 2010. Duration and level of transgene expression after gene electrotransfer to skin in mice. *Gene Ther.* 17: 839-845.

78. van den Berg, J. H., B. Nujien, J. H. Beijnen, A. Vincent, H. van Tinteren, J. Kluge, L. A. Woerdeman, W. E. Hennink, G. Storm, T. N. Schumacher, and J. B. Haanen. 2009.

Optimization of intradermal vaccination by DNA tattooing in human skin. *Hum. Gene Ther.* 20: 181-189.

79. Rabinovich, B. A., Y. Ye, T. Etto, J. Q. Chen, H. I. Levitsky, W. W. Overwijk, L. J. Cooper, J. Gelovani, and P. Hwu. 2008. Visualizing fewer than 10 mouse T cells with an enhanced firefly luciferase in immunocompetent mouse models of cancer. *Proc. Natl. Acad. Sci. U. S. A.* 105: 14342-14346.

80. Gibson, D. G., L. Young, R. Y. Chuang, J. C. Venter, C. A. Hutchison 3rd, and H. O. Smith. 2009. Enzymatic assembly of DNA molecules up to several hundred kilobases. *Nat. Methods* 6: 343-345.

81. Ingulli, E. 2007. Tracing tolerance and immunity in vivo by CFSE-labeling of administered cells. *Methods Mol. Biol.* 380: 365-376.

82. Kearney, E. R., K. A. Pape, D. Y. Loh, and M. K. Jenkins. 1994. Visualization of peptide-specific T cell immunity and peripheral tolerance induction in vivo. *Immunity* 1: 327-339.

83. Schorpp, M., R. Jager, K. Schellander, J. Schenkel, E. F. Wagner, H. Weiher, and P. Angel. 1996. The human ubiquitin C promoter directs high ubiquitous expression of transgenes in mice. *Nucleic Acids Res.* 24: 1787-1788.

84. de Koning, H. D., D. Rodijk-Olthuis, I. M. van Vlijmen-Willems, L. A. Joosten, M. G. Netea, J. Schalkwijk, and P. L. Zeeuwen. 2010. A comprehensive analysis of pattern recognition receptors in normal and inflamed human epidermis: upregulation of dectin-1 in psoriasis. *J. Invest. Dermatol.* 130: 2611-2620.

85. Stenler, S., A. Andersson, O. E. Simonson, K. E. Lundin, Z. Y. Chen, M. A. Kay, C. I. Smith, C. Sylven, and P. Blomberg. 2009. Gene Transfer to Mouse Heart and Skeletal Muscles Using a Minicircle Expressing Human Vascular Endothelial Growth Factor. *J. Cardiovasc. Pharmacol.*

86. Zhang, X., M. W. Epperly, M. A. Kay, Z. Y. Chen, T. Dixon, D. Franicola, B. A. Greenberger, P. Komanduri, and J. S. Greenberger. 2008. Radioprotection in vitro and in vivo by minicircle plasmid carrying the human manganese superoxide dismutase transgene. *Hum. Gene Ther.* 19: 820-826.

87. Hsieh, E. A., C. M. Chai, B. O. de Lumen, R. A. Neese, and M. K. Hellerstein. 2004. Dynamics of keratinocytes in vivo using HO labeling: a sensitive marker of epidermal proliferation state. *J. Invest. Dermatol.* 123: 530-536.

88. Biernaskie, J., M. Paris, O. Morozova, B. M. Fagan, M. Marra, L. Pevny, and F. D. Miller. 2009. SKPs derive from hair follicle precursors and exhibit properties of adult dermal stem cells. *Cell. Stem Cell.* 5: 610-623.

89. Bedoui, S., G. M. Davey, A. M. Lew, and W. R. Heath. 2009. Equivalent stimulation of naive and memory CD8 T cells by DNA vaccination: a dendritic cell-dependent process. *Immunol. Cell Biol.* 87: 255-259.

90. Bins, A. D., M. C. Wolkers, M. D. van den Boom, J. B. Haanen, and T. N. Schumacher. 2007. In vivo antigen stability affects DNA vaccine immunogenicity. *J. Immunol.* 179: 2126-2133.

91. Hovav, A. H., M. W. Panas, S. Rahman, P. Sircar, G. Gillard, M. J. Cayabyab, and N. L. Letvin. 2007. Duration of antigen expression in vivo following DNA immunization modifies the magnitude, contraction, and secondary responses of CD8+ T lymphocytes. *J. Immunol.* 179: 6725-6733.

92. Dooriss, K. L., G. Denning, B. Gangadharan, E. H. Javazon, D. A. McCarty, H. T. Spencer, and C. B. Doering. 2009. Comparison of factor VIII transgenes bioengineered for improved expression in gene therapy of hemophilia A. *Hum. Gene Ther.* 20: 465-478.

93. De Giovanni, C., G. Nicoletti, A. Palladini, S. Croci, L. Landuzzi, A. Antognoli, A. Murgo, A. Astolfi, S. Ferrini, M. Fabbi, A. M. Orengo, A. Amici, M. L. Penichet, L. Aurisicchio, M. Iezzi, P. Musiani, P. Nanni, and P. L. Lollini. 2009. A multi-DNA preventive vaccine for p53/Neu-driven cancer syndrome. *Hum. Gene Ther.* 20: 453-464.

94. Geusens, B., N. Sanders, T. Prow, M. Van Gele, and J. Lambert. 2009. Cutaneous short-interfering RNA therapy. *Expert Opin. Drug Deliv.* 6: 1333-1349.

95. Anonymous *J Gene Med* Clinical Trial Site.

96. Azzoni, A. R., S. C. Ribeiro, G. A. Monteiro, and D. M. Prazeres. 2007. The impact of polyadenylation signals on plasmid nuclease-resistance and transgene expression. *J. Gene Med.* 9: 392-402.

97. Miller, A. M. and D. A. Dean. 2008. Cell-specific nuclear import of plasmid DNA in smooth muscle requires tissue-specific transcription factors and DNA sequences. *Gene Ther.* 15: 1107-1115.

98. van den Berg, J. H., B. Nuijen, T. N. Schumacher, J. B. Haanen, G. Storm, J. H. Beijnen, and W. E. Hennink. 2010. Synthetic vehicles for DNA vaccination. *J. Drug Target.* 18: 1-14.

99. McNaughton, B. R., J. J. Cronican, D. B. Thompson, and D. R. Liu. 2009. Mammalian cell penetration, siRNA transfection, and DNA transfection by supercharged proteins. *Proc. Natl. Acad. Sci. U. S. A.* 106: 6111-6116.

100. Han, X., J. H. Bushweller, D. S. Cafiso, and L. K. Tamm. 2001. Membrane structure and fusion-triggering conformational change of the fusion domain from influenza hemagglutinin. *Nat. Struct. Biol.* 8: 715-720.

101. Skehel, J. J., K. Cross, D. Steinhauer, and D. C. Wiley. 2001. Influenza fusion peptides. *Biochem. Soc. Trans.* 29: 623-626.

102. Wadia, J. S., R. V. Stan, and S. F. Dowdy. 2004. Transducible TAT-HA fusogenic peptide enhances escape of TAT-fusion proteins after lipid raft macropinocytosis. *Nat. Med.* 10: 310-315.

103. Sugita, T., T. Yoshikawa, Y. Mukai, N. Yamanada, S. Imai, K. Nagano, Y. Yoshida, H. Shibata, Y. Yoshioka, S. Nakagawa, H. Kamada, S. Tsunoda, and Y. Tsutsumi. 2007. Improved cytosolic translocation and tumor-killing activity of Tat-shepherdin conjugates mediated by co-treatment with Tat-fused endosome-disruptive HA2 peptide. *Biochem. Biophys. Res. Commun.* 363: 1027-1032.

104. Carlotti, F., M. Bazuine, T. Kekarainen, J. Seppen, P. Pognonec, J. A. Maassen, and R. C. Hoeben. 2004. Lentiviral vectors efficiently transduce quiescent mature 3T3-L1 adipocytes. *Mol. Ther.* 9: 209-217.

105. Ma, H., J. Zhu, M. Maronski, P. T. Kotzbauer, V. M. Lee, M. A. Dichter, and S. L. Diamond. 2002. Non-classical nuclear localization signal peptides for high efficiency lipofection of primary neurons and neuronal cell lines. *Neuroscience* 112: 1-5.

106. Lavorini-Doyle, C., S. Gebremedhin, K. Konopka, and N. Duzgunes. 2009. Gene delivery to oral cancer cells by nonviral vectors: why some cells are resistant to transfection. *J. Calif. Dent. Assoc.* 37: 855-858.

107. Carpentier, E., S. Paris, A. A. Kamen, and Y. Durocher. 2007. Limiting factors governing protein expression following polyethylenimine-mediated gene transfer in HEK293-EBNA1 cells. *J. Biotechnol.* 128: 268-280.

108. Kreiss, P., B. Cameron, R. Rangara, P. Mailhe, O. Aguerre-Charriol, M. Airiau, D. Scherman, J. Crouzet, and B. Pitard. 1999. Plasmid DNA size does not affect the physicochemical properties of lipoplexes but modulates gene transfer efficiency. *Nucleic Acids Res.* 27: 3792-3798.

109. van den Berg, J. H., K. Oosterhuis, W. E. Hennink, G. Storm, L. J. van der Aa, J. F. Engbersen, J. B. Haanen, J. H. Beijnen, T. N. Schumacher, and B. Nuijen. 2010.

Shielding the cationic charge of nanoparticle-formulated dermal DNA vaccines is essential for antigen expression and immunogenicity. *J. Control. Release* 141: 234-240.

110. U.S. National Institutes of Health. 2010:

111. U.S. Food and Drug Administration. 2010. PROVENGE® (sipuleucel-T). 2010:

112. Anonymous 2006. Sipuleucel-T: APC 8015, APC-8015, prostate cancer vaccine--Dendreon. *Drugs R. D.* 7: 197-201.

113. Brewer, J. M. 2006. (How) do aluminium adjuvants work? *Immunol. Lett.* 102: 10-15.

114. Rhee, E. G., R. P. Kelley, I. Agarwal, D. M. Lynch, A. La Porte, N. L. Simmons, S. L. Clark, and D. H. Barouch. 2010. TLR4 ligands augment antigen-specific CD8+ T lymphocyte responses elicited by a viral vaccine vector. *J. Virol.* 84: 10413-10419.

115. Cekic, C., C. R. Casella, C. A. Eaves, A. Matsuzawa, H. Ichijo, and T. C. Mitchell. 2009. Selective activation of the p38 MAPK pathway by synthetic monophosphoryl lipid A. *J. Biol. Chem.* 284: 31982-31991.

116. Zhong, Z., X. Wei, B. Qi, W. Xiao, L. Yang, Y. Wei, and L. Chen. 2010. A novel liposomal vaccine improves humoral immunity and prevents tumor pulmonary metastasis in mice. *Int. J. Pharm.* 399: 156-162.

117. Smith, K. A., Z. Qiu, R. Wong, V. L. Tam, B. L. Tam, D. K. Joea, A. Quach, X. Liu, M. Pold, U. M. Malyankar, and A. Bot. 2010. Multivalent immunity targeting tumor-associated antigens by intra-lymph node DNA-prime, peptide-boost vaccination. *Cancer Gene Ther.*

118. Lu, Y., K. Ouyang, J. Fang, H. Zhang, G. Wu, Y. Ma, Y. Zhang, X. Hu, L. Jin, R. Cao, H. Fan, T. Li, and J. Liu. 2009. Improved efficacy of DNA vaccination against prostate carcinoma by boosting with recombinant protein vaccine and by introduction of a novel adjuvant epitope. *Vaccine* 27: 5411-5418.